NUREG/CR–5883
BNL–NUREG–52330

Health Risk Assessment of Irradiated Topaz

Prepared by
K. Nelson, J. W. Baum

Brookhaven National Laboratory

Prepared for
U.S. Nuclear Regulatory Commission

AVAILABILITY NOTICE

Availability of Reference Materials Cited in NRC Publications

Most documents cited in NRC publications will be available from one of the following sources:

1. The NRC Public Document Room, 2120 L Street, NW., Lower Level, Washington, DC 20555

2. The Superintendent of Documents, U.S. Government Printing Office, P.O. Box 37082, Washington, DC 20013-7082

3. The National Technical Information Service, Springfield, VA 22161

Although the listing that follows represents the majority of documents cited in NRC publications, it is not intended to be exhaustive.

Referenced documents available for inspection and copying for a fee from the NRC Public Document Room include NRC correspondence and internal NRC memoranda; NRC bulletins, circulars, information notices, inspection and investigation notices; licensee event reports; vendor reports and correspondence; Commission papers; and applicant and licensee documents and correspondence.

The following documents in the NUREG series are available for purchase from the GPO Sales Program: formal NRC staff and contractor reports, NRC-sponsored conference proceedings, international agreement reports, grant publications, and NRC booklets and brochures. Also available are regulatory guides, NRC regulations in the *Code of Federal Regulations*, and *Nuclear Regulatory Commission Issuances*.

Documents available from the National Technical Information Service include NUREG-series reports and technical reports prepared by other Federal agencies and reports prepared by the Atomic Energy Commission, forerunner agency to the Nuclear Regulatory Commission.

Documents available from public and special technical libraries include all open literature items, such as books, journal articles, and transactions. *Federal Register* notices, Federal and State legislation, and congressional reports can usually be obtained from these libraries.

Documents such as theses, dissertations, foreign reports and translations, and non-NRC conference proceedings are available for purchase from the organization sponsoring the publication cited.

Single copies of NRC draft reports are available free, to the extent of supply, upon written request to the Office of Administration, Distribution and Mail Services Section, U.S. Nuclear Regulatory Commission, Washington, DC 20555.

Copies of industry codes and standards used in a substantive manner in the NRC regulatory process are maintained at the NRC Library, 7920 Norfolk Avenue, Bethesda, Maryland, for use by the public. Codes and standards are usually copyrighted and may be purchased from the originating organization or, if they are American National Standards, from the American National Standards Institute, 1430 Broadway, New York, NY 10018.

NUREG/CR–5883
BNL–NUREG–52330
RO

Health Risk Assessment of Irradiated Topaz

Manuscript Completed: December 1992
Date Published: January 1993

Prepared by
K. Nelson, J. W. Baum

C. Daily, NRC Project Manager
C. Jones, NRC Project Manager

Brookhaven National Laboratory
Upton, NY 11973

Prepared for
Division of Regulatory Applications
Office of Nuclear Regulatory Research
U.S. Nuclear Regulatory Commission
Washington, DC 20555
NRC FIN A3982

ABSTRACT

Irradiated topaz gemstones are currently processed for color improvement by subjecting clear stones to neutron or high-energy electron irradiations, which leads to activation of trace elements in the stones. Assessment of the risk to consumers required the identification and quantification of the resultant radionuclides and the attendant exposure. Representative stones from Brazil, India, Nigeria, and Sri Lanka were irradiated and analyzed for gamma ray and beta particle emissions, using sodium iodide and germanium spectrometers; and Geiger-Muller, plastic and liquid scintillation, autoradiography, and thermoluminescent-dosimetry measurement techniques. Based on these studies and other information derived from published literature, dose and related risk estimates were made for typical user conditions. New criteria and methods for routine assays for acceptable release, based on gross beta and gross photon emissions from the stones, were also developed.

TABLE OF CONTENTS

LIST OF FIGURES

LIST OF TABLES

EXECUTIVE SUMMARY

This study provides information on the radionuclides involved in the production of "blue" topaz by neutron and electron irradiation and on the attendant potential exposure. Based on this information, several instruments and techniques were tested and evaluated for possible use by licensees to ensure compliance with NRC regulations on the release of activity in stones. Suggested new dose criteria and measurement methods are outlined for this purpose.

Radionuclides Produced

Fifty-one colorless gemstones from Brazil, India, Nigeria, and Sri Lanka were irradiated with neutrons at BNL's 60 MW research reactor. The thermal neutron fluence ranged from 3×10^{16} to 9.2×10^{18} neutrons/cm^2, while the fast neutron fluence ranged from 1.8×10^{18} to 1×10^{18} neutrons/cm^2. The relative contribution of either thermal or fast neutrons to the total activity in an irradiated topaz could not be established because of the inability to shield thermal neutrons (the integrity of thermal neutron shielding could not be maintained). Radionuclides produced from neutron activation included ^{182}Ta, ^{59}Fe, ^{46}Sc, ^{51}Cr, ^{54}Mn, ^{124}Sb, ^{77}As, ^{183}Ta, ^{77}Ge, ^{72}Ga, ^{32}P, and ^{24}Na.

Thirty-six colorless topaz gemstones from Brazil, India, Nigeria, and Sri Lanka were subjected to 2.5 coulombs per kilogram of 17 MeV electrons produced by a linear accelerator. The radioactive nuclides created emitted only positrons (511 keV) and relatively low intensity or low-energy beta emissions. The radionuclides produced by high-energy electron treatment include ^{64}Cu, ^{68}Ga, ^{49}Cr, and ^{18}F, but, positive identification was not possible because of their relatively short half-lives (< 1 day). However, the presence of the target elements, Cu, Ga, and Zn, was confirmed by x-ray fluorescence analysis (a minimum detectable level of 0.5 to 50 ppm).

Storing activated topaz at the irradiation facility to allow for radioactive decay will reduce radiation exposure. Such storage is common practice at some topaz distribution centers. The required storage time will vary depending upon the activation process and resulting radioactivity. Other nuclides, often identified in neutron-activated topaz, include ^{187}W, ^{140}La, ^{198}Au, ^{64}Zn, and ^{24}Na. However, these nuclides originate from (a) surface contamination due to human sweat and oils, and (b) chipping of tungsten-carbide drills during gem cutting. All surface contamination, with the exception of ^{24}Na, was removed by a 1-hour ultrasonification cleaning before analysis.

The activity per gram of the gemstones per unit fluence varied widely for any particular country of origin, sometimes by several orders of magnitude. This variation was due to the differences in the amount of specific precursor nuclides in the individual topaz. For this reason alone, recommendations can not be made about limiting or encouraging using topaz from a specific country of origin to minimize activity levels. Although the amount of precursor nuclide varied greatly, the distribution of activity in an individual topaz was uniform, as demonstrated by autoradiography on bare and covered film.

Photon Measurements

The individual gamma- or positron-emitting nuclides in irradiated topaz were easily identified and quantified by using a germanium detector. Although the energy resolution is outstanding, because of its low detection efficiency, this instrument may have limited usefulness in a commercial operation. Counting times of approximately 60 minutes were

needed to quantify nuclides at the NRC-exempt concentration or general public release levels using the germanium detector.

A NaI well-type detector (2" thick by 1.75" diameter) also could be used to quantify gamma or positron emissions in an individual topaz. Although a NaI detector is more efficient than a germanium detector for gamma or positron produced annihilation radiation, the energy resolution of the NaI detector can not approach that of the germanium detector. To meet exempt concentration limits, the NaI sensitivity (net cpm/nCi) must be determined for each nuclide identified by germanium gamma spectroscopy. If only single-channel NaI analysis were available to determine release concentrations, then the nuclide having the lowest NaI sensitivity (net cpm/nCi) should be used as a cutoff value for topaz containing a mixture of several gamma-emitting nuclides. NaI multichannel analysis could be used only if the resolution of the detector allowed detection of all gamma-emitting nuclides. An empirical equation was developed to calculate the NaI counting time necessary to detect exempt concentration levels at twice background based on the NaI sensitivity expressed as net cpm/nCi for the 40 to 1,400 keV energy window. All gamma-emitting nuclides identified in BNL topaz, ^{46}Sc, ^{54}Mn, ^{182}Ta, and ^{59}Fe, can be detected at a 99.9% confidence level in less than one minute using a shielded well type NaI detector and a minimum gem mass of 0.2 grams. If the detector is not shielded, then the background count rate for the 40 to 1,400 keV energy window would increase and, therefore, the required counting period would also increase. The counting time necessary to detect an exempt concentration of ^{134}Cs in a 0.2, 0.5, and 1.0 g topaz was calculated to be 9.1, 1.5, and 0.4 minutes, respectively, at the 99.9% confidence interval. These results are based on a NaI sensitivity of 700 cpm/nCi for ^{134}Cs and a shielded detector.

Beta-Particle Measurements

GM counters, beta scintillation detectors (liquid and solid), and gas-flow proportional counters were used to analyze beta activity emitted from activated topaz. With a shielded GM detector, an analysis time as long as 3 hours would be required to detect an exempt concentration level of ^{54}Mn and ^{35}S at twice background levels of radiation in a 0.2 g topaz. The counting time required varies inversely with the mass of the stone. For example, a 1 g topaz containing ^{35}S could be identified at an exempt concentration level if the counting time was reduced to five minutes. However, exempt concentration levels of ^{46}Sc, ^{182}Ta, ^{59}Fe, and ^{32}P in a 0.5 g or larger topaz can be detected with a shielded GM detector at twice background levels of radiation in one minute or less. The most restrictive nuclide, ^{54}Mn (by virtue of the low β emission - 4 keV per disintegration), would require a counting time of approximately 7 minutes for a 1 g topaz. The GM sensitivities were nearly equal for the gamma/beta emitting nuclides, ^{46}Sc, ^{182}Ta, and ^{59}Fe. The GM response to ^{32}P was approximately six times as great as the response to the above gamma/beta emitters. GM sensitivity for ^{54}Mn and ^{14}C (or ^{35}S) was so low that they could not be detected in a reasonable counting time at exempt concentrations.

However, when the detection level was based on the National Council on Radiation Protection and Measurements' (NCRP) negligible individual risk level of 10^{-7} (an annual effective dose equivalent of < 0.25 mrem) rather than on the NRC's criteria on exempt concentration, all the nuclides identified yielded twice background levels of radiation with a table facet area as low as 0.0625 cm^2.

Pure beta-emitting nuclides are of special concern. Based on our study, the pure beta-emitting nuclides considered likely to be produced by neutron irradiation were ^{32}P, ^{35}S, and ^{36}Cl. However, sulphur, chlorine, and phosphorus, the precursor elements of these

pure beta-emitting nuclides, were conspicuously absent when gems were analyzed by photon-induced x-ray emission (PIXE). The PIXE minimum detectable levels (MDLs) for these elements are 1,000 ppm for phosphorous, 425 ppm for sulfur, and 250 ppm for chlorine. It is, therefore, unlikely that detectable amounts of ^{36}Cl could be produced by thermal neutron activation. We could identify ^{32}P in irradiated topaz by observing the GM response (net cpm) with 0, 80, and 450 mg/cm^2 filtration. We did not further quantify pure beta emitters in topaz, because we used only nondestructive tests on activated topaz.

Several other detection methods were studied. A 0.01" plastic scintillator was as effective in detecting beta radiation over a wide energy range as a GM detector at the same source-to-detector distance. At low energies, the scintillator's net response is about three times greater. A plastic scintillator and/or bare photomutiplier tube can be used as a low-energy screening device. Autoradiographic analysis was conducted on irradiated topaz containing varying quantities of radioactivity. An approximately equal response per activity concentration (nCi/g of topaz) occurred for ^{182}Ta, ^{54}Mn, ^{46}Sc, and ^{59}Fe. An increased response to ^{32}P was noted, but the results could not be quantified because of the difficulty in making synthetic topaz containing a known amount of ^{32}P.

LiF thermoluminescent dosimetry chips (0.125" x 0.125" x 0.035") were placed for about 18 days directly on the table facet of irradiated topaz containing varying amounts of ^{46}Sc, ^{59}Fe, ^{182}Ta, and ^{51}Cr. These exposures gave responses ranging from 23 to 39 mR/(nCi g). For a topaz containing these nuclides and ^{32}P, the response ranged from 94 to 1,089 mR/(nCi g). The latter result is semiquantitative, because the response of TLD to a known concentration of ^{32}P in topaz is undetermined and difficult to simulate.

In summary, the GM detector is reliable and inexpensive to operate. The detector responds efficiently to radiation, but poorly to photon radiations. Therefore, its sensitivity to some isotopes is insufficient. Thus, an additional gamma sensitive detector, such as a NaI well detector, is needed.

Risk Estimates

Risk estimates for skin and breast cancer from exposure to irradiated topaz worn as a pendant were compared to the NCRP's negligible individual risk level (NIRL) of 10^{-7}. The integrated first-year risk of an irradiated topaz in contact with the skin or three inches from breast tissue was a small fraction of the NIRL level. For the risk from beta-particle exposure, the first-year estimates from a pendant containing six 1-gram stones, worn 8 hours per day were less than 1/1000 of the NIRL level for all isotopes identified in this study. For the risk from gamma-ray exposure, the first year estimates for the same topaz pendant were 0.58 (^{54}Mn) to 0.08 (^{51}Cr) of the NIRL level.

ACKNOWLEDGEMENT

The authors thank Dr. Robert Ryan and his colleagues at Rensselaer Polytechnic Institute for providing electron beam irradiation of samples; Dr. Eugene Foord, United States Geological Survey, and Dr. James Shigley, Gemological Institute of America, for help in obtaining topaz samples; and Dr. Garman Harbottle, Dr. Anant Moorthy, and Dr. Keith Jones of BNL for technical assistance in the analysis of the gems.

Much of the work reported here was submitted to the Graduate School of the University of Minnesota by Kevin L. Nelson in partial fulfillment of the requirements for the degree of Doctor of Philosophy.

The advice and suggestions from Cynthia Jones, Christine Daily, and other members of the NRC staff; Dr. Donald Barber, University of Minnesota (thesis advisor); Charles B. Meinhold (technical review); Dr. Avril Woodhead (editorial review), and our secretaries Grace Nubla and Karen Rose are greatly appreciated.

1. INTRODUCTION[1]

Since the beginning of the century precious and semi-precious gems have been irradiated to enhance their color. Reports of the intensification of diamond coloration by exposure to radium appeared as early as 1914 (Crookes, 1914). The first report of the production of blue topaz after irradiation was by F. H. Pough and T.H. Rogers in 1947. Since then, there have been various reports on topaz irradiation using an assortment of treatments, such as gamma rays, neutrons, and electrons. Unfortunately, these reports give little, if any, information on the radionuclides, or the levels of radioactivity produced during irradiation, or the type of detection equipment necessary to ensure that radiation levels are within acceptable limits. This research is intended to answer these questions, and estimate the risks of wearing irradiated topaz.

Today, gemstones are frequently treated to alter their color with good to excellent results. Table 1 lists the gemstones in which irradiation has successfully enhanced color. The enhancement of topaz creates a blue color, which has excellent stability at ambient or normal temperature and light. During the last decade, more than one million carats of irradiated blue topaz have entered the world market (Fournier, 1988). Currently, the only characteristic that can distinguish natural from irradiated blue topaz is a thermoluminescent peak (λ = 0.670 to 0.625 μm) that occurs at about 302°C (at 7°C/sec) in the latter which is not present in the natural mineral (Petrov and Berdesinski, 1975).

The blue topaz industry has grown dramatically through the years and now accounts for a $675 million in the worldwide market. The largest percentage of this market results from (a) wholesale distribution of blue topaz (4,000 kg of blue topaz were sold for $200 million in 1987), and (b) retail sales (3,000 kg of blue topaz were sold for $300 million in 1987)[2]. These figures do not reflect the cost of diamonds, gold, or other precious gems or metals used in the mountings. Table 2 summarizes this information. Also, the table shows that an increasing amount of blue topaz is being produced outside the United States. According to information supplied by the American Gem Trade Association, the countries listed in Table 3 are involved in the blue topaz industry (American Gem Institute, 1987). Assuming that 75 percent of worldwide sales occur in the United States and that the average weight of a topaz is two carats, 5.6 million blue topaz gems per year are purchased here.

NRC Information Notice 90-62 (1990) alerted all importers and distributors of irradiated gemstones, and all non-power reactor licensees that to import neutron-irradiated topaz, an NRC distribution license must be obtained. NRC has continued to work with U.S. Customs Officials to monitor all incoming shipments of non-precious gemstones.

---

[1]Various terms and acronyms specific to the gem and radiation technologies are defined in Appendices A and B, respectively.

[2]Letter dated August 18, 1987 from Peggy Willett, American Gem Trade Associates, Inc., to Stanley Lasuk, NRC.

Table 1. Gemstones Most Frequently Irradiated to Enhance Color[a]

Gemstone	Original color	Final color	Frequency used[b]	Stability
Amethyst	Colorless to yellow or pale green	Brown, amethyst "Smoky", rose	Occasionally	Good
Beryl; blue ("Maxixe" type)	Pale pink or colorless	Deep blue	Always	Poor
Beryl; yellow	Colorless	Yellow	Commonly	Good
Diamond; colored	Off white	Various shades of green/yellow brown/blue	Occasionally Many[c]	Excellent
Pearl; cultured		Blue and gray	Occasionally Some[c]	Good
Sapphire	Yellow	Intense yellow or orange color	Occasionally	Very poor
Spodumene	Colorless/pink	Green	Rarely	Poor
Topaz: blue	Colorless	Blue	Usually Most[c]	Excellent
Topaz; yellow/orange	Yellow/orange	Intensifies yellow or orange color	Occasionally Many[c]	Good
Tourmaline; green, blue	Green, blue	Darker green, blue	Occasionally	Excellent
Tourmaline; pink, red ("rubellite"), purple		Intensifies initial color	Occasionally Some[c]	Excellent
Zircon[d]	Colorless	Brown to red	Always	Good

[a]Jewelers Information Manual, 3rd ed., Feb. 1988.

[b]Jewelers Information Manual frequency designations; Rarely 0-10%; Occasionally 10-25%; Commonly 25-50%; Usually 50-95%; Always 100%.

[c]Jeweler's Gemstone Reference (Sept. 1985) frequency designations; Most 90% or more; Many 60-90%; Some 30-60%.

[d]Zircon is only heat treated but contains naturally occurring radionuclides (Reprinted from C.E. Ashbaugh III, "Gemstone Irradiation and Radioactivity," Gems & Gemology , Vol. 24, No. 4, pp. 196-213, 1988).

Table 2. The Blue Topaz Industry-1987[a]

Activity	Estimated number of people involved (non-overlapping)	Estimated percent of yearly income[d]	Estimated international yearly weight in kg	Estimated international yearly dollar volume in millions	Approximate U.S. market share, %
Mining	4,000	95	181,600	15	*
Cutting	10,000	95	6,000	20	*
Color processing	200	75	6,000	15	40[c]
Wholesale distribution	1,000	30	5,000	125	35[c]
Wholesale jewelry manufacturing and sales	10,000	30	4,000	200[b]	40
Retail sales	10,000	15/20	3,000	300[b]	80

*Not applicable.
[a]Letter written to Mr. Stanley Lasuk, NRC, Region III, from Peggy Willett, August 18, 1987.
[b]Blue topaz only; gold and diamonds not included.
[c]1986 figures exceeded 95%.
[d]Applies to people listed in second column.

Table 3. Worldwide Blue Topaz Industry[a]

Country	Mining	Cutting	Neutron and/or electron irradiation and/or heat treatment	Wholesale blue topaz distribution	Wholesale jewelry mfg. and sales
Australia	X		X		
Brazil	X	X	X		X
Canada			X		
China		X	X (?)		
England			X	X	
France					X
Germany		X	X	X	X
Hong Kong		X		X	X
India	X		X (?)		
Italy					X
Japan					X
Korea		X			
Nigeria	X				
Sri Lanka	X	X			
Sweden			X		
Switzerland				X	
Taiwan		X			X
Thailand		X		X	X
U.S.A.			X	X	X

[a]Letter written to Mr. Stanley Lasuk, NRC, Region III, from Peggy Willett, August 18, 1987.
Note: (?) indicates strong possibility, but no evidence.

Three major types of irradiation facilities are used to enhance topaz: gamma ray facilities (i.e., ^{60}Co), linear accelerators, and nuclear research reactors. The 1.17 and 1.33 MeV ^{60}Co gamma rays convert the near-colorless topaz to a low-intensity, light-blue color called "Cobalt Blue" in the trade (Ashbaugh, 1988). A more intense blue has been created by interaction with high-energy electrons (10 to 20 MeV) produced by a linear accelerator (LINAC) (Schmetzer, 1987). Nuclear reactors generate fast neutrons with an average energy of 2 to 3 MeV, although the energy of the neutrons to which the topaz is exposed may range from thermal energies (0.025 eV or less) to higher energies (5 to 20 MeV). The medium-blue color created by neutron irradiation is called "London Blue." Table 4 summarizes various methods of treating topaz and the suspected color centers.

Topaz contains impurities which are made radioactive during exposure to electron beams via (γ,n) reactions and neutron beam bombardment via (n,γ), (n,2n), (n,p), or (n,α) reactions. The larger the fluence delivered, the larger is the amount of induced activity produced in topaz. Therefore, the dose delivered to the topaz is an important consideration in studying induced activity. Some time is necessary to allow for radioactivity to decay before the irradiated topaz can be handled at extremity exposure rates less than several mR/hr. Exposure of the individuals that retrieve and work with irradiated topaz, immediately after an irradiation, must be maintained within the occupational exposure limits. The level of their exposure to radiation will depend on several factors, including: (a) the type of treatment (e.*g.*, ^{60}Co vs. neutron treatment), (b) the radiation fluence delivered to the topaz, and (c) the nuclides and activity levels created by the irradiation. If the radiation protection principles of time, distance, and shielding are followed, it is anticipated that the exposure of the individuals handling topaz immediately after irradiation can be maintained within occupational exposure limits. Grinding or cutting the irradiated topaz should be restricted, because of the added radiation exposure caused by inhalation of radioactive particulates. Current NRC limits restrict the yearly occupational whole-body radiation dose to 5 rems and yearly skin dose to 30 rems (Code of Federal Regulations, 1991). Low levels of radioactivity can remain in irradiated topaz for months to years after treatment. Some of the primary gamma-emitting radionuclides found in irradiated topaz include ^{182}Ta, ^{46}Sc, ^{54}Mn, and ^{59}Fe (Ashbaugh, 1988). The level of activation produced from these isotopes and others that may be present depends on the type of irradiation treatment, the geologic origin of the gem, the total thermal/fast neutron fluence, and the amounts of precursor elements present. Elements identified spectroscopically in topaz at less than 300 ppm are Co, Cr, Ni, Ge, Mn, and Cu (Heide, 1966). These nuclides could be made radioactive during coloration treatments. Also, Foord et al., (1988) identified three types of natural topaz: (a) rhyolitic (rich in F); (b) pegmatites and greisens; and (c) hydrothermal (rich in OH). They also found the fluorine content to be inversely related to water content. Trace and minor elements included Li, Fe (as much as 0.3 % wt), Cr, and Ge. Chromium was found in hydrothermal topaz. These interrelationships between these elements and radiation are not understood fully and require further investigation; however, they are included in this discussion to account for the wide variety of activated nuclides that might be expected after coloration treatment.

Table 4. Methods of Treating Colorless Topaz and the Suspected Color Centers in Irradiated Topaz[a]

First Treatment	Resulting Color	Additional Treatment(s)		Final Color
Gamma rays i.e., ^{60}Co	(a) Colorless (b) Brown	Heat treatment at 100-200°C		(i) Colorless (ii) Blue X-centers* "Cobalt Blue"
Electron beam 10 to 20 Mev	Brown or greenish brown	Heat treatment at 100-200°C		Blue X- and Y-centers*
Nuclear reactor	Steely, dark blue or gray	10 to 20 MeV electrons	120 to 480°C 1 to 6 hrs.	Blue X-centers* "London Blue" "American Blue"
	Brown, yellow, green or blue	10 to 20 MeV electrons	120 to 315°C 1 to 6 hrs.	"Super Sky Blue"

*F color centers may also be involved.

[a]Reprinted with permission from Journal of Gemmology, Volume 20, K. Schmetzer, "Colour and Irradiation-Induced Defects in Topaz Treated with High-Energy Electrons," 1987.

NRC regulations do not prohibit neutron irradiation of products. However, they prohibit both the import and domestic distribution of consumer products containing radioactivity that results from producing or using special nuclear material, except in accordance with a distribution license issued by the NRC (Code of Federal Regulations, 1984). This license requires that the radioactivity in the product must not exceed the exempt concentrations specified in 10 CFR 30.70 (Code of Federal Regulations, 1984). However, these limits were not based on solid, nonsoluble materials (such as topaz), that remained outside the body.

In addition, current regulations require specific justification for the distribution of radioactive products designed for application to humans. Long-standing NRC policy on consumer products specifies that the authorization of radioactivity in toys, novelties, and adornments (such as jewelry) is inappropriate (Atomic Energy Commission, 1965). In 1982, the NRC prohibited the manufacture and import of cloisonne jewelry and similar products containing uranium (Nuclear Regulatory Commission, 1983, 1984).

The NRC has not established "de minimus" levels below which the radioactivity in consumer products might be disregarded. European countries have established release limits greater than the NRC's exempt limits listed in 10 CFR 30.70, and the European limit of 74 Bq/g (2 nCi/g) is considered by some in the industry as a more realistic limit (Ashbaugh, 1988). The determination of specific gamma and beta emitting radioisotopes found in neutron- and electron-beam-irradiated topaz is essential in estimating individual and population doses.

The overall objective of our study was to quantify the concentrations of activity possible in irradiated gems, to identify the specific nuclides responsible for the radiations, and to measure or calculate the dose to people attributable to the induced activity. However, there was little quantitative information in the literature on gamma and beta emitting nuclides that would allow us to make generalizations. Such information was especially incomplete for pure beta emitters, because they present a difficult analytical challenge in the presence of nuclides that emit both beta particles and gamma rays. In this study, the types of pure beta emitting nuclides that could be expected were identified and their activity concentrations were measured in activated topaz. Such analyses are essential in evaluating the health risk associated with distributing and wearing such gems.

Another factor investigated was the distribution of the activity in the gem. If the induced activity was not uniformly distributed, then certain beta emitting nuclides could go undetected yet still result in concentrations exceeding the exempt concentration limits. Also, errors in calculated estimates of dose would occur if the mixture of radionuclides was not homogeneous.

BNL irradiated topaz gems from several countries with neutrons in a high-flux nuclear reactor to maximize the induction of radioactivity, allowing measurements to be completed in a reasonable time. Worst case scenarios were completed on which to formulate upper estimates of health risks and to make correlations between the country of origin, type of emissions, and the magnitude of induced activity. Such correlations were considered to evaluate if one could safeguard occupational and public health on the basis of country of origin alone.

To determine if we could deduce activity concentrations from the color of topaz gems or the type of treatment, we compared the most commonly used coloration regimens. The identity and activity concentrations of radionuclides found with each type of treatment was established.

Some publications suggest that low concentrations of radionuclides with short half-lives are induced in topaz (Nassau, 1985; Ashbaugh, 1988). If this is invariably true, simple storage of gems until the activity concentrations have decayed to inconsequential levels would eliminate any health risks associated with the manufacture, distribution, and use of such gems.

Different types of calibrated, charged-particle and gamma-ray detectors were used to measure low concentrations of induced activity in topaz, and the best combination of resolution, efficiency, and counting protocols was determined. Factors were examined that influence the accurate determination of activity (i.e., geometry and background radiation). In choosing the best instrument (or instruments) and measurement protocols, we considered the cost of the instrument, the technical expertise of the expected users, and the circumstances under which the measurements would be made. This study answered the question, "Is it possible to measure the activity in gems at radioactive concentrations that are at or below those exempted from regulation by the U.S. Nuclear Regulatory Commission?", as listed in the Code of Federal Regulations 10 CFR 30.70 (1984).

Quantitative and accurate answers to the above questions are important for both health and economic reasons, because the topaz industry grosses about $675 million dollars per year in the United States.

2. PREVIOUS RESEARCH

2.1 Radiation Dose from Irradiated Topaz

Publications on dose equivalents or exposures from topaz is rare. Although radiation dose equivalent (rem) is usually stated in all studies of topaz irradiation, the distinction between the measurement of radiation exposure in air (Roentgens or R) and the radiation dose equivalent is not clear. In the literature, exposure and dose are related by the following equation (Johns and Cunningham, 1978).

$$D_{med} = (f_{med})\ (X)\ (A_{eq}) \qquad (1)$$

where

D_{med} = dose (or dose rate) in medium, rads

f_{med} = f factor

$$= 0.0869\ \frac{\mu_{en}/\rho_{med}}{\mu_{en}/\rho_{air}}$$

X = exposure (or exposure rate) measured in air, roentgens

A_{eq} = equilibrium correction factor, i.e., the fraction of the photon beam transmitted through an equilibrium thickness of air.

μ_{en}/ρ = mass energy-absorption coefficient, cm^2/g

The equilibrium correction factor is often neglected because it is nearly 1.0 for most energies and differs from 1.0 by only 1.5% for ^{60}Co in air. This equation cannot be used for photon energies greater than 3 MeV and may not be used in the buildup region where electronic equilibrium is not established.

Table 5 compares the mass energy-absorption coefficients, μ_{en}/ρ, for 80 keV and 1.5 MeV photons in air, water, and topaz ($Al_2SiO_4F_2$).

Table 5. Comparison of Mass Energy-Absorption Coefficients, μ_{en}/ρ (cm^2/g)

Medium	80 keV	1.5 MeV
topaz	0.0285	0.0250
air	0.0243	0.0254
water	0.0262	0.0282

Data for air and water from Attix et al. (1968).

The gamma ray dose from topaz would be about 86 percent of the exposure measurement from irradiated topaz at 80 keV and 1.5 MeV. For air and topaz, the f factor varies only

slightly from 80 keV to 1.5 MeV, because air and topaz have essentially the same atomic number and the same number of electrons per gram, and, therefore, have similar mass energy absorption coefficients.

The dose equivalent is related to the absorbed dose by the following equation (ICRP, 1977):

$$H_T = DQN \quad (2)$$

where

H_T = dose equivalent, rem
D = absorbed dose, rad
Q = quality factor
= 1 for beta and gamma emissions
N = product of other modifying factors, such as absorbed dose rate and fractionation. Usually assumed to be equal to 1.

In 1977, the ICRP introduced the concept of effective dose equivalent because of the differences in sensitivity among organs and tissues. This recommendation was based on the principle that the risk of a stochastic effect should be equal, whether the whole body is uniformly irradiated, or whether the radiation dose is non-uniformly distributed. To account for this varying degree of tissue sensitivity, weighing factors, w_T, are used to calculate an effective dose equivalent, H_E, from the following equation:

$$H_E = \sum w_T H_T \quad (3)$$

where H_T is the dose equivalent in rems, to tissue T. Whole-body dose equivalent for members of the general public, H_E, is limited to 1 mSv (100 mrem) in a year (Code of Federal Regulations, Section 20.1301, 1991).

We concluded that measurements of exposure in roentgens, absorbed dose in rads, or estimates of dose equivalent in rems are roughly equivalent in topaz for the energy range of interest, 80 keV to 1.5 MeV.

Most reported measurements of exposure from irradiated topaz involve the use of Geiger-Muller (GM) detectors. However, because the response of GM detectors is energy-dependent, direct measurement of exposure cannot be made unless the activated nuclides are known and the GM detector has been calibrated to those specific nuclide(s). Crowningshield (1981) measured a parcel of 100 blue Brazilian topaz and obtained 12 mR/hr at contact with a GM counter, while an individual 10 carat topaz in contact with the GM detector caused approximately 0.2 mR/hr. Using a Victoreen Model 290 GM survey meter with a pancake probe Model 489-110 B, Ashbaugh (1988) reported a net count rate of 35 cpm (background of 40 cpm) from a neutron-irradiated blue topaz (4.62 carats) containing 0.75 nCi of ^{46}Sc, and 70 cpm from a 4.72 carat gem containing 2.0 nCi of ^{182}Ta. Thus, 0.86 nCi of ^{46}Sc and 1.1 nCi of ^{182}Ta were required to produce a count rate of 40 cpm above background. Therefore, the exposures reported in the literature from a single irradiated topaz varied from several hundredths of a mrem/hr (Ashbaugh, 1988) to several

tenths of a mrem/hr (Crowningshield, 1981). Our studies suggest that it is unlikely that unshielded GM detectors would be of value in evaluating exempt concentration levels in topaz because the background counting rates for GM detectors are in this same range.

2.2 Irradiation Methods

2.2.1 Gamma Irradiation

Most published reports of irradiated topaz involve the use of gamma facilities. Nassau and Prescott (1975) used ^{60}Co gamma rays to deliver a total dose of 10 Mrads at a dose rate of 0.7 Mrads/hr to 86 colorless topaz samples from Minas Gerais, Brazil. Thirty-two stones turned brown to dark brown after irradiation, and twenty-one of these turned blue after heating in a muffle furnace at 250°C overnight. The color that was produced was not uniform. The initial brown color was produced at two radiation dose rates; one rate produced a fast fading yellowish color when exposed to light at a half-color saturation dose of 0.058 Mrads while the other rate, at a half-color saturation dose of 12.6 Mrads, produced a slowly fading dark brown color. Color saturation dose was determined by a polarized optical spectrometer and measured as the absorption coefficient of the strongest absorption peak (at 0.5 μm) at a given dose. Nassau and Prescott had difficulty in equating half coloration dose with the polarized optical spectrophotometer measurements. Dickinson and Moore (1967) reported that colorless topaz turned amber-yellow upon exposure to 5 MR from ^{60}Co gamma rays.

Nassau (1985) recommended dose rates of less than 5 Mrads/hr to avoid an excessive buildup of temperature inside topaz during gamma irradiation, depending on the size of the topaz. He reported a sequence of color change due to gamma irradiation as colorless →yellow→brown→reddish brown→very dark brown. Initial colorization was observed at 1 Mrad. According to Nassau, tens to many thousands of Mrads produced an olive-green component, which, upon heating at 200°C to 300°C (the length of time not given), evolved into a light-blue color.

Ashbaugh (1988) reported the production of a light blue color ("Cobalt Blue") upon exposure of near colorless topaz to ^{60}Co gamma rays at dose rates as high as several Mrads/hr. Higher dose rates created a steely gray-blue color. He suggested that large ^{60}Co sources could be used in a prescreening method to determine which topaz turns light blue and, therefore, might become darker with other types of treatment.

2.2.2 Neutron Irradiation

The blue color produced by neutron bombardment of topaz is usually uniformly deep, regardless of the size of the topaz, because neutrons have excellent penetrating properties. Unfortunately, radioactive byproducts are produced with such treatment. Several studies suggested that thermal neutrons (less than 0.025 eV) create the majority of radioactive isotopes in topaz, but fast neutrons (greater than several MeV) produce the blue color (Ashbaugh, 1988; Nassau, 1985). The blue color produced by neutron bombardment of topaz was called "London Blue" (Ashbaugh, 1988).

The dose required to produce a blue topaz by neutron bombardment can vary by more than one magnitude. Nassau (1984) suggested that a dose of up to 40,000 Mrads would produce a stable deep blue; he also reported that 1,000 Mrads created a stable "inky" or "steely" blue after heating (Nassau, 1985). The depth of color was not correlated with dose.

Various methods have been suggested to reduce the thermal neutron activation component. Ashbaugh (1988) and Nassau (1985) mentioned using a cadmium- or boron-lined container to reduce the thermal neutron fluence. Ashbaugh also suggested using uranium convertor plates to reduce the thermal neutron fluence by absorption, while increasing the fast, color-producing, neutron fluence. Convertor plates attenuate or reduce the thermal neutrons and release fast neutrons by fission.

2.2.3 Electron Beam Irradiation

Although the NRC does not regulate electron beam irradiation, the isotopes produced by this treatment are important because often neutron and electron treatments are combined. Electrons with energies between 10 and 20 MeV have been used to create or enhance blue color in topaz. Nassau (1985) recommended using cold running water to cool the topaz during irradiation, thus preventing temperature buildup within the gem.

In addition, electrons must be energetic enough to completely penetrate the topaz, or a large negative charge will build up internally and cause fracturing (Ashbaugh, 1988). The "Sky Blue" color that is produced by electron beams requires doses of between 7,000 and 10,000 Mrads.

Nassau (1985) reported that induced activity increased with increasing electron energy, although no specific examples of this reaction were cited. The induced activity began at about 15 MeV. In this same work, tens of thousands of Mrads were required to create a deep-blue color. The specimens had to be less than 15 mm in diameter and/or less than approximately 150 carats to maximize this treatment. Schmetzer (1987) used 10 to 20 MeV electrons to study X- and Y-color centers (hole centers) in blue topaz; he did not mention the dose rate nor the total dose delivered.

Ashbaugh (1988) used electrons between 10 to 15 MeV and a current of several hundred microamps to create blue topaz; dose rates up to and exceeding several hundred Mrads/hr were required. At these large dose rates (250 to 500 Mrads/hr), the internal temperature of topaz increased at a rate of 50°C to 100°C per minute. Because of this increase, Schmetzer (1987) speculated that the color is bleached in the core and appears only at the surface.

2.2.4 Combination Radiation Treatments

The combination radiation treatment regimen most commonly mentioned in the literature involved neutron bombardment followed by treatment with electron beams (Fournier, 1988). After heating (121°C to 482°C for 1 to 6 hrs), a dark blue color called "American"/"Electra"/"California"/"Swiss" or "Super Sky Blue" was produced. The electron-beam radiation dose required to enhance the medium blue color produced by neutron bombardment was 1,000 to 10,000 Mrads.

2.3 Isotope Identification and Radioactivity Produced

The number of publications identifying the radiation treatment facilities in the last ten years is several times the number of those identifying the activated radionuclides and their associated concentration levels in topaz. Activation of topaz is possible during neutron or electron beam bombardment or other particle-beam treatments. Gamma irradiation does not induce radioactivity (Nassau, 1985); however, high-energy photons (bemsstrahlung) produced in stopping high-energy electrons can activate elements through the photo-neutron reaction; this effect generally occurs with photons above a few MeV in energy.

Benada (1972) conducted an activation analysis of a 2.42 g piece of Nigerian topaz found in a fluvial deposit. Using a fluence rate of 1 x 10^{12} thermal neutrons/(cm^2 sec) and an irradiation time of 72,000 sec (20 hrs), ^{40}K, ^{46}Sc, ^{59}Fe, ^{141}Ce, and ^{182}Ta were detectable 27 days after bombardment. The results reported as parts per million (ppm) for ^{46}Sc, ^{141}Ce, and ^{182}Ta showed concentration levels of 9.30, 0.5, and 4.3 nCi/g, respectively. Unfortunately, only one topaz was analyzed. The results for ^{40}K and ^{59}Fe were not reported.

Table 6 summarizes the results of Crowningshield (1981), who noted the following isotopes and activity for about 100 deep blue topaz gemstones from Brazil which were, presumably, subjected to neutron bombardment (the neutron fluence and time between irradiations and measurements is unknown).

Table 6. Induced Activity in Topaz[a]

Activity, μCi (Bq)	Nuclide
0.1 (3,700)	^{46}Sc
0.002 (74)	^{182}Ta
0.002 (74)	^{54}Mn
0.001 (37)	^{59}Fe

[a]Taken from Crowningshield, 1981

Nassau (1985) and Ashbaugh (1988) found that induced activity increased as the electron energy was increased; the minimum energy needed to create induced activity varied. Nassau reported that activation began at approximately 15 MeV, and that a storage and decay period of a few days to a few weeks was needed before radiation levels were low enough to allow handling of the gems. Ashbaugh reported that the minimum electron energy needed to induce activity was about 12 MeV. He indicated that an (x-ray neutron) interaction produced ^{69}Ge (with a radioactive half-life of 36 hrs).

2.4 Radiation Detection Equipment

A thorough understanding of radiation detection equipment and information on radiation exposure is necessary to estimate the health risk from irradiated blue topaz. Domestic processors will need to understand the equipment and its limitations to assess quantities such as exempt release concentration levels. The minimum detectable levels and quality-control procedures for the counting equipment specifically required for irradiated blue topaz are not normally available in the literature.

Ashbaugh (1988) stated that a GM counter worked well for "low levels" of beta radiation and "somewhat higher levels" of gamma emitters. A GM efficiency of 1 to 20 percent and 0.1 to 2 percent was given for a beta and a gamma emitter, respectively. In general, he concluded that GM counters are less than 5 percent efficient for quantifying radioactivity in topaz, and further, the response per nCi depended on the size of the stone and the type of radiation emitted.

Ashbaugh also stated that NaI(Tl) and germanium detectors were used in conjunction with multichannel analyzers to quantify gamma activity. However, minimum detectable levels, counting geometries, and counting times were not given.

Autoradiography (the use of radiation-sensitive film to detect the presence of radiation) was suggested by Webster (1983) as a method to detect radium-treated diamonds, but he did not mention irradiated topaz.

2.5 Color Centers in Irradiated Blue Topaz

Color in gemstones can be created by five basic mechanisms (Fritsch and Rossman, 1987):

- dispersed metal ions; e.g., Cr^{+3} (octahedral); e.g., emerald
- charge transfer; e.g., $Fe^{+2} \rightarrow Fe^{+3}$; e.g., aquamarine
- color centers; e.g., unknown blue color-center; e.g., topaz
- band theory; e.g., cinnabar
- physical optics; e.g., opal

The blue color in topaz is thought to be caused by color centers. Ionization-induced electron and hole formation and migration processes are primarily responsible for creating color centers. The initial interaction of fast neutron reactions with atoms of topaz is an elastic or inelastic collision with a single atom (Levy, 1985). Slow or thermal neutrons also can interact with atoms, most often by undergoing a (n,γ) reaction. The atom is displaced if the energy transferred is about 25 eV. Additional displacements may occur if the displaced atom possesses enough energy. For example, 500 atoms in Al_2O_3 can be displaced by a 1 MeV neutron. An electron will primarily interact with lattice electrons. If the electron is sufficiently energetic, electron-hole ionization pairs are formed. Atoms also can be displaced if the electron has a large initial energy, i.e., electrons produced by a linear accelerator. For example, a 0.67 MeV electron is needed for a Ge atom to acquire the necessary 25 eV displacement energy. X-rays, gamma rays, and other neutral species do not interact with topaz until charged species, such as photoelectrons or electron-positron pairs, are produced. Once recoil electrons (or positrons) are created, they interact in all ways associated with primary electrons. Gamma-ray damage results from a two-step process. Initially, recoil electrons are produced, which create electron hole pairs and ion pairs in their paths. Consequently, gamma-ray-induced damage is limited by the penetration of the gamma rays to the point where the recoil electrons are produced. Optical absorption processes (e.g., valence to conduction band transitions) result in the interaction of low-energy photons with solids.

Crystals contain up to 10^{16} defects per cm^3 or about 1 ppm before irradiation (Levy, 1985). Some of these defects are electron and/or hole traps at normal temperatures. In addition, radiation-induced defects can trap ionization electrons and holes. Usually, holes are trapped more quickly than electrons. Often, the recombination of electrons with trapped holes and holes with trapped electrons is accompanied by the emission of light, i.e., luminescence. These recombination reactions have cross sections much larger than those for electron-hole trapping and can account for more than 99 percent of the ionization-induced changes. The remaining charged particles are trapped on defects and create the color centers responsible for the coloring.

Nassau (1983) predicted that the energy required to create a stable color-center in topaz was 5 eV. Schmetzer (1987) measured the absorption spectra after irradiation of Brazilian, Nigerian, and Zimbabwean topaz, using a polarized absorption spectroscope and

determined that several blue color centers existed in the irradiated gem, i.e., at least two blue hole-type X-centers and one bluish-violet hole-type Y-center. He found that the concentration of X-centers predominated in natural blue topaz, in gamma and neutron-irradiated topaz, and in the uniform light-blue area of topaz irradiated with electron beams. Neutron-irradiated blue topaz had a higher concentration of X-centers than gems from all other radiation regimens, and the homogeneous distribution of X-centers gave a more uniform color. In this case, trace elements, which are associated with higher concentrations of color centers, are less important in the coloration process. Not all topaz turned blue because some stones lacked the electron or hole-center precursors necessary for the forming color centers. Dark bluish-violet Y-centers (at concentrations similar to neutron-irradiated X-centers) were found in the dark blue patchy areas of electron-irradiated topaz. It is speculated that both X- and Y-color centers are necessary to create the darker blue colors required for commercial topaz. Table 4 summarizes the various methods of producing blue topaz and lists the color-center precursors.

Raju (1981) speculated that the increase in hardness of topaz following neutron irradiation was caused by clustering of point defects, i.e., color centers. He found that the hardness of neutron-irradiated topaz crystals (VHN) was proportional to the total neutron dose. Hardness was determined by indentation with a Vickers microhardness indenter. Hardness attributable to radiation was reduced by heat. Raju's results are summarized in Table 7.

Table 7. Measurement of Hardness (VHN) in Topaz After Neutron Irradiation[a]

Hours of irradiation	VHN (kg/mm^2)	
	Before heating	After heating
Non-irradiated	0.168	**
Irradiated*		
48	0.275	0.197
60	0.357	0.209
72	0.515	0.223
84	0.742	0.234

[a] Reprinted with permission from The International Journal of Applied Radiation and Isotopes, Vol. 32, K.S. Raju, "Topaz-On Neutron Irradiation," 1981, Pergamon Press Ltd.
* Irradiated at 10^{13} neutrons/(cm^2 sec)
**Not determined.

2.6 Estimates of Somatic Risk

Cancer induction is one of the most important somatic effects of low-dose ionizing radiation. Possible biologic outcomes from the wearing of pendants, necklaces, or rings bearing

such as bone and stomach in our study because of the small quantity of radioactivity produced by irradiation of topaz and the rapid falloff of radiation dose with distance. However, their potential risks were accounted for by assuming that the total risk from all other organs was equal to that for breast or thyroid.

In considering radiation-ascribed carcinogenesis, the following considerations are important (NAS/NRC, 1980):

- Radiation-induced cancers are indistinguishable from those resulting from other factors.
- The incidence of cancer varies by several orders of magnitude depending on such factors as the histologic type and site of origin of the neoplasm, age, sex, and environmental factors.
- Depending on the histologic type and site of cancer, latency periods typically vary from a few years for leukemia, to about ten years for solid tumors following irradiation.
- The incidence of irradiation-induced human breast and thyroid cancer is greater in women, while the radiation risks from other cancers is about equal in the two sexes.
- The risk of cancer induction from low-dose radiation cannot be accurately predicted because of the uncertainty of the dose-response curve at low doses. Most current studies use a linear model for breast and thyroid cancer, and a linear-quadratic model for other sites.
- Linear extrapolations from high-dose to low-dose regions provide an upper boundary in risk estimations for low-dose, low-LET radiations.
- Bias and confounding factors including, for example, the healthy worker effect and smoking, can complicate the problem of accurately determining the expected number of cases in the cohort.
- Extrapolations between the incidence of radiation-induced cancers in animals and humans is highly speculative.

Risk is often expressed in absolute or relative terms. Attributable risk is the absolute increase in the frequencies of cancer attributable to radiation, and it is usually expressed in terms of excess deaths or cases per rad (or gray) or alternately, excess per rad per 10^6 person-years. Risk is often estimated by regression analysis, using a linear dose-response model. Relative risk is the ratio of the number of cases in an exposed population to the number in a comparable non-exposed population. The relative risk is generally expressed as a standardized mortality ratio, wherein adjustments are made for age, sex, and years of study. Studies are continually being reevaluated to determine whether the selection of the comparison group was appropriate. Unless otherwise specified, risk coefficients are assumed to be independent of age. The increased risk for young individuals would be balanced by the lower risk for older individuals at the time of exposure. Overall risk combines the probability of a radiation dose causing an effect, the chance of the exposure occurring, and the radiation dose received.

Irradiated gemstones emit a mixture of beta and photon energies that vary widely in energy, half-life, and relative isotopic abundance, depending on their origin, trace amounts of impurities, treatment (with neutrons, gamma radiation, and/or electrons), time since treatment, and self-absorption that is a function of the stone's size and weight.

Exposure rate (R/hr) at one foot from photon sources can be approximated as 6CE for sources with energies between 0.07 and 4 MeV, where C is number of curies and E is energy in MeV (BRH, 1970). This equation yields a dose per photon-MeV of 4.5×10^{-14} rem at one foot or 7.2×10^{-13} rem at 3 inches.

The beta-particle dose at 7 mg/cm^2 in tissue for a range of β emitters having average beta particle energies from 0.1 to 10 MeV was calculated using the VARSKIN Code (Traub et al., 1987). The results are summarized in Table 8. When expressed as the product of (average dose over an area of radius greater than the range of the most energetic beta particle) times (that area), the results show that dose per beta particle emitted from the gem may be expressed approximately as 6.2 ($\pm$ 20%) x 10^{-8} rem-cm^2 for average beta particle energies from 143 KeV to 1,242 KeV.

Table 8. Parameters of Beta Particle Dosimetry

Isotope	Average β Particle Energy (KeV)	βs/ disintegration	Dose per 10^8 β particles[a] (rem-cm^2/10^8 βs)
^{35}S	48.6	1	0.88
^{45}Ca	77.1	1	2.4
^{65}Zn	143	1	5.7
^{90}Sr	196	1	5.1
^{22}Na	215	0.9	5.9
^{36}Cl	251	1	5.6
^{32}P	695	1	5.3
^{90}Y	934	1	6.9
^{28}Al	1,242	1	7.4

[a]Dose-area product at 7 mg/cm^2 depth in tissue.

These dose conversion factors may be used with the latest recommended risk factors summarized in ICRP Publication 60 (ICRP, 1991). This document suggests that there is a risk of cancer mortality of 4×10^{-2} per person-Sv (4×10^{-4} per person-rem) for whole-body exposures, or the sum of the organ-weighted dose equivalent values: the latter is termed the effective dose (E) which replaces the effective dose equivalent, H_E.

Exposures to beta particles from gemstones primarily affect the skin. Gamma exposures are likely to occur to breast tissues and the thyroid gland. Total risk, R, is estimated as the sum of risks to the breast, thyroid, whole body, and skin. To estimate the gamma risks, the gems are assumed worn at an effective distance of 3 inches from breast tissue and 3 inches from the thyroid gland. The sum of gamma risks to all other organs in the whole body is assumed to be equal to the risk to either of these two organs.

Since the organ-weighting factors for breast and thyroid are both 0.05, the total gamma ray risk R_γ is:

$$\begin{aligned} R_\gamma &= D_\gamma \times 3 \times 0.05 \times 4 \times 10^{-4}/\text{rem} \\ &= 6 \times 10^{-5} D_\gamma \end{aligned} \qquad (4)$$

where D_γ is photon dose in rem at 3 inches from the gemstone.

This risk coefficient may be combined with the photon dose conversion factor to yield a risk per photon-MeV:

$$\begin{aligned} R_\gamma &= 6 \times 10^{-5}/\text{rem} \times 7.2 \times 10^{-18} \text{ rem/photon-MeV} \\ &= 4.3 \times 10^{-17}/\text{photon-MeV} \end{aligned} \qquad (5)$$

The β risk estimate, R_β, based on the probability of skin cancer, was summarized in ICRP Publication 60 (ICRP, 1991), from Shore (1990) as follows:

> The incidence of skin cancer is proportional to the area of skin exposed to ionizing radiation and also to ultraviolet radiation (UVR). The absolute risk estimate for the UVR exposed skin of the body, a total area of about 3000 cm^2, is 6.7×10^{-4} per person year gray. For the skin shielded from UVR, representing a total area of about 15,000 cm^2, this risk is estimated to be 2.0×10^{-4} per person year gray. The total risk is estimated to be 8.7×10^{-4} per person year gray when all of the skin of the body is exposed to ionizing radiation.
>
> Risks have been estimated by summing of the risks for UVR exposed and shielded areas, averaging risks for both sexes, and assuming a lethality of induced skin cancers of 0.2%. No reduction in risk is assumed for protracted exposures even though such a reduction is very likely.

The average whole-body cancer risk for a lifetime exposure from age 18 to 64 years was 2×10^{-4}/Sv (2×10^{-6}/rem), based on fatal cancer risk derived from the relative risk model. The dose should be evaluated at the depth of the basal cell layer, which varies between 20 μm and 100 μm over the whole body. When expressed as risk per cm^2 of skin exposed, this yields an average value of $2 \times 10^{-6}/\text{rem}/18000\ cm^2 \approx 10^{-10}/(\text{rem } cm^2)$. The non-fatal skin cancer risk would be approximately 500 times this value or $5 \times 10^{-8}/(\text{rem } cm^2)$.

3. EXPERIMENTAL METHODS

Colorless topaz (often referred to as "white" topaz in the trade) was obtained from various distributors to determine if the difference in induced radioactivity was correlated with country of origin. Unless otherwise specified, all the stones were precut, polished, and weighed between 0.1 g and 1.6 g (i.e., 0.5 carats to 8 carats). Colorless topaz stones were chosen from countries mining the largest percentage of topaz (except Australia). Unless topaz was mined from the same geological strata, the activation products were expected to vary greatly. Stones were primarily of brilliant or pendeloque cut. Definitions of carat size and types of topaz cuts are given in Appendix A. Appendix B gives the radiation terminology and acronyms frequently used in this study.

Because topaz is found in pegmatites and in high-temperature, highly acidic, igneous rocks, such as quartz or beryl, it is necessary to identify its mineral composition. In part, mineral composition accounts for differences in the activated products found in neutron-irradiated beryl, quartz, and topaz. The minerals are identifiable by differences in density and refractive index. Table 9 lists the differences in density and refractive indices for topaz and for minerals often misidentified as topaz.

All polished and faceted topaz stones were viewed with a Duplex II refractometer (Gem Instruments Santa Monica, CA 90406) before experimentation.

Table 9. Density and Refractive Indices for Topaz and Other Minerals[a]

Mineral	Density, g/cm^3	Refractive Index
Topaz	3.53 - 3.56	1.61 - 1.62
Beryl	2.68 - 2.90	1.75 - 1.76
Quartz	2.65	1.54 - 1.55

[a]From Webster, 1983.

Optical contact was made between the hemicylinder of the refractometer and the gemstone by using a liquid with a refractive index greater than 1.80 (the upper limit of the refractometer's range). The liquid, supplied by Gem Instruments, was composed of methylene iodide, sulfur, and tetraiodoethylene.

The refractometer could measure refractive indices of 1.3 to 1.8, and birefringences as small as 0.01. The refractometer measured the critical angle between the thick glass of the hemicylinder and the topaz. The scale was designed so that the critical angle was read in refractive indices and not in degrees. Yellow monochromatic light from a utility lamp with a 30-watt, 10.8 volt tungsten-halogen bulb (Gem Industries) enabled the experimenter to determine the most accurate refractive indices on flat surfaces.

Table 10 shows the sources and forms of topaz used in this study.

Table 10. Sources and Forms of Topaz Used in this Study

Supplier	State	Country of Origin	Cut	Polished
A	New York	Rondonia, Brazil	Yes	Yes
		Minas Gerias, Brazil	Yes	Yes
			Yes	Yes
		Sri Lanka	Preforms	Yes
		Africa		
B	New York	Nigeria	Yes	Yes
		Nigeria	Rough	No
C	Florida	Sri Lanka	Yes	Yes
		India	Yes	Yes
D	New York	Brazil	Yes	Yes
E	Colorado	USA	Rough	No
		Minas Gerias, Brazil	Rough	No

3.1 Neutron Coloration Treatment

Topaz was irradiated in the 60 MW High Flux Beam Reactor (HFBR) at Brookhaven National Laboratory (BNL). Table 11 gives the usable fluences and maximum dimensions of the irradiation chamber. The stated fluence was reported not to vary by more than 5 percent. The fluence was determined periodically by the reactor technical services group who have many years experience in activation experiments. These same people also packed, inserted, and removed the irradiation containers from the reactor, and continually monitored the irradiation. Each experiment was recorded in a log book.

Differences in neutron fluence are reflected in the different concentrations of activation products. The activation cross-section is generally neutron energy (or velocity)-dependent. Temperature control is important, because the cross-section will vary at elevated temperatures. This "spectral hardening" results in the selective loss of lower energy neutrons and, therefore, less thermal activation than anticipated.

Table 11. HFBR Irradiation Facilities[a]

Facility	Maximum fluence rate, neutrons/(cm^2 sec)		Usable sizes (inches)	
	Thermal	Fast (>1 MeV)	Diameter	Length
V-10 Reflector	2.7×10^{14}	7.5×10^{11}	15/16	3
V-11 Reflector	1.5×10^{14}	9.0×10^{10}	5/8	3
V-12 Reflector	3.8×10^{14}	8.3×10^{11}	15/16	3
V-14 Core-edge	8.3×10^{14}	9.0×10^{13}	3/4	3
V-15 In-core	2.0×10^{14}	3.0×10^{14}	3/4	3

[a]Ambient temperature was 50-60°C.

Neutron fluence monitors were used because refueling of the reactor causes the neutron-energy spectrum and, therefore, the neutron fluence to change. Table 12 gives the neutron fluences used in this study.

Table 12. Summary of BNL HFBR Irradiation Conditions

Gem #	Country of Origin	Thermal fluence (n/cm^2)	Fast fluence (n/cm^2)	Total Irradiation Time (min)
1 - 10	India	1×10^{18}	6×10^{14}	111
11-13, 15, 18, 19	Sri Lanka	*	1.1×10^{18}	24,351
14, 16, 17	India	*	1.1×10^{18}	24,351
20 - 24	Brazil	3×10^{18}	8.33×10^{15}	185
25 - 30	Brazil	6.6×10^{17}	1×10^{18}	55
31 - 36	Sri Lanka	9.21×10^{18}	1×10^{18}	185
37 - 41	Brazil	3.1×10^{17}	1.8×10^{14}	34
42 - 46	Brazil	3×10^{16}	1.8×10^{13}	3.3
47 - 51	Nigeria	1×10^{18}	2.8×10^{15}	62

* Cadmium shield partially melted.

An attempt was made to maximize the fast neutron fluence for some stones within any batch of topaz of the same national origin. This was done to assess neutron activation due to fast neutrons above any background level of thermal neutron activation. Other fluences chosen for study depended on the concentration level (nCi/g), and the minimum detectable levels achievable with a gamma spectroscopy system.

All samples were washed in an ultrasonic bath containing 2N HNO_3 before being packed in 99.99 percent aluminum to reduce the activation products produced from fingerprints and sweat. The nitric acid residues did not result in long-lived activation products of any consequence.

All sealed hyperpure quartz vials in which the fluence monitors were placed and their aluminum wrappings were marked with Higgins India ink, which does not produce disturbing radioactivity during neutron bombardment.

Topaz stones and fluence monitors (standards) were packaged so that the stones were singly aligned along the axial gradient. The fluence monitors were placed near the top and bottom of the string of topaz to measure variations along the axis. Radial variation of the

fluence within an irradiation chamber had been measured at ±1.5 percent (Yeh and Harbottle, 1986). We assumed that the topaz would be seen as an infinitely thin source by the neutrons (i.e., the fluence was not disturbed by the gems) because the maximum radial dimension of a single topaz gem was less than 1 cm.

After neutron irradiation in the HFBR, the topaz was stored for radioactive decay for two days to assure that radiation exposure levels would be reduced to a level that was safe to handle. The stones were then submerged in approximately 9-10 ml of 2N HNO_3 and cleaned for half an hour in a Bransonic 2200 ultrasonic bath. After half an hour, they were transferred to a clean beaker containing approximately 9-10 ml of 2N HNO_3 and cleaned ultrasonically for another half an hour.

3.2 Electron Coloration Treatment

Although the NRC does not regulate electron beam irradiation (some states do), some stones were treated this way to anticipate any problems that could arise with dual neutron- and electron-beam treatment. BNL topaz was irradiated with 17 MeV electrons from electron beams at the Rensselaer Polytechnic Institute (RPI) LINAC; treatment took four hours.

Topaz gems to be irradiated were packaged in a bucket with an inner cylinder. The bucket was made of aluminum, approximately 1/16" thick and a 1-1/2" space between the outside wall of the bucket and an inner aluminum cylinder was filled with topaz. The bucket was rotated rapidly and moved up and down during irradiation.

The irradiation was conducted at 200 mA (peak) and 440 μA (average) measured at the bucket with a pulse rate of 240 pulses per sec. The klystron was operated at 1300 MHz. Electrons from the L-band LINAC were extracted after the third (of eight) section through a 30-degree magnet. The electron beam (in the shape of an ellipse) was 1- to 2-cm wide horizontally as it struck the bucket about 8 inches from the window. The beam's cross-sectional area was 2 to 4 cm^2 at the bucket. The charge per unit mass to the target was 2.5 coulombs/kg of topaz, while the total electron charge to the bucket was 5.3 coulombs.

To cool the topaz during treatment and prevent cracking, water flowed through the bucket by gravity. The temperature of the water after passage through the bucket was 14°C, and it then was sent through a heat exchanger before being recirculated to the bucket.

After irradiation, exposure rates from the bucket can be several R/hr at contact. A week-long cooling period usually allows radiation levels to decrease to the mR/hr range.

After irradiation, the personnel at RPI anneal or heat the topaz at 88°C for two hours to drive off the brown color produced during irradiation. Annealing at this temperature for longer periods (e.g., 12 hours) will bleach out the blue color, which can be restored by irradiation.

3.3 Equipment for Radiation Detection

Many different types of radiation detection equipment are needed to correctly identify and quantify the activated nuclides in topaz; the best combination of resolution, efficiency, and counting times is necessary to accurately assess low levels of radioactivity. Consideration must be given to the cost and to the technical expertise required to operate these devices because of the wide range of situations in which they might be used.

A description of the radiation detection equipment used in our study is summarized in the following sections. Also, a summary of the counting equipment (non-germanium gamma spectroscopy) and non-counting equipment with the manufacturer's model and serial number is given in Appendices C and D, respectively.

3.3.1 Gamma Spectroscopy Detectors

The neutron- and electron-beam activated topaz was transferred to counting vials and placed in an automatic sample changer or introduced manually into gamma-spectroscopy counting systems. Appendix E lists the three counting systems used for the analyses. All gamma-spectroscopy detectors were coupled to ND-6600 multichannel analyzers (MCAs).

The detector designated as Princeton Gamma Tech (PGT) 6A was surrounded on five sides by various sizes of steel bricks (4" minimum). The top remained open to accept samples from the automatic sample changer. The bottom section of the shield closest to the detector was composed of cadmium bars to reduce characteristic lead x-rays. The Ge(Li) detector designated as Ortec 2 was surrounded by a 6" thick steel-encased lead shield from Gamma Products.

For the PGT 12 detector, samples from the automatic sample changer were dropped into a standardized counting geometry in which the bottom of the sample coincided with the center line of the horizontal Ge(Li) detector. In this way, the counting geometry of each specimen was reproduced and exactly controlled. A 60 hertz pulser, which fed into the preamplifier, was used for dead-time correction for the PGT 12 detector.

Routine performance tests (see Appendix F) were conducted on all detectors, and the results were logged. If a detector failed any of the tests listed in Appendix F, it was removed until the problem was resolved. The frequency of all gamma-ray spectroscopy-detector tests met, or exceeded, those recommended by ANSI (1978).

It was first necessary to determine if a point-source geometry was approximated for gamma-spectroscopy analysis conducted on the Ge(Li) or on intrinsic germanium detectors. As a general rule, the source-to-detector crystal (not endcap) should be at least twice the size of the largest crystal dimension to be considered as a point source. The largest dimension of all germanium crystal elements used in this study was 53 mm, giving us a desired source-to-detector distance of 106 mm (10.6 cm, or 4.17 inches). At this distance, the counting times necessary to detect the exempt concentrations of nuclides in irradiated topaz would be excessively long. Our compromise was to select a source-to-detector geometry that varied with the activity of the stone and permitted relatively short counting times (1 to 2 hours).

Figure 1 gives an example of a efficiency curve for point source geometry at various source-to-detector distances. As shown on these log-log efficiency curves, a linear best-fit curve was generated by a power function derived from the Grapher software package (Golden Software, Inc.). Multinuclide gamma standards (Amersham QCY.44) were used to generate all the gamma-spectroscopy efficiency curves, which were derived only from the 122 to 1333 keV (or 1836 keV) energy range. This choice was appropriate, because all the isotopes identified in this study and other studies (Ashbaugh, 1988) were found in this region. This clustering also eliminated the need to include the curvalinear crossover region below approximately 120 keV (for intrinsic germanium detectors). Its inclusion of this crossover region would have created difficulty in curve-fitting.

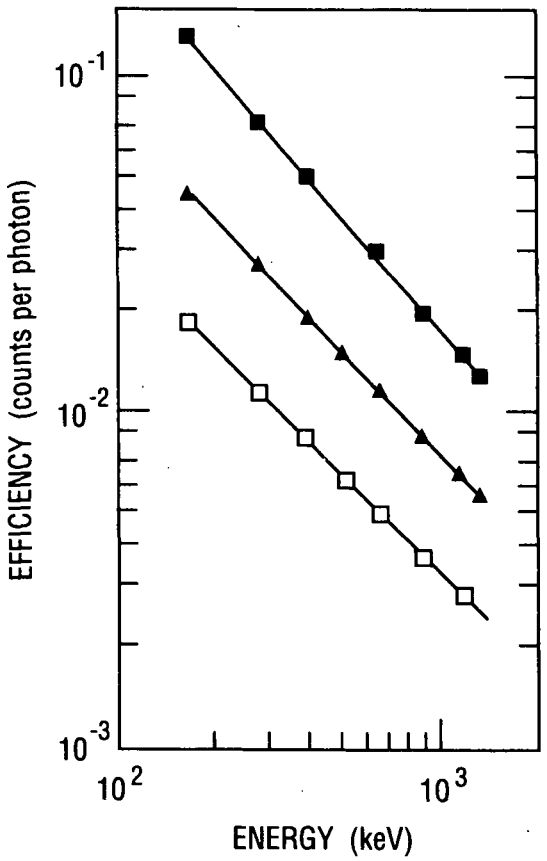

Figure 1. **PGT 6A germanium detector efficiency curves for selected endcap-to-source distances; ■=¼ in. above endcap; ▲=1 in. above endcap; □=2 in. above endcap.**

Next, it was necessary to determine if the physical form of the standard (liquid vs. ground topaz), mesh size of the ground topaz (30 mesh vs. 400 mesh), or the degree of saturation (saturated ground topaz vs. dried ground topaz) affected the efficiency curve. Table 13 and Figure 2 compare the efficiencies for various Amersham multinuclide gamma standards. The liquid standard (dashed line) in Figure 2 should result in the highest efficiency if attenuation made a difference in determining the efficiency of gamma spectroscopy. Both of the mesh standards (dried and saturated) have slightly greater efficiencies than the liquid standard, as the figure shows. However, all standards are within statistical uncertainty of each other. Figure 2 indicates that within the manufacturer's stated measurement error of ±10% for the multinuclide gamma standard, all standards, regardless of their density or physical form, have approximately the same efficiency curve. This result indicates that an efficiency curve derived from a liquid standard of unit density would closely approximate the efficiency in irradiated topaz (ρ=3.5 g/cm) for the energy range 122 to 1836 keV.

Table 13. Comparison of Gamma Spectroscopy Efficiencies Versus Mesh Size and Degree of Saturation

Energy keV	30 mesh Amersham 1-1 saturated topaz	30 mesh Amersham 1-3 saturated topaz	Amersham 1-4 liquid (before move)*	Amersham 1-4 liquid (after move)*	400 mesh Amersham 1-5 saturated topaz	400 mesh Amersham 1-5 dried topaz
88	$1.57\pm.03\times10^{-2}$	$1.34\pm.02\times10^{-2}$	$1.76\pm.02\times10^{-2}$	$1.76\pm.02\times10^{-2}$	$1.81\pm.03\times10^{-2}$	$1.81\pm.02\times10^{-2}$
122	$1.88\pm.03\times10^{-2}$	$1.65\pm.02\times10^{-2}$	$1.97\pm.02\times10^{-2}$	$2.00\pm.02\times10^{-2}$	$2.10\pm.03\times10^{-2}$	$2.14\pm.03\times10^{-2}$
166	$1.64\pm.03\times10^{-2}$	$1.45\pm.03\times10^{-2}$	$1.83\pm.02\times10^{-2}$	$1.81\pm.02\times10^{-2}$	$1.90\pm.04\times10^{-2}$	$1.95\pm.03\times10^{-2}$
279	$1.14\pm.03\times10^{-2}$	$9.59\pm.23\times10^{-3}$	$1.14\pm.02\times10^{-2}$	$1.20\pm.03\times10^{-2}$	$1.18\pm.05\times10^{-2}$	$1.23\pm.04\times10^{-2}$
392	$7.66\pm.11\times10^{-3}$	$7.30\pm.08\times10^{-3}$	$8.42\pm.08\times10^{-3}$	$8.40\pm.08\times10^{-3}$	$8.73\pm.13\times10^{-3}$	$8.55\pm.11\times10^{-3}$
514	$5.62\pm.09\times10^{-3}$	$5.31\pm.07\times10^{-3}$	$6.16\pm.06\times10^{-3}$	$6.09\pm.08\times10^{-3}$	$6.77\pm.13\times10^{-3}$	$6.43\pm.11\times10^{-3}$
662	$4.70\pm.05\times10^{-3}$	$4.36\pm.03\times10^{-3}$	$4.99\pm.03\times10^{-3}$	$5.00\pm.03\times10^{-3}$	$5.37\pm.04\times10^{-3}$	$5.31\pm.04\times10^{-3}$
898	$3.42\pm.04\times10^{-3}$	$3.28\pm.03\times10^{-3}$	$3.71\pm.03\times10^{-3}$	$3.73\pm.03\times10^{-3}$	$3.96\pm.04\times10^{-3}$	$3.86\pm.04\times10^{-3}$
1173	$2.70\pm.03\times10^{-3}$	$2.56\pm.02\times10^{-3}$	$2.85\pm.02\times10^{-3}$	$2.86\pm.02\times10^{-3}$	$2.97\pm.03\times10^{-3}$	$3.08\pm.02\times10^{-3}$
1333	$2.35\pm.03\times10^{-3}$	$2.28\pm.02\times10^{-3}$	$2.52\pm.02\times10^{-3}$	$2.54\pm.02\times10^{-3}$	$2.68\pm.03\times10^{-3}$	$2.70\pm.02\times10^{-3}$
1836	Not determined	Not determined	Not determined	$1.87\pm.02\times10^{-3}$	$1.95\pm.03\times10^{-3}$	$1.93\pm.02\times10^{-3}$

Note: All standards were in glass, screw-top vials with a paraffin seal between the vial and the aluminum screw-on cap. All standards were counted on Princeton Gamma Tech 6A using a similar geometry (source approximately 2" from detector endcap).

* During these studies the gamma-spectroscopy equipment was moved to a different building.

The topaz stones were initially counted for 30 to 60 minutes on a calibrated Ge(Li) detector, in an attempt to account for any short-lived gamma emitters (T 1/2 < 6 days) that might remain two to three days after irradiation. After decay of the short-lived gamma emitters (approximately 1-2 weeks), a longer counting time of 60 to 300 minutes was used to obtain better statistics.

Table 14 lists the isotopes found routinely during short-term (1/2 to 1 hour) gamma spectroscopy analysis or during long-term counts (>1 hour). Also listed are the minimum detectable levels (nCi/g) of nuclides necessary for detecting 50 net counts for all the counting geometries and counting times used in this study. We note that counting geometry 105 was at the greatest source-to-detector distance and required the least analysis time. This geometry was used to assess highly activated topaz shortly after its removal from the HFBR.

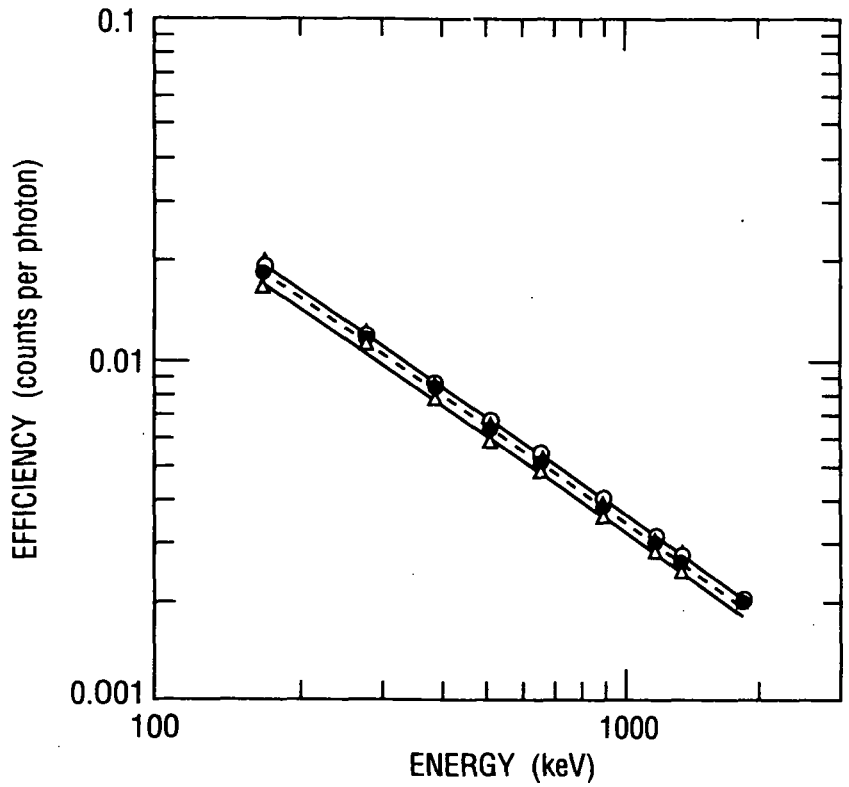

Figure 2. Comparisons of gamma spectroscopy efficiency. All standards counted on Princeton Gamma Tech (6A). Standards contain Amersham multigamma solution. All standards counted at fixed distance. Standards approximately 1 cm^3. Lower solid line - 30 mesh saturated topaz standard; dashed line - liquid standard and 400 mesh dried (saturated initially) topaz standard; upper solid line - 400 mesh saturated topaz standard; dashed line - 400 mesh dried (saturated initially) topaz standard.

Table 14. Minimum Detectable Levels (nCi/g) for a 1g Topaz for Different Counting Geometries[a]

Isotope	Energy keV	Counting Geometry 105[b]	107[c]	109[d]	123[e]	JC[f]	10 CFR 30.70 exempt conc. (nCi/g)
^{182}Ta	1,189.0	1.04	0.41	0.30	0.51	0.35	0.4
^{182}Ta	1,221.0	0.64	0.26	0.19	0.32	0.21	0.4
^{46}Sc	889.0	0.13	0.05	0.04	0.06	0.04	0.4
^{59}Fe	1,099.0	0.28	0.11	0.08	0.14	0.09	0.6
^{59}Fe	1,292.0	0.42	0.16	0.12	0.21	0.14	0.6
^{51}Cr	320.1	0.49	0.20	0.14	0.24	0.17	20.0
^{77}As	239.0	2.27	0.96	0.63	1.11	**	0.8
^{183}Ta	354.0	0.47	0.20	0.13	0.23	**	0.001
^{72}Ga	629.9	0.37	0.15	0.10	0.18	**	0.4
^{54}Mn	834.8	0.12	0.05	0.03	0.06	**	1.0
^{24}Na	1,368.6	0.19	0.08	0.06	0.10	**	2.0
^{124}Sb	602.7	0.09	0.04	0.03	0.05	0.03	0.2

**Not determined.
[a]Liquid Amersham multigamma standard used for efficiency determination.
[b]30 min. live count time; PGT 12; approx. 6" distance from source to endcap.
[c]200 min. live count time; PGT 12; approx. 1" distance from source to endcap.
[d]100 min. live count time; PGT 12 source in contact with endcap.
[e]60 min. live count time; PGT 12; approx. 2" distance from source to endcap.
[f]150 min. live count time; PGT 6A; approx. 1-3/4" distance from source to endcap.

Table 14 shows the minimum detection levels for various counting times and distances. Because three different calibrated Ge(Li) detectors were used, a randomly selected irradiated topaz was counted on all the detectors on a biweekly basis to assure intracomparability of the concentrations of gamma-emitting radionuclides. The relative efficiency of all germanium detectors used in this study, compared to a 3" x 3" NaI(Tl) detector at a 25 cm source-to-detector distance, ranged from 15 to 21 percent at 1,332 keV. Resolution, as measured by full width, half maximum (FWHM) at 1,332 keV, ranged from 1.62 to 2.00 keV. Appendix E gives the detectors' efficiency and resolution. Selected irradiated stones were placed directly on top of the PGT 6A detector and counted for 24 hours to account for nuclides with low-intensity, primary gamma emissions, and/or low NRC exempt concentrations.

The energy (keV) per channel calibration for each detector was automatically calculated using two prominent, widely separated peaks.

The Nuclear Data 6600 peak search package was used to determine the centroid, FWHM, and intensity information for each peak in the marker-defined portion of the data spectrum for the specified analog-to-digit converter group. The algorithm supplied by the Nuclear Data computer was used for peak identification.

A user-supplied sensitivity factor was used in determining whether an area would be accepted as a peak. The product of the sensitivity factor and the square root of the background count had to be greater than the background-subtracted peak area in order to be accepted as a peak. The minimum sensitivity factor used in this study was two.

Gamma energies used in gamma spectroscopy analysis were based on gamma intensity, lack of possible coincidence, and summation peak problems (see Table 15).

The calibration sources used in gamma spectroscopy were prepared by pipetting into glass vials known amounts of National Institute of Standards and Technology (NIST)-traceable Amersham mixed gamma standard QCY.44 (Solution number R8/270/50). The dimensions of the round glass vials were 5.7 cm high x 1.3 cm diameter, and the inside diameter was 1.2 cm. Several gamma-spectroscopy standards were used in the study including:

- NIST-traceable multinuclide liquid standard (approximately 0.5 ml).
- Two 30/80-mesh ground topaz samples, saturated with NIST-traceable liquid standard simulating a medium-sized gem (approximately 0.4 g).
- One 30/80-mesh ground topaz sample, saturated with NIST-traceable liquid standard simulating a large-sized gem (approximately 1.0 g).
- One 400-mesh ground topaz sample, saturated with NIST-traceable liquid standard simulating a medium-sized gem (approximately 0.4 g).
- One 400-mesh ground topaz sample, saturated with NIST-traceable liquid standard and then dried, simulating medium-sized gem (approximately 0.4 g).

Gamma emissions from the standard were given by Amersham in units of gamma rays emitted per sec per gram, and were multiplied by the mass of the standard added to the vial to obtain gamma rays per second. The ground topaz samples were unirradiated. Efficiency E was determined from equation 6:

$$E = \frac{N}{(\gamma s)(g)(1-d)} \qquad (6)$$

where

E	=	efficiency or counts per photon for the energy in question
N	=	net counts rate in photopeak of interest, counts per second
γs	=	photons per second per gram of original standard
g	=	grams of secondary standard
d	=	dead time (fraction)

Table 15. Peak Selection for Gamma Spectroscopy Quantification[a]

Nuclide	Energy, keV (and % rel. intensity)	Coincidence peaks; keV (and % rel. intensity)	Summation peaks; keV (and % rel. intensity)
^{22}Na	1,275 (100%)	^{72}Ga;1,276 (2%)	^{60}Co;1,173 (100%) + ^{182}Ta;100 (14%) ^{214}Bi;1,120 (15%) + ^{182}Ta;152 (7%) ^{46}Sc;1,121 (100%) + ^{182}Ta;152 (7%) ^{182}Ta;1,121 (35%) + ^{182}Ta;152 (7%) ^{58}Co;811 (99%) + ^{125}Sb;463 (10%)
^{24}Na	1,369 (100%)	^{77}Ge;1,368 (3%)	None
^{46}Sc	889 (100%)	None	^{125}Sb;463 (10%) + ^{125}Sb;428 (30%)
	1,121 (100%)	^{182}Ta;1,121 (35%) ^{214}Bi;1,120 (15%)	None
^{54}Mn	835 (100%)	^{72}Ga;834 (96%)	^{182}Ta;68 (41%) + ^{214}Bi;768 (5%) ^{124}Sb;723 (11%) + ^{182}Ta;114 (19%)
^{58}Co	810 (99%)	^{72}Ga;810 (2%)	^{125}Sb;636 (11%) + ^{125}Sb;176 (7%) ^{134}Cs;569 (15%) + ^{214}Pb;242 (8%)
^{60}Co	1,173 (100%)	None	^{214}Bi;609 (46%) + ^{134}Cs;563 (8%) ^{134}Cs;605 (98%) + ^{134}Cs;569 (15%)
	1,332 (100%)	None	^{182}Ta;1231 (12%) + ^{182}Ta;100 (14%) ^{214}Bi;1155 (17%) + ^{125}Sb;176 (7%) ^{124}Sb;723 (11%) + ^{214}Bi;609 (46%)
^{65}Zn	1,116.0 (50.75%)	None	^{134}Cs;605 (98%) + ^{22}Na;511 (180%) ^{134}Cs;605 (98%) + ^{58}Co;511 (30%) ^{124}Sb;603 (96%) + ^{22}Na;511 (180%) ^{124}Sb;603 (96%) + ^{58}Co;511 (30%)

See footnote at end of table

Table 15. Peak Selection for Gamma Spectroscopy Quantification[a] (continued)

Nuclide	Energy, keV (and % rel. intensity)	Coincidence peaks; keV (and % rel. intensity)	Summation peaks; keV (and % rel. intensity)
^{113}Sn	No strong γ lines		
^{124}Sb	1,691 (48%)	None	^{214}Bi;1,120 (15%) + ^{134}Cs;569 (15%) ^{182}Ta;1,121 (35%) + ^{134}Cs;569 (15%) ^{46}Sc;1,121 (100%) + ^{134}Cs;569 (15%) ^{46}Sc;889 (100%) + ^{134}Cs;802 (9%)
^{125}Sb	428 (30%)	None	^{214}Pb;295 (19%) + ^{144}Ce;134 (11%) ^{214}Pb;242 (8%) + ^{226}Ra;186 (3%)
^{134}Cs	605 (30%)	^{125}Sb;601 (18%) ^{124}Sb;603 (96%)	^{22}Na;511 (180%) + ^{144}Ce;92 (5%) ^{58}Co;511 (30%) + ^{144}Ce;92 (5%) ^{125}Sb;428 (30%) + ^{125}Sb;176 (7%)
	796 (86%)	None	^{226}Ra;186 (3%) + ^{214}Bi;609 (46%)
^{144}Ce	134 (11%)	None	None
^{182}Ta	1189 (16%)	None	^{182}Ta;68 (41%) + ^{214}Bi;1,120 (15%) ^{182}Ta;1,121 (35%) + ^{182}Ta;68 (41%) ^{182}Ta;68 (41%) + ^{46}Sc;1,121 (100%) ^{214}Pb;352 (37%) + ^{54}Mn;835 (100%)
	1221 (27%)	None	^{182}Ta;68 (41%) + ^{214}Bi;1,155 (17%) ^{46}Sc;1,121 (100%) + ^{182}Ta;100 (14%) ^{182}Ta;1,121 (35%) + ^{182}Ta;100 (14%) ^{214}Bi;1,120 (15%) + ^{182}Ta;100 (14%) ^{134}Cs;796 (85%) + ^{125}Sb;428 (30%)

[a]Taken from ICRP, 1983.

As defined for gamma spectroscopy analysis, gamma activity was calculated using equation 7. In addition, branching ratios (ratios of multiple disintegrations from the isotope in question) were taken into consideration:

$$a = \frac{N}{(E)(F)(M)(37\text{dps/nCi})(1-d)} \qquad (7)$$

where

a	= nCi/g of sample
N	= net counts per second in photopeak of interest
E	= overall efficiency in counts per photon for the energy in question
F	= fractional intensity (relative) of energy in question, photons/disintegration
M	= mass of topaz, g
d	= dead time fraction; approximately 0 for low energy gamma spectroscopy analysis.
dps	= disintergrations per second
nCi	= 10^{-9} curies

The major gamma-, positron-, and beta-emitting nuclides found in neutron-irradiated topaz. Table 16 gives a more complete listing of gamma- and positron-emission from selected nuclides is given in Table 17. This also includes a listing of naturally occurring nuclides from the uranium series which may interfere with low-level counting of irradiated topaz. Values for gamma-ray energies, relative intensities, gamma MeV/transformation, and beta MeV/transformation for our calibrations and calculations were taken primarily from ICRP Publication #38 (ICRP, 1983).

Analyses conducted on the PGT 12 intrinsic-germanium coaxial detector also were reported in units of parts per million (ppm). After counting the standards, the mean values of the calibration coefficient (counts per minute per milligram per unit concentration) were computed and these mean values were applied to the unknown samples. The gamma spectra were processed by a Brookhaven-generated computer program called INTRAL, coupled to a VAX computer. Final elemental concentrations, in ppm, were obtained from the in-house programs, ELCALC and SAMPCALC.

Ohio Red mineral and dried arsenic and gallium standards were used to monitor neutron fluence. Table 18 gives the concentrations of elemental oxides identified in the Ohio Red standard. Although not an NIST or United States Geological Survey (USGS) primary standard, the Ohio Red standard was compared to NIST and USGS primary standards and its concentration levels were determined by numerous measurements at independent laboratories (Harbottle, 1976). The mass of Ohio Red standards used in the study ranged from 0.0025g to 0.1g. The Ohio Red standard had been fired at about 1,050°C before use.

Table 16. Major Beta Emissions for Nuclides Discussed in this Study

Nuclide	T½[a] day	Mode of decay[b]	Gamma energy, keV[a]	Rel. intensity, %[a]	Max. β energy, keV[c]	Ave. β energy, keV[a]	Rel. intenstiy, %[a]	Means of production
^{22}Na	950	β^+ 90%	511	180	545	215	90	^{19}F (α,n)
		EC 10%	1,275	100				
^{24}Na	0.63	β^-	1,369	100	1,390	554	100	^{23}Na (n,γ)
^{46}Sc	84	β^-	889	100	357	112	100	^{45}Sc (n,γ)
			1,121	100				
^{51}Cr	28	EC	320	10	No β^-s			^{50}Cr (n,γ)
^{54}Mn	313	EC	835	100	No β^-s			^{55}Mn (n,2n)
^{58}Co	71	β^+ 15%	511	30	474	201	15	^{59}Co (n,2n)
		EC 85%	811	99				^{55}Mn (α,n)
^{59}Fe	45	β^-	192	3	273	81	46	^{58}Fe (n,γ)
			1,099	56	466	149	53	
			1,292	44				
^{60}Co	1,924	β^-	1,173	100	318	96	100	^{59}Co (n,γ)
			1.332	100				
^{65}Zn	244	β^+ 1%	511	3	330	143	1.5	^{64}Zn (n,γ)
		EC 99%	1,116	51				
^{72}Ga	0.58	β^-	601	5	650	217	15	^{71}Ga (n,γ)
			630	25	667	224	22	
			786	3	956	342	27	
			834	96	1,048	381	2	
			894	10	1,477	569	9	
			1,051	7	1,927	774	3	
			1,464	4	2,528	1,055	9	
			1,597	4	3,158	1,354	10	
			1,861	5				

See footnotes at end of table

Table 16. Major Beta Emissions for Nuclides Discussed in this Study (continued)

Nuclide	$T_{1/2}$[a] day	Mode of decay[b]	Gamma energy, keV[a]	Rel. intensity, %[a]	Max. β energy, keV[c]	Ave. β energy, keV[a]	Rel. intenstiy, %[a]	Means of production
^{77}As	1.63	β^-	162	0.1	451	141	2	$^{76}Ge\ (n,\gamma)^{77}Ge + ^{77m}Ge \rightarrow \beta^-$ --
			239	1.6	690	232	97	
			250	0.4				
			521	0.6				
^{113}Sn	115	EC	255	1.9	No β^-s			$^{112}Sn\ (n,\gamma)$
^{124}Sb	60	β^-	603	96	212	59	9	$^{123}Sb\ (n,\gamma)$
			646	7	612	194	52	
			723	11	867	292	4	
			1,691	48	1,580	594	5	
					2,303	919	23	
^{125}Sb	1011	β^-	176	7	610	216	14	$^{124}Sn\ (n,\gamma)$
			428	30				
			463	10				
			601	18				
			607	5				
			636	11				
^{134}Cs	753	β^-	563	8	89	23	27	$^{133}Cs\ (n,\gamma)$
		EC	569	15	658	210	70	
			605	98				
			796	85				
			802	9				
			1,365	3				
^{144}Ce	284	β^-	134	11	310	49	20	fission
						90	76	

See footnotes at end of table

Table 16. Major Beta Emissions for Nuclides Discussed in this Study (continued)

Nuclide	T½[a] day	Mode of decay[b]	Gamma energy, keV[a]	Rel. intensity, %[a]	Max. β energy, keV[c]	Ave. β energy, keV[a]	Rel. intenstiy, %[a]	Means of production
^{182}Ta	115	β^-	68	41	258	71	29	^{181}Ta (n,γ)
			100	14	437	129	20	
			152	7	522	157	40	
			179	3		181	5	
			222	8				
			229	4				
			264	4				
			1,121	35				
			1,189	16				
			1,221	27				
			1,231	12				
^{183}Ta	5	β^-	99	7	620[d]	190	92	^{182}Ta (n,γ)
			108	11				^{183}W (n,p)
			160	3				
			161	9				
			162	5				
			210	5				
			244	9				
			246	27				
			292	4				
			313	4				
			354	11				
^{198}Au	3	β^-	412	96	961	315	99	^{197}Au (n,γ)

[a]Taken from ICRP, 1983. Values rounded to nearest whole number.
[b]Taken from ICRP, 1983 and Bureau of Radiological Health, 1970. Mode of decay: β+=positron, EC=electron capture, β-=beta
[c]Taken from NCRP, 1978b. Values rounded to nearest whole number.
[d]Taken from Bureau of Radiological Health, 1970.

Table 18. Concentration of Oxides in the Ohio Red Standard

Elemental Oxide	Derived From Comparison to USGS Six Rock Standards, ppm	Derived From Comparison to Kings College, London Standard, ppm*	Used in this Study, ppm
Fe_2O_3	75,900 ± 2,500	83,700 ± 800	75,857.80
Na_2O	1,840 ± 70	1,930 ± 100	1,840.77
K_2O	41,100 ± 2,100	40,300 ± 400	41,114.90
Rb_2O	191 ± 18	231	190.98
Cs_2O	10.81 ± 0.77		10.81
BaO	785 ± 57	756 ± 10	785.20
CoO	25.36 ± 1	24.54 ± 1	25.35
ZnO	120 ± 8	118 ± 7	120.00
Cr_2O_3	133 ± 7	119 ± 9	133.00
Sc_2O_3	30.71 ± 1.3	(27.6)	30.69
La_2O_3	58.6 ± 2.2	55.4	58.60
CeO_2	135 ± 5	120 ± 4	136.10
Eu_2O_3	2.04 ± 0.11	(1.53)	2.04
Lu_2O_3	0.87 ± 0.10		0.87
Sm_2O_3	9.62 ± 0.54	(7.41)	9.62
MnO	320 ± 13	(326)	320.00
HfO_2	7.40 ± 0.38		7.40
ThO_2	17.65 ± 0.63		17.66
Ta_2O_5	2.18 ± 0.63		2.18

*Errors based on standard deviation of four independent determinations.
Note: Values in ( ) are approximate.

All liquid standards, i.e., Ga and Ge, were heat-sealed in small quartz vials before irradiation. The vials were made from ultra-high-purity quartz tubing obtained from a West German manufacturer and having an inside diameter of 3 mm, an outside diameter of 4 mm, and a length of approximately 20 mm. To avoid contamination, rubber or cloth fingercots were worn when handling these vials. The measured versus stated fluence rates were computed and compared.

The fluence rate was calculated using equation 8 (Bureau of Radiological Health, 1970).

$$dps = \frac{(\delta)(f)(m)(1-e^{-\lambda t})(e^{-\lambda \phi})(6.02 \times 10^{23})(a)}{A} \qquad (8)$$

where

dps	=	disintegrations per second at time of counting
ϕ	=	time between end of bombardment and counting
δ	=	activation cross section, cm^2/(atom neutron)
f	=	fluence rate, neutrons/(cm^{-2} sec)
t	=	duration of exposure to neutron fluence rate
e	=	base of natural log (2.718)
λ	=	radioactive decay constant
m	=	mass of standard, g
A	=	atomic weight of parent
a	=	fractional abundance of parent

Note: ϕ, t, and $1/\lambda$ have the same units, e.g. s, min, or h.

The data on neutron capture cross-section were obtained from BNL-NCS-31451 and McLane et al., (1988).

Previous studies indicated a lack of agreement between the calculated and measured fluences for chromium, hafnium, and lutetium (Yeh and Harbottle, 1986). Because of this variance, these nuclides, found in the Ohio Red standards, were not used to calculate neutron fluence rate.

A well-type NaI detector (2" thick by 1.75" diameter) also was used to detect gamma activity in irradiated topaz (Figure 3). The NaI detector was housed in a sliding-top steel shield (6" thick) in the counting room, and the counting time was 300 sec. Energy and efficiency calibrations were checked before each use with NIST-traceable Amersham multigamma standards and tertiary ^{46}Sc, ^{59}Fe, ^{54}Mn, and ^{182}Ta standards. The end channel ($\sim$1400 keV) of the region of interest was set to include the 1332 keV ^{60}Co peak. The first counting channel ($\sim$40 keV) of the region of interest included the 67 keV peak from ^{182}Ta, and the 122 keV peak ($\sim$100 keV) from the ^{57}Co found in the Amersham standard. The amplifier's coarse and fine gain were optimized using an oscilloscope. The lower channel in the region of interest was varied with several nuclides to determine the best signal-to-noise ratio.

3.3.2 GM Detectors

The radiation from topaz was measured with an unshielded GM meter (Ludlum Model 12 with 44-9 thin window probe) and a shielded GM (Eberline HP-210) pancake detector. The

irradiated topaz was centered directly on, or very close to, the screen protecting the thin window (1.4 mg cm^{-2} to 2.0 mg cm^{-2}) for both detectors of the GM probe.

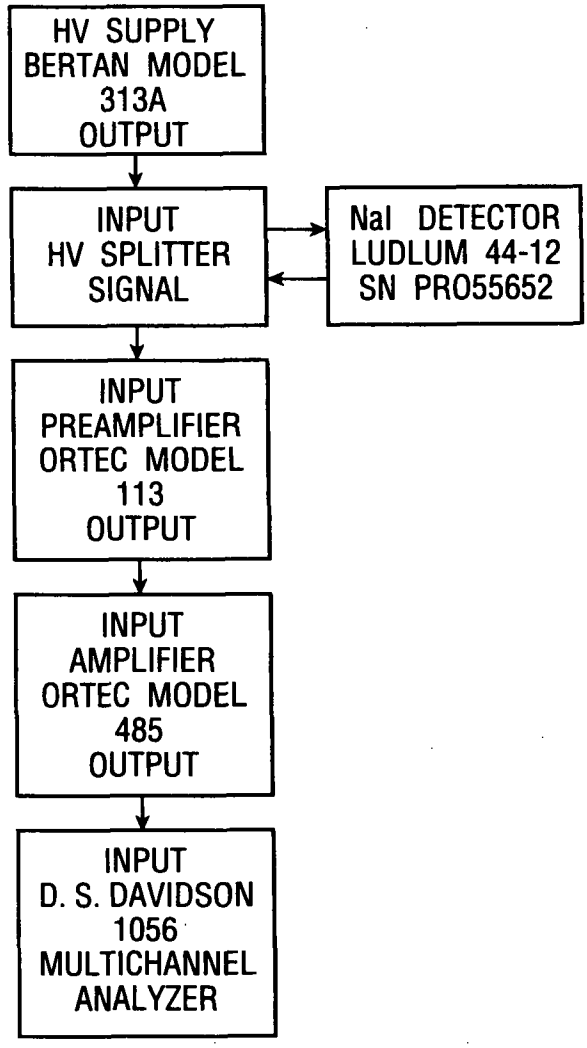

Figure 3. Counting setup for the NaI(Tl) detector

A determination of efficiency was made for each GM detector; in practice, these were always within 25% of the manufacturers' stated value. The efficiency was periodically checked and compared to previous measurements to assure that the response of the detector remained constant.

Studies of beta absorption were conducted using calibrated 99.99 percent aluminum filtration sets prepared by Brookhaven's Chemistry Department. Shielded GM analysis was conducted on topaz at a minimum of three weeks after irradiation to allow the short-lived byproducts to decay. The GM probe was an Eberline Model HP-210L (1.4 mg cm^{-2} to 2.0 mg cm^{-2} mylar window thickness) with lead shield. The topaz was placed on a plastic template with the table facet facing the GM tube; the distance from the top of the plastic template to the bottom of the detector was 5.5" mm. The plastic template was placed in the depression of the aluminum sample tray. The aluminum filters, topaz, and plastic template were held in place during counting by a sample holder supplied by Ludlum (Model 180-2). A sample drawer (with a 47-mm diameter depression) could be positioned 1/8" to 2" from the detector's face. The sample holder was modified to decrease the source-to-detector distance as much as possible. The decrease in beta counts due to source-to-detector distance and the density of air at standard temperature and pressure (STP) was taken into consideration. A value of 1.295 mg cm^{-2} is given for dry air at STP and approximately 1.2 mg cm^{-2} cm^{-1} path length for the usual laboratory conditions (ICRU, 1972 and Overman and Clark, 1960). All filters were placed as close to the detector as possible to avoid scattering. An Eberline "Smart" radiation monitor, Model SRM-200, with data logging capability, was connected to the GM probe. Dead-time corrections became important at rates of 5,000 cpm (ORTEC, 1976).

The probe was surrounded by 2" x 4" x 8" lead blocks, which were surveyed for gross activity with a GM instrument (Ludlum Model 3 with 44-9 pancake probe). The blocks were surveyed for removable contamination using wipes coated with a liquid scintillation detector. No radiation above background levels was detected.

The filters that were used ranged from 1.7 mg cm^{-2} density thickness to 798.2 mg cm^{-2}. In making absorption measurements, the filters were interposed, one at a time, until the counting rate dropped to background levels of radiation, or until it became constant, indicating the presence of gamma emitters.

Simulated topaz stones were used to test the sensitivity of the shielded GM counting setup. Plastic disks 1/4" thick, with 9/32" or 13/32" diameter holes drilled almost completely through the plastic, were used to contain simulated topaz stones. The holes were filled with 30/80 mesh topaz (approximate density 2 g cm^{-3}) to the top surface of the disk. Standardized solutions of ^{182}Ta, ^{46}Sc, ^{59}Fe, ^{54}Mn, ^{36}Cl, and ^{14}C were added to the ground topaz and the activity per gram for each disk was calculated. The readily obtainable ^{14}C was used to simulate ^{35}S because of similar maximum and average beta energies. These isotopes were chosen because they represented the majority of activity found or suspected in irradiated topaz. All disks and standardized solutions were evaporated (30°C to 50°C for 12 hours) before counting to minimize beta attenuation. Ge(Li) analysis was used to account for any residual activity remaining on the interior surface of the glass vials used in preparing the standards. To minimize any possible absorption on the side of the vial, a nonradioactive carrier was added to the vial before the radioactive material was introduced. After the activity of a known mass of standard was determined by gamma spectroscopy, the material was removed to manufacture tertiary standards.

"Infinitely" thin beta sources were used to determine the counting efficiencies of the shielded GM detector and 0.01"-thick plastic scintillator. The sources were prepared by pipetting a known mass of NIST- traceable solution onto an aluminum planchet and slowly drying the sources under a heat lamp. Sources of 1/4" to 1/2" diameter were prepared. The aluminum planchet was placed on the top of the 6 mm plastic disk used to count the topaz stones with the SRM 200 GM detector.

Ground topaz was prepared by breaking up the rough Nigerian topaz and grinding the material in a mortar to granular size. The U.S.A. Standard Testing Sieves, manufactured by W.S. Tyler, Inc. (Mentor, OH.44060), and meeting ASTM E-11 specifications, were used to segregate the topaz into various sizes. Mesh sizes (with square openings) correspond to metric or English units, i.e., a 400 mesh is equivalent to a 38- micrometer or 0.0015-inch opening, and 30 mesh is equivalent to a 600-micrometer or 0.0234-inch opening.

3.3.3 Quantification of Beta Emitters

It is important to identify and quantify all beta emitters because of the possibility of producing nuclides that emit only beta radiation and the role that these beta emitters play in radiation exposure of the skin (see Results). Table 19 lists potential pure beta emitters with an atomic number ≤ 100. Considering the isotopes listed, ^{32}P and ^{35}S would be important in considering skin irradiation from topaz because of the combination of maximum beta energy, half-life, means of production, and the abundance of parent, and exempt concentration limits (0.2 and 0.6 nCi/g, respectively).

Methods for determining concentrations of the precursors for beta emitting isotopes ^{35}S, ^{32}P and ^{36}Cl are listed in Table 20. The beta scintillator and gas-flow counter offers the greatest possibility for beta detection and discrimination at nCi/g levels. Gas-flow proportional counters have an overall efficiency of 30 to 50 percent for the detection of alpha (^{210}Po) and beta (^{14}C) particles according to various manufacturers. Plastic scintillators have an overall efficiency of about 10 percent for ^{14}C, and 85 percent for ^{90}Sr (0.01" thick x 1.5" diameter scintillator with 0.8 mg cm^{-2} aluminized mylar window).

3.3.3.1 Plastic Scintillation Detector

A 1-inch diameter, 0.01-inch thick plastic scintillator (Bicron B1) attached to an Eberline SRM 200 monitor was used to count beta activity from irradiated topaz. The plastic scintillators were affixed to the PM tube with optical coupling grease. A mica screw endcap covered the end of the PM tube to prevent light transmission. The high voltage plateau was determined by using NEN beta reference sources, i.e., ^{14}C, ^{36}Cl, ^{90}Sr, and Amersham gamma reference sources, i.e., ^{241}Am and ^{54}Mn. The latter two isotopes were chosen because they have no beta emissions. Irradiated topaz was counted with, and without the plastic scintillator on the PM tube after optimizing the amplifier and the discriminator.

Typical setup values were as follows: dead time = 7.35×10^{-5} sec, HV = 737 volts for the 0.01" scintillator, and 752 volts for the PM tube without a scintillator. The plastic scintillator and sample holder were surrounded by 2" lead bricks. The scintillator was held in position above the sample holder by tight-fitting styrofoam. The probe was positioned so that the gems were separated from the mica endcap by only a few millimeters. A GM counting geometry and spacing of 11.5 mm from the depression in the sample tray holder to the endcap was maintained.

Table 19. Pure Beta Emitters with A ≤ 100

Nuclide	T½[a]	Max. β energy, keV[b]	Relative intensity[b]	Means of production	% abundance of parent[c]
^{3}H	12 yr	19	100	*	7
^{14}C	5,730 yr	156 (ave = 50)	100	*	fraction of a %
^{32}P	14 day	1,710 (ave = 695)	100	^{31}P (n,γ) ^{32}S (n,p) ^{35}Cl (n,α)	100 95 76
^{35}S	87 day	167 (ave = 49)	100	^{34}S (n,γ) ^{35}Cl (n,p)	4 76
^{33}P	25 day	249	100	^{33}S (n,p)	1
^{36}Cl	3 x 10^{5} yr	714	98	^{35}Cl (n,γ)	76
^{45}Ca	163 day	257	100	^{44}Ca (n,γ)	2
^{55}Cr	4 min	2,590	[d]	^{54}Cr (n,γ)	2
^{63}Co	52 sec	3,600	[d]	^{64}Ni (n,γ)	1
^{63}Ni	96 yr	66	100	^{62}Ni (n,γ)	4
^{69}Zn	57 min	905	100	^{68}Zn (n,γ)	19
^{90}Y	64 hr	2,284	100	^{89}Y (n,γ)	100
^{99}Tc	2 x 10^{5} yr	292	100	^{98}Mo (n,γ)	24

*Naturally occurring.
[a]Taken from ICRP, 1983. Values rounded to the nearest whole number.
[b]Taken from NCRP, 1978b. Values rounded to the nearest whole number.
[c]Taken from Bureau of Radiological Health, 1970. Values rounded to the nearest whole number.
[d]Not listed in NRCP, 1978b.

Table 20. Some Methods for Quantifying S, P, and Cl

Instrumentation	Comments
Proton Induced X-ray Emission (PIXE)	Lower limit of detection (LLD) determined in this study. Parts per million sensitivity level could be increased by the use of large Ge(Li) detectors.
X-ray fluorescence	Resolution of 8 to 11 eV. Good S/N ratio except at low energies. S, P, and Cl would be expected at low energies (<8 KeV). Reviewed in this study.
Scanning Electron Microscope (SEM)	LLD about 100 to 1,000 ppm.
Plasma emission techniques	Not sensitive to ppm levels
Neutron activation	Good for gamma or positron emitters
Wet chemistry	Not recommended for concentrations less than a few ppm.
Beta scintillator (liquid and solid)	Reviewed in this study.
Gas flow counter	Reviewed in this study.

When the bare PM tube counting was conducted, the irradiated gems were placed on the PM tube and the endcap screwed on the PM tube. Thus, the endcap provided an effective light barrier. The end cap was checked for imperfections before use.

Plastic scintillators consist of fluorescent organic compounds dissolved in a solidified polymer matrix. Aromatic compounds, such as PPO and POPOP, are added to increase the scintillation efficiency. A general purpose plastic scintillator should have the following characteristics:

- excellent transparency to its own scintillation light for good light collection,
- high scintillation efficiency (the ability to convert absorbed radiation to detectable light),
- highly polished surfaces,
- wavelength of scintillation light and a refractive index compatible with common photomultiplier tubes.

The plastic scintillator used at BNL fluoresced in the blue region of the visible spectrum and matched well with the PM tube supplied by Bicron.

3.3.3.2 Gas-Flow Proportional Counter

A windowless gas-flow proportional counter (manufactured by Eberline) was used to quantify the activity from charged particles emitted from irradiated topaz. The proportional counters were operated in the voltage region where the multiplication (10 to 1,000) results in a millivolt pulse. The pulse size depended on the type of radiation being measured, i.e., primary ionization. The sample-to-wire distance was 3/8". A minimum purge time of 30 seconds with P-10 gas (90% argon, 10% methane) was used before each count. A Canberra counter/timer (Model 1776) and high voltage supply (Model 3002) were used in conjunction with the counter. Varying thicknesses of calibrated aluminum absorbers surrounded by a plastic rim were interposed between the gem and the wire element of the counter. The two-inch diameter E-3A absorbers (S/N 406) were supplied by Tracerlab.

3.3.3.3 Liquid Scintillation Detector

A Searle Analytic 92 liquid scintillation counter (Model 6892) was used to distinguish between the different types of radiation emitted from irradiated topaz, i.e., beta versus gamma radiation. Unquenched ^{14}C, ^{3}H, and ^{32}P standards were used to generate pulse-height curves. Typical efficiencies expected for unquenched liquid standards were 60 percent for ^{3}H, and 95 percent for ^{14}C and ^{32}P. Standards and topaz stones were counted in 5 ml of Beckman Ready-Solv HP scintillation cocktail (Lot #5702241). White plastic screw-top vials were used. For comparison, 22-mm low-background glass (zero ^{40}K content) and minimal radium (^{226}Ra) content vials with hard, white plastic screw-caps lined with metal foil were used in liquid scintillation counting.

3.3.4 ZnS Detector

A shielded 2"-diameter ZnS detector prepared at Brookhaven was used to determine alpha activity in pulverized, unirradiated samples of topaz (<200 mesh). The sample drawer containing a 2" aluminum planchet with a thinly dispersed layer of sample was placed only 3 to 4 mm from the detector face. An ^{241}Am source (NIST-traceable) was used to determine the detector's efficiency before, and after counting was completed. A typical manufacturer's ZnS detector (0.8 mg cm^{-2} aluminized mylar window, 1-1/2" diameter) has an overall efficiency of about 60 percent for ^{239}Pu. A preamplifier and amplifier were used to shape the pulse output of the detector.

3.4 X-Ray Fluorescence

X-ray fluorescence (XRF) was used to identify elements found in topaz. Absorption of x-rays results in the excitation of electrons in the inner shells surrounding the atomic nucleus. The atoms then remit their own characteristic x-rays that can be identified and counted. A Ge(Li) detector was used for counting. The energy of x-ray fluorescence emissions varies characteristically from element to element on the periodic table (Bureau of Radiological Health, 1970).

3.5 PIXE

Accelerated protons, either focused or unfocused, were used for trace-element analysis of sulfur, chlorine, and phosphorus. The common term for this procedure is PIXE (Proton Induced X-ray Emission). This system was coupled to a 3-mm deep by 30 mm^2 area Si(Li) detector, which has considerably better sensitivity than conventional x-ray fluorescence because of a lower background. Simultaneous detection of proton-induced x-rays and gamma rays enables rapid determination of both major and trace elements in thin, homogeneous samples. This method was successfully used to examine the composition of six USGS rock standards (Carlsson and Akselsson, 1981). The atomic numbers of elements that can be detected by this technique include Z = 3, 5, 9, 11-13 from gamma ray analysis, and Z = 13-92 from x-ray analysis. We used a proton energy of 2.5 MeV during the approximately 15-minute irradiations.

Topaz samples used in PIXE analysis were ground to a 400-mesh consistency and mixed with conductive graphite powder (Fisher Scientific). This mixture was pressed to a pellet of 5- to 6-mm diameter by 1- to 2-mm thickness with a 3,000 psi hydraulic press. The powdered topaz accounted for 25 to 50 percent of the volume of the pellet. Several representative samples of nonirradiated topaz were selected from each topaz lot listed in Table 9 for PIXE analysis. The system was calibrated with a NIST standard containing sulfur, chlorine, and phosphorus (NBS SRM 89).

3.6 Autoradiography

Autoradiographs were made of topaz approaching 10 CFR 30.70 exempt concentration limits to test this method as a potential screening technique for irradiated gemstones. Kodak X-OMAT AR film was chosen because of its high sensitivity for beta and low-energy gamma emissions. The film was double-coated on a blue base, and could be processed manually or automatically. We used a 7-1/2 watt Kodak GBX-2 safelight filter (red) recommended by Kodak.

The film packet was kept in a drawer in the darkroom (with low relative humidity and at room temperature). The 8-1/2" x 11" film was withdrawn slowly from its storage box to avoid static discharge. Radiation sources were not stored in the darkroom nor in the surrounding area. The table facet of the topaz was placed in direct contact with the film. Although the use of fluorographic and intensifying screens, -70 °C exposure conditions, and other techniques could enhance the sensitivity of the film by at least one magnitude (Swanstrom and Slank, 1978), they were not used to better approximate the conditions more frequently anticipated in the field. All films were manually processed in the following way:

(a) the film was placed in Kodak GBX developer and replenisher for five minutes at 20 °C. We did not allow the film to adhere to the sides of the developing tank;

(b) the film was removed and rinsed in 16 °C to 22 °C tap water for about 15 seconds;

(c) the film was placed in the Kodak X-ray fixer for 10 minutes at 20 °C;

(d) the film was removed and rinsed in tap water for approximately 15 to 30 seconds;

(e) the film was allowed to dry in the darkroom.

The developer, fixer, and procedures used in this study follow those recommended by Kodak (Hahn, 1983). Variations in film density as great as 25 percent can be expected for similar radiation exposures. The film was calibrated with NEN ^{14}C and ^{210}Bi reference sources to account for this difference.

Spot densities were read manually with a Macbeth TD502 optical densitometer. This unit was calibrated before each use with a Macbeth opal-glass density strip, ranging from 0 optical density to 4.98.

3.7 TLD Measurement

Lithium fluoride (LiF) thermoluminescent dosimeters (TLDs), supplied by Harshaw, were used to directly determine exposure from the irradiated topaz. The dimensions of the chips were 1/8" x 1/8" x 0.035". They were placed on the table facet (largest facet) of topaz, with a table-facet surface area as large as or larger than the surface area of the chip. Harshaw LiF TLD-700 chips were chosen for the following reasons:

- they have a dose-rate independence to more than 10 R/second; they are energy-independent for photons of approximately 10 keV to several MeV, with only a slight overresponse between 15 keV and 200 keV (maximum overresponse factor occurs at 30 keV and is about equal to 1.25 ;
- they are approximately tissue equivalent;
- they can measure exposures from mR to 10^5 R range;
- they show a long-term retention of the response (only a 5 percent loss at room temperature for one year);
- the reproducibility of the response for any single chip is two to five percent;
- the spread of sensitivity within a batch of chips is small (±15 percent for three sigma deviation, or ±10 percent for one sigma deviation).

The gamma-ray dose-rate independence and gamma-ray energy-response were not determined in this study because they are well known.

The chips were initially annealed at 400°C for one hour, cooled for ten minutes, and then heated to 80°C for 24 hours to remove all trapped carrier sites. The TLDs were pre-irradiated at Brookhaven's Calibration Facility, using a ^{60}Co gamma source. A total dose of 200 mR was delivered to the chips at one meter using a decay-corrected dose rate of 1.52966 R/hr. Only chips falling within one standard deviation of the mean (n = 40) were used. TLD chips were read out on a Harshaw Series 2000 reader. The following checks were performed (tolerance levels are given in parenthesis) before the readout:

- 90-sec upper temperature setting (220°C for Harshaw LiF TLD-700);
- zero adjustment;
- charge collected in 30 seconds due to dark current (should be less than 0.25 nC);
- 10-sec reference light-source reading (should be 60.0 ± 0.5 nC).

All chips underwent a 30-second, 220 °C readout cycle. This cycle reached 100 °C within three seconds, and then increased at a constant rate until 220 °C. The temperature was allowed to return to 50 °C (maximum) before the next readout. After all the chips had been read out, readings of the dark current and reference light source were taken again. Annealing was conducted immediately before the chips were to be used again. Although post-irradiation, pre-evaluation annealing was recommended (Harshaw/Filtrol, 1988), we did not do so because of the short exposure time (approximately two weeks) and small amount of fading from the LiF TLD-700 chips.

3.8 Statistical Methods

Various statistical methods were used in this study. The peak area error associated with peaks identified by gamma spectroscopy analysis was determined as follows (Nuclear Data, Inc., 1981):

$$\% \text{ peak error} = \frac{\sqrt{\text{net area} + 2 \text{ bkg}}}{\text{net area}} \times 100 \qquad (9)$$

where the net area and background (bkg) were determined by a Nuclear Data software package.

Gaussian (bell shaped) peaks were assumed in the analysis. The peak error took into account the following sources of error, including the magnitude of the error as stated by the American National Standards Institute (ANSI, 1978):

(a) preparation and calibration of the standard source (±3%);
(b) reproducibility of net energy-peak counts (±2%);
(c) determination of efficiency of calibration (±3%);
(d) accuracy of live-time determination and pile-up corrections (±2%).

To minimize these errors, the following procedures were followed whenever possible:

- to minimize (a), intercomparisons of multiple standards were conducted;
- to minimize (c), calibration was done by using a power function to fit the data points on a semi-log scale. This was typically from 150 keV to 1800 keV for detectors used in this study.
- to minimize (d), automatic live-time corrections, we used a pulser and a sample-to-detector distance, which minimized dead-time corrections to $<<1\%$.

Confidence intervals associated with multiple standards for individual isotopes on GM, NaI, and scintillator (plastic) detectors were determined by the following equation:

$$\text{Mean Value} \pm \tau \sqrt{s^2/n} \qquad (10)$$

where τ is the critical value of the t distribution for a $(1-\alpha/2) \times 100$ confidence interval and

$$\text{Standard Error of the estimator} = \sqrt{s^2/n} \tag{11}$$

where

s^2 = the sample variance
= $\sum (x_i - \bar{x})^2/(n-1)$
x_i = individual measurement
$\bar{x}$ = the mean of all measurements
n = the total number of measurements

The uncertainty in the measurement of individual standards and individual irradiated topaz, when analyzed on a GM, NaI, or scintillator (plastic or liquid) counter, was determined by the following equation:

$$N \pm \sqrt{G + b} \tag{12}$$

where

N = net count rate, counts per time interval
G = gross count rate, counts per time interval
b = background count rate, counts per time interval
t = counting period

Note: N, G, b, and t have the same units of time (i.e., seconds or minutes).

Statistical assumptions in these calculations include the following:

- the radioactive half-life is long compared to the counting time of the detector;
- losses due to the detector's resolving time have been corrected or were small;
- statistical variations due to sample preparation or detector geometry were not considered, but were assumed to be smaller than variations in counting.

4. RESULTS

Topaz can be activated by three types of neutron absorption processes:

(1) thermal absorption: occurs with low or thermal energy neutrons (E<0.5 eV). Thermal neutrons have a most probable energy of 0.025 eV. This value corresponds to neutrons having a velocity of 2,200 m/s at room temperature.

(2) resonance absorption: occurs with intermediate (or epithermal) neutron energies (0.5 eV<E<10 keV).

(3) threshold activation: occurs with neutrons of intermediate and high energies (10 keV<E<20 MeV). Neutrons from fission are initially emitted with energies up to 14 MeV and have an average energy of about 2 MeV.

Slow or thermal neutron reactions are usually of the type A (n,γ) B, where B usually decays by beta emission followed by gamma radiation.

There are three types of predominate reactions for fast neutrons:

- A (n,p) B;
- A (n,α) B;
- A (n,2n) B.

Neutron-proton reactions generally have neutron thresholds in the range of 1 to 3 MeV. Thresholds for (n,α) and (n,2n) reactions are usually in the range of 10 to 20 MeV.

Table 21 gives the cross-sections of thermal neutron activation for precursors of nuclides found in this or other studies of neutron-irradiated topaz. When there was no information on individual nuclides, the natural form of the element was listed.

Table 22 lists common interferences with neutron activation that should be considered if the amount of the parent (precursor) nuclide is to be determined.

Ohio Red mineral standards were placed, at a minimum, at the top and bottom of each topaz irradiation packet to assure that neutron irradiation would be uniform, so that neutron activation could be compared. The packets were arranged so that the topaz and standards did not overlap, thus avoiding a "shadow shielding" effect. Results conducted at thermal neutron fluences from 3×10^{16} to 9.21×10^{18} thermal neutrons/cm^2 in all HFBR irradiation ports showed that the axial and radial variations were less than ±5 percent. Appendix G lists the count rate of the photopeak of various nuclides found in Ohio Red standards for several HFBR topaz irradiations.

4.1 BNL Neutron Irradiation

Examination of all neutron-irradiated blue topaz revealed that a fast neutron fluence of about 1×10^{18} neutron/cm^2 was necessary to cause a color change. The fluence rate ranged from 7.5×10^{11} to 3×10^{14} fast neutrons/(cm^2 sec) with irradiation times of 405 hr and 0.93 hr, respectively. Table 23 gives the results of gamma-induced activity (nCi/g of gem) from neutron bombardment at BNL.

Table 21. Cross-Sections (Barns) of Thermal Neutron Activation Precursors of Radionuclides Suspected to be Found in Topaz[a]

Nuclide	Ref: Bureau of Radiological Health, 1970	Ref: BNL-NCS-31451 1982	Ref: McLane, et.al, 1988
^{23}Na	0.53	0.53	
Si(nat)		0.16	
^{31}P	0.19	0.20	
S(nat)		0.52	
Cl(nat)	33	33	
^{45}Sc	24		28
Cr(nat)	3.1	3.1	
^{50}Cr			15
Fe(nat)	2.5	2.6	
^{59}Co	37	37	
Ni(nat)	4.8	4.6	
Cu(nat)	3.8	3.8	
Zn(nat)	1.1		1.1
Ga(nat)		3.0	
Cd(nat)	2,450	2,446	
Sb	5.7		
^{181}Ta	21	21	
^{182}Ta		8,253	
^{186}W		38	
^{197}Au	99	99	

[a]Cross-section rounded to two significant figures.

Table 22. Interferences with Neutron Activation[a]

Reaction	Abundance of parent, %	Thermal neutron activation cross-section, barns	Interference(s) and comments
$^{23}Na(n,2n)^{22}Na$	100.0		Occurs between 15 to 120 MeV
$^{23}Na(n,\gamma)^{24}Na$	100.0	0.53	$^{24}Mg(n,p)^{24}Na$ $^{27}Al(n,\alpha)^{24}Na$
$^{31}P(n,\gamma)^{32}P$	100.0	0.20	$^{30}Si(n,\gamma)^{31}Si$--β^---$^{31}P(n,\gamma)^{32)}P$* $^{32}S(n,p)^{32}P$ $^{35}Cl(n,\alpha)^{32}P$ $^{75}As(n,\alpha)^{72}Ga$ $^{70}Zn(n,\gamma)^{71,71m}Zn$--$\beta^-$-- $^{71}Ga(n,\gamma)^{72}Ga$ $^{70}Ge(n,\gamma)^{71}Ge$--β^---$^{71}Ga(n,\gamma)^{72}Ga$
$^{34}S(n,\gamma)^{35}S$	4.2	0.49	$^{35}Cl(n,p)^{35}S$ $^{38}Ar(n,\alpha)^{35}S$
$^{45}Sc(n,\gamma)^{46}ScTa$	100.0	24	$^{46}Ti(n,p)^{46}Sc$
$^{50}CR(n,\gamma)^{51}Cr$	4.3	15	$^{54}Fe(n,\alpha)^{51}Cr$
$^{58}Fe(n,\gamma)^{59}Fe$	0.3	2.6	$^{59}Co(n,p)^{59}Fe$ $^{62}Ni(n,\alpha)^{59}Fe$
$^{55}Mn(n,2n)^{54}Mn$	100.0	Not applicable	Occurs at neutron energy >10 MeV $^{54}Fe(n,p)^{54}Mn$
$^{71}Ga(n,\gamma)^{72}Ga$	39.8	3.0	$^{72}Ge(n,p)^{72}Ga$ $^{75}As(n,\alpha)^{72}Ga$ $^{70}Zn(n,\gamma)^{71,71m}Zn$--$\beta^-$-- $^{71}Ga(n,\gamma)^{72}Ga$ $^{70}Ge(n,\gamma)^{71}Ge$--β^---$^{71}Ga(n,\gamma)^{72}Ga$

See footnotes at end of table

Table 22. Interferences with Neutron Activation[a] (continued)

Reaction	Abundance of parent, %	Thermal neutron activation cross-section, barns	Interference(s) and comments
$^{76}Ge(n,\gamma)^{77}Ge$	7.7	0.10	$^{76}Ge(n,\gamma)^{77}Ge + ^{77m}Ge \text{--}\beta^{-}\text{--} ^{77}As$
$^{181}Ta(n,\gamma)^{182}Ta$	100.0	21.00	$^{182}W(n,p)^{182}Ta$ $^{180}Hf(n,\gamma)^{181}Hf \text{--}\beta^{-}\text{--} ^{181}Ta(n,\gamma)^{182}Ta$
$^{182}Ta(n,\gamma^{183}Ta$			$^{183}W(n,p)^{183}Ta$ Threshold at 288 keV

[a]Adapted from Koch, 1960.
*Limiting irradiation time to 1 week or less minimizes this reaction.

Table 23. nCi/g of Gem Measured at 0 Days Following Irradiation at BNL's HFBR[a]

1. Gem #	2. ^{46}Sc	3. ^{59}Fe	4. ^{182}Ta	5. ^{182}Ta	6. ^{51}Cr	7. ^{183}Ta	8. ^{183}Ta	9. ^{77}As ($x10^3$)	10. ^{72}Ga ($x10^3$)	11. ^{24}Na ($x10^3$)
1	5.3	4.7								
2	33.7	6.8	1.6(0.3)	0.9(0.2)						
3	22.0	2.6								
4	3.1	4.6	0.7(0.2)	1.3(0.2)						
5	9.6	3.3								
6	25.8	5.0								
7	3.1	3.7	0.8(0.2)	0.5(0.1)						
8	17.1	4.6	1.0(0.2)	1.2(0.2)						
9	35.1	4.0(0.5)								
10	5.2	1.9			1.2(1.2)					
11	22.4	1.6(0.2)	43.4	44.3						
12	56.0	6.4	1.1(0.4)	1.1(0.3)						
13	16.8	1.1(0.2)	6.2	5.7	2.3(1.8)					
14	952	95.3	5.3(0.8)	5.4						
15	74.5	8.4	0.9(0.2)	0.9(0.2)	43.5					
16	827	231	30.1	29.3						
17	1160	176	15.6	13.3						
18	20.3	3.2	3.8	3.0	16.5(4.7)					
19	21.2	3.9	1.0(0.3)	1.1(0.3)	20.7(3.0)					
20	255	14.9		3.0(0.9)	55.5			1.1(0.3)	77.5	4.9
21	326	7.9(1.2)		3.1(1.6)				1.9(0.3)	134	3.8
22	2130	38.6		5.0(2.0)				2.4(0.6)	70.7(10.3)	3.1(0.5)
23			50.5	54.6		36.3(5.3)	37.3(8.1)	3.9		1.7(0.3)

See footnotes at end of table

Table 23. nCi/g of Gem Measured at 0 Days Following Irradiation at BNL's HFBR[a] (continued)

1. Gem #	2. ^{46}Sc	3. ^{59}Fe	4. ^{182}Ta	5. ^{182}Ta	6. ^{51}Cr	7. ^{183}Ta	8. ^{183}Ta	9. ^{77}As ($x10^3$)	10. ^{72}Ga ($x10^3$)	11. ^{24}Na ($x10^3$)
24	1000	15.4						2.0(0.5)	82.2(8.9)	4.0(0.5)
25	732	7.3(2.1)	784	727.5		119(17.9)	127(48.8)	3.3(0.8)	112	1150.0
26	108	6.8(3.2)	29.5(8.0)	18.3(3.6)				4.3(0.7)	129.2	1100.0
27	180	8.8(1.2)	476	421.3		80.7(12.8)	74.6(28.1)	8.2(0.9)	92.2(11.2)	1100.0
28	13.3	13.0(2.3)	9.5(4.6)	17.6(3.5)	8.7			3.0(0.5)	64.5(10.1)	1100.0
29	1.5(0.6)		59.7(6.7)	49.1(5.5.)		14.5(6.3)	28.0	10.6	73.5(12.3)	1100.0
30	272	6.7	14.1(1.7)	10.1	12.7(4.7)			4.9(0.6)	154(17.7)	1100
31	3.4	0.3(0.1)	7.3	7.4		13.5	24.5(4.8)	33.0	358.7	981
32	6.5	0.9(0.1)	1.7(0.3)	2.4	4.1(0.6)			17.3	188.2	992
33	2.5(0.4)	0.4(0.1)		1.3(0.2)	3.5(0.4)			23.6	251.3	986
34	3.3(0.4)	0.2(0.1)	7.0(2.1)	7.7(0.3)		8.6	15.0(5.5)	31.6	336.9	958
35	4.2		54.7	51.7	4.2(1.9)	104	128	30.0	409.5	888
36	3.9(0.6)		1190	1150		2150	2090	22.2	298.8	822
37	2.8	2.3(0.6)							3.6	
38	11.5	2.3(0.6)			8.8(4.4)			0.3	6.2	0.5
39	143	2.3(0.9)							18.9	0.4
40	81.4	3.3(0.8)	2.0(0.7)	3.2(0.6)					17.3	0.5
41	11.4	2.6(0.6)						0.3(0.3)	5.4	0.5
42	14.7								0.9	0.02 (0.005)
43	2.0	0.6(0.3)							1.2	0.05 (0.008)
44	0.3(0.1)	0.4(0.1)							0.4	0.4

See footnotes at end of table

Table 23. nCi/g of Gem Measured at 0 Days Following Irradiation at BNL's HFBR[a] (continued)

1. Gem #	2. ^{46}Sc	3. ^{59}Fe	4. ^{182}Ta	5. ^{182}Ta	6. ^{51}Cr	7. ^{183}Ta	8. ^{183}Ta	9. ^{77}As ($x10^3$)	10. ^{72}Ga ($x10^3$)	11. ^{24}Na ($x10^3$)
y45	1.4(0.2)	0.4(0.1)							0.3	0.04 (0.005)
46	0.5(0.2)	0.4(0.3)							0.4	0.04 (0.007)
47	19.8	22.3	55.5	55.4	1.6(1.0)				27.6	1.8
48	37.7	9.4	4.6	4.5				0.3(0.1)	54.1	2.0
49	178	5.8	1.5(0.3)	2.2(0.3)				1.1	31.3	2.0
50	25.4	11.7	1.1(0.3)	1.0(0.2)				1.2	13.8	1.9
51	205	5.5	3.0(0.5)	3.1				0.7	35.5	1.9

[a]One sigma peak error estimates greater than 10% are given in parenthesis. Gems removed from the reactor at the following times:
All other one sigma peak errors are less than 10%.
Peaks chosen for quantification:

^{46}Sc 889 keV
^{59}Fe 1099 keV
^{182}Ta (column 4) 1189 keV
^{182}Ta (column 5) 1221 keV
^{51}Cr 320 keV
^{183}Ta (column 7) 354 keV
^{183}Ta (column 8) 209 keV
^{77}As 239 keV
^{72}Ga 630 keV
^{24}Na 1369 keV

1-10 removed 11/17/88 #25-36 removed 1/3/89
#11-19 removed 11/21/88 #37-46 removed 1/17/89
#20-24 removed 1/4/89 #47-51 removed 2/24/89

In general, the results of gamma spectroscopy analysis showed that for all irradiated topaz, regardless of origin, the ^{59}Fe concentration level (nCi/g of gem) remained constant while the ^{46}Sc concentration varied. The ^{77}As:^{72}Ga ratio was always less than one. When the ^{46}Sc:^{182}Ta ratio was greater than one, ^{51}Cr was found, but ^{183}Ta was not present.

In some irradiated gems, the concentration of ^{183}Ta was approximately 200 percent greater than the concentration of ^{182}Ta. This result was puzzling if ^{183}Ta was produced from ^{182}Ta via a (n,γ) reaction. A possible explanation was that tungsten found in the saws used to cut the topaz may contaminate the stone and become activated, creating larger than expected amounts of ^{183}Ta via the $^{183}W(n,p)^{183}Ta$ reaction. The level of ^{77}As could not always be determined because the length of the interval between irradiation and the initial gamma spectroscopy analysis.

When activity (nCi/g of gem) ratios (see Table 24) were compared with topaz color, we found that HFBR- irradiated topaz was blue only when the ^{72}Ga:^{24}Na ratio was less than one. Ratios of 10 or greater resulted in a brown or cinnamon color, while intermediate ^{72}Ga:^{24}Na ratios resulted in a clear or slightly tinged blue. It seems possible that the parent elements, Na and/or Ga, participate in creating the color centers necessary for blue color.

The activity per gram of topaz for the nuclides ^{24}Na, ^{46}Sc, ^{51}Cr, ^{59}Fe, ^{72}Ga, ^{77}As, ^{182}Ta, and ^{183}Ta was measured, and the results were converted to activity at O days following HFBR irradiation. We note that during any irradiation both thermal and fast neutrons were present and, theoretically, both contributed to the induced activity. The increase in activity concentration of a particular isotope for a particular country of origin was reviewed to determine if fast or thermal neutrons dominated the activation process. There were only sufficient number of samples of Brazilian topaz to establish a relationship between nCi g^{-1} of gem and thermal (or fast) neutron fluence.

As Figures 4 and 5 show, the range of activity (nCi/g) in Brazilian topaz was about two to three magnitudes for ^{59}Fe but less than one magnitude for ^{46}Sc. Still, we anticipated that for any nuclide present in trace quantities (ppm level or less), a mean or average concentration value in topaz for either a given thermal or fast neutron fluence would not be representative of a particular country of origin. This conclusion is based on the non-normal distribution of activity in irradiated topaz.

Figures 6 and 7 give the total gamma activity per gram of topaz plotted as a function of thermal or fast neutron fluence for irradiated topaz from India, Sri Lanka, Brazil, and Nigeria. Each point represents an individual stone. For Brazilian topaz, the activity per gram of gem increased with thermal neutron fluence but tended to saturate or slightly decrease with increasing fast neutron fluence. Results from other countries could not be obtained because we lack data covering a wide range of neutron fluences.

On 4/22/89, a 24-hour (86,400 sec), live-time gamma spectroscopy analysis was conducted on neutron irradiated stones to determine if long-lived gamma emitters were present in low concentrations. At least two gems from each irradiation were selected and were counted on the endcap of the germanium detector to maximize efficiency. We did not quantify these values because of small, photopeak net areas and large peak errors. Topaz that had a high total gamma activity (determined by previous analysis using a calibrated geometry) was selected. Table 25 lists the nuclides and the number of photopeaks.

Table 24. Comparisons of Activity Ratio for Neutron Irradiated Topaz at BNL[a]

Gem #	$^{46}Sc/^{59}Fe$	$^{77}As/^{72}Ga$	$^{72}Ga/^{24}Na$
1	1.12	N.D.*	N.D.
2	4.94	N.D.	N.D.
3	8.44	N.D.	N.D.
4	0.67	N.D.	N.D.
5	2.94	N.D.	N.D.
6	5.20	N.D.	N.D.
7	0.84	N.D.	N.D.
8	3.71	N.D.	N.D.
9	8.95	N.D.	N.D.
10	2.75	N.D.	N.D.
11	14.42	N.D.	N.D.
12	8.70	N.D.	N.D.
13	15.98	N.D.	N.D.
14	9.98	N.D.	N.D.
15	8.85	N.D.	N.D.
16	3.58	N.D.	N.D.
17	6.59	N.D.	N.D.
18	6.26	N.D.	N.D.
19	5.33	N.D.	N.D.
20	17.08	0.01	15.99
21	41.49	0.01	35.33
22	55.19	0.03	22.80
23	N.D.	N.D.	N.D.
24	65.13	0.02	20.31
25	100.74	0.03	0.10
26	15.95	0.03	0.12
27	21.20	0.04	0.20
28	1.03	0.05	0.06
29	N.D.	0.14	0.07

See footnotes at end of table

Table 24. Comparisons of Activity Ratio for Neutron Irradiated Topaz at BNL[a] (cont'd)

Gem #	$^{46}Sc/^{59}Fe$	$^{77}As/^{72}Ga$	$^{72}Ga/^{24}Na$
30	40.01	0.03	0.14
31	14.11	0.09	0.37
32	7.87	0.09	0.19
33	7.73	0.09	0.25
34	19.42	0.09	0.35
35	N.D.	0.07	0.46
36	N.D.	0.07	0.36
37	1.2	N.D.	N.D.
38	5.04	0.05	12.10
39	62.87	N.D.	47.00
40	24.36	N.D.	36.10
41	4.39	0.05	12.00
42	N.D.	N.D.	39.05
43	3.38	N.D.	25.12
44	1.24	N.D.	0.95
45	3.00	N.D.	8.56
46	1.33	N.D.	9.40
47	0.89	N.D.	15.13
48	4.00	0.04	27.30
49	33.70	0.04	15.90
50	2.17	0.09	7.36
51	37.04	0.02	18.78

[a]Activity, nCi/g, calculated for time=0 following irradiation.
*Not determined.

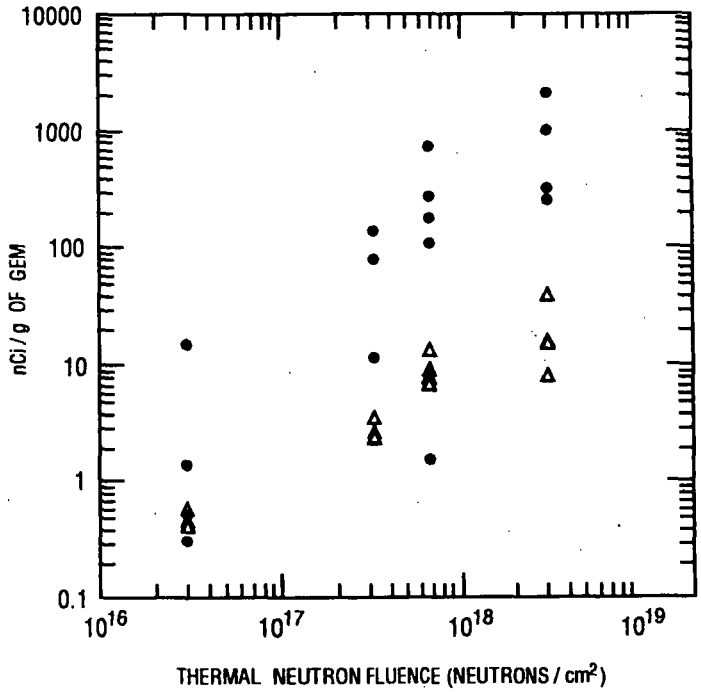

Figure 4. **Induced activity in Brazilian topaz versus thermal neutron fluence; ●, ^{46}Se, △, ^{59}Fe.**

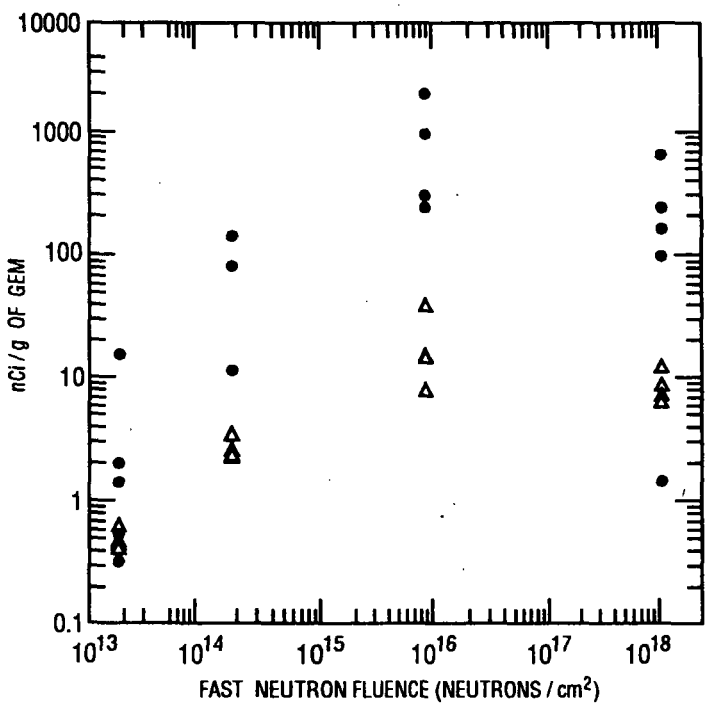

Figure 5. **Induced activity in Brazilian topaz versus fast neutron fluence; ●, ^{46}Se, △, ^{59}Fe.**

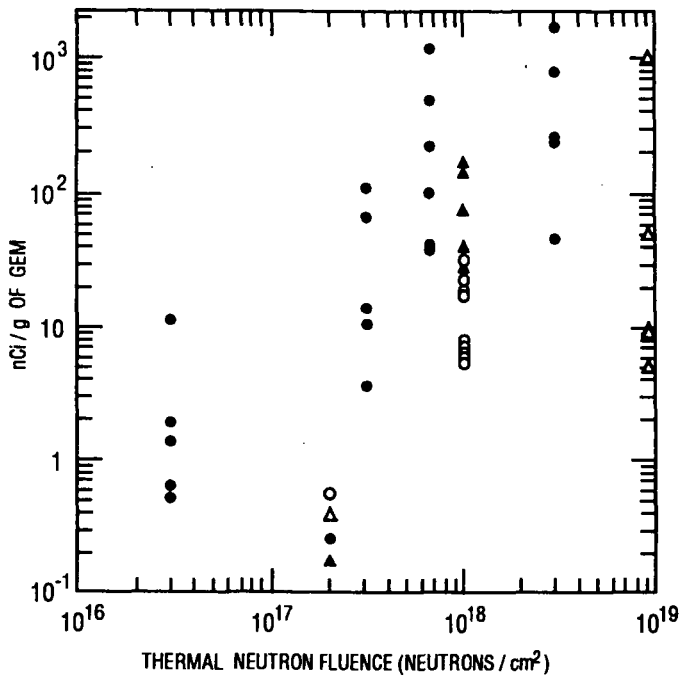

Figure 6. **Total induced activity in BNL topaz versus thermal neutron fluence. Total gamma nCi/g of gem at time=30 days following neutron irradiation. ○=India, △=Sri Lanka, ●=Brazil, ▲=Nigeria.**

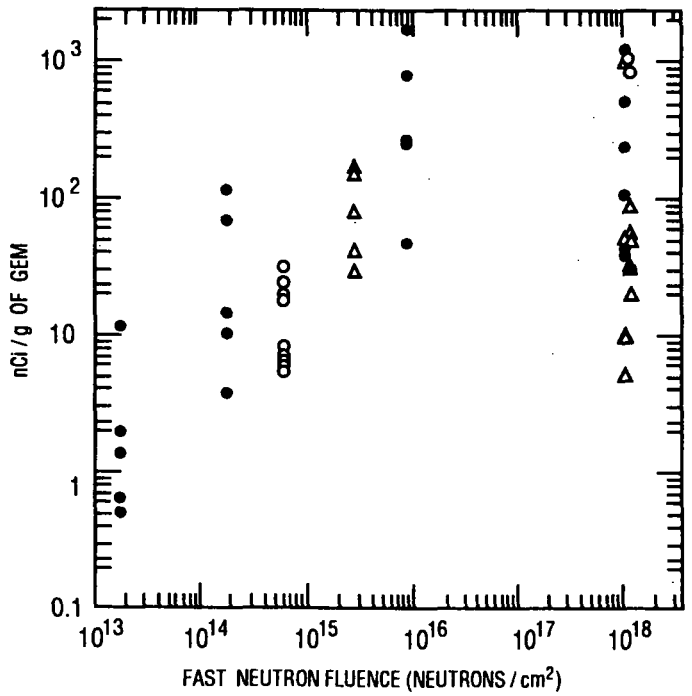

Figure 7. **Total induced activity in BNL topaz versus fast neutron fluence. Total gamma nCi/g of gem at time=30 days following neutron irradiation. ○=India, △=Sri Lanka, ●=Brazil, ▲=Nigeria.**

Table 25. Gamma-Emitting Nuclides Identified by Long-Term Ge(Li) Analysis

Nuclide	# of photopeaks
^{182}Ta	18[a]
^{59}Fe	3[b]
^{54}Mn	1
^{46}Sc	2[c]
^{124}Sb	2
^{51}Cr	1

[a]Includes 1120 and 1289 keV peaks shared with ^{46}Sc and ^{59}Fe, respectively.
[b]Includes 1289 keV peaks shared with ^{59}Fe.
[c]Includes 1120 keV peaks shared with ^{46}Sc.

In a 24-hour count, the net area of the ^{54}Mn peak at 834.8 keV contained 6,298 counts above a background of 660,906 counts. Similarly, the ^{124}Sb peak at 602.7 keV (98.1% relative intensity) had a net count of 53,464 (2,640,000 background counts), while the 1,691 keV peak (50% relative intensity) had 4,403 net counts (52,055 background counts).

These nuclides and peak lines were confirmed during a 80,000 sec live-time count performed ten days later using the same stones in the same geometry.

4.2 Reduction of Surface Contamination

Care was taken to reduce the removable contamination caused by handling the gems that would be counted by gamma spectroscopy. Certain isotopes have been identified incorrectly as being incorporated in irradiated topaz because surface contamination was not removed before irradiation. This misidentification was particularly important for neutron irradiated topaz.

Periodically, the acid wash used to clean irradiated stones was analyzed by gamma spectroscopy to assess the activated isotopes that could be removed from the topaz. Table 26 shows a typical analysis. Approximately 10 ml of the wash was placed in a standard liquid scintillation vial and counted for 2,700 sec (live-time). Activities were determined by assuming an endcap counting geometry of the detector. The activities were determined at 0 days after irradiation.

Table 26. Gamma Spectroscopy Analysis of Acid Wash

Isotope	T½, hr	γ energy, keV	net dps
^{24}Na	15.0	1,369	13,817
^{187}W	23.9	480	582
^{187}W	23.9	686	1,023
^{140}La	40.3	488	314
^{140}La	40.3	1,596	342
^{198}Au	64.6	412	40
^{65}Zn	5,851.2	1,116	17

Sweat and oil from handling the topaz could contribute to the ^{24}Na, ^{65}Zn, and ^{198}Au found in the acid wash. Commercial tungsten carbide drills are usually relatively inexpensive, and although they provide good performance, they occasionally chip and contaminate the sample, resulting in the presence of ^{187}W after neutron irradiation (Harbottle, 1976). Although the largest activity concentration in the acid wash was due to ^{24}Na, the amount of ^{24}Na was small compared to the concentration identified in topaz following post-acid wash.

If thin-walled quartz vessels are used to hold the topaz during neutron irradiation and analysis, the following activated isotopes would be expected in the quartz container (because of the mineral content of the vessel): ^{181}Hf, ^{153}Sm, ^{140}La, ^{24}Na, ^{175}Yb, and ^{198}Au. This expectation was confirmed by gamma spectroscopy analysis of quartz vessels that had undergone neutron irradiation. Irradiated topaz should be removed from quartz containers to avoid interference from these isotopes.

4.3 Electron Beam Irradiation

Cut topaz was irradiated with a 17 MeV electron beam at the Rensselaer Polytechnic Institute (RPI) LINAC Laboratory. Examples of all the topaz listed in Table 9 were irradiated. The energy of the electrons was determined by RPI LINAC technicians.

BNL Ge(Li) and shielded end-window GM measurements of electron-irradiated topaz showed the presence of a positron emitter(s) (511 keV) with no other significant gamma lines, and weak or nonexistent beta emissions. The half-lives (T½) of the radionuclides were less than one day. Positron emitters with T½ of either (a) less than 10 minutes, or (b) greater than one day were not considered as possibilities. We assumed that all the nuclides created by RPI LINAC irradiation were produced by a (γ,n) reaction. Table 27 lists the potential photonuclear or photodisintegration (x,n) cross-sections of the nuclides of concern in topaz irradiation. This table includes the approximate photonuclear cross-sections up to 17 MeV, resonance, and integrated cross-sections in this energy region.

Based on the photonuclear cross-sections and emission characteristics of previously identified nuclides in irradiated topaz, and the elements found in non-irradiated topaz, the most likely precursor nuclides that may interact are (in descending order of likelihood): ^{133}Cs, ^{70}Ge, ^{69}Ga, ^{65}Cu, ^{63}Cu, ^{55}Mn, ^{64}Zn, ^{50}Cr, ^{66}Zn, and ^{19}F. Of the photonuclear

reactions possible with these parent nuclides, ^{133}Cs, ^{70}Ge, ^{55}Mn, and ^{66}Zn would result in daughter products with half-lives greater than one day and were, therefore, unlikely to occur. Photonuclear reactions with ^{68}Cu would result in a daughter nuclide with a half-life of less than ten minutes that was unlikely to be detected during analysis.

The daughter products of the parent nuclides, ^{69}Ga, ^{65}Cu, ^{64}Zn, ^{50}Cr, and ^{19}F, were the most likely to be produced by electron irradiation. These daughter products included ^{68}Ga ($T_{1/2}$=1.13 hrs), ^{64}Cu ($T_{1/2}$=12.7 hrs), ^{63}Zn ($T_{1/2}$=0.64 hrs), ^{49}Cr ($T_{1/2}$=0.70 hrs), and ^{18}F ($T_{1/2}$=1.83 hrs).

The presence of Cu, Ga, and Zn had been confirmed by x-ray fluorescence and proton-induced x-ray fluorescence. It would be necessary for a gem to have concentrations of 0.5 to 50 ppm to be detected by this method. Although fluorine-19 has a relatively low photonuclear cross-section, interaction is very likely because of the large amounts initially present in topaz. This is also true for chromium, commonly listed as a major impurity in topaz.

4.4 NaI(Tl) Detector Analysis

We used a 2" thick by 1.75" diameter NaI(Tl) well-type detector in association with a D.S. Davidson 1056 B multichannel analyzer to determine the sensitivity of the detector to gamma emissions. Before the counting of irradiated topaz began, the keV/channel and efficiency were determined, using NIST-traceable multigamma standards (see Figure 8). The bottom of the well was the most efficient for counting gemstones (efficiency is reduced approximately 5 percent, 15 mm above the bottom). The amplifier coarse and fine gain controls were optimized using an oscilloscope. The following gamma sensitivities (net cpm/(nCi) were determined with liquid standards (initial activity determined by Ge(Li) analysis) for two energy ranges - 100 to 1400 keV, and 40 to 1400 keV (Table 28).

Table 27. Photonuclear Cross Sections[a]

Reaction	Threshold MeV	Approximate Cross Section, mbarns: 8 MeV	10 MeV	12 MeV	14 MeV	16 MeV	17 MeV	Resonance peaks up to 17 MeV: MeV	mbarns	Integrated Cross Section: Energy Range	MeV-barns
$^{19}F(\gamma,n)$	10.45			1.8	1.9	2.8	2.4	12.4	3.7	0-15 MeV	12
$^{19}F(\gamma,xn)$				3.5	5.7	4.5	13.5	12.5	7.5	for $(\gamma,xn)+(\gamma,2-xn)$	
								16.1	3.2		
$^{23}Na(\gamma,n)$	12.47				2.0	6.2				0-27 MeV	119
$^{23}Na(\gamma,n)+(\gamma,p)$					3.0	10.0				for $(\gamma,n)+(\gamma,np)$	
$^{27}Al(\gamma,n)$	12.96				1.0	4.5	12.0	17.0	12.0	0-17 MeV	4
$^{27}Al(\gamma,n)+(\gamma,np)+(\gamma,2n)$					1.0	4.3	5.5	17.0	5.7	12.5-24 MeV	115
$^{28}Si(\gamma,n)$	17.14						0			0-17 Mev	0
$^{31}P(\gamma,n)$	12.48				3.4	5.5	9.5	16.2	10.0	Th-22 Mev	120
								14.8	7.2	Th-28.6 MeV	179
$^{32}S(\gamma,n)$	15.10					2.2	4.0	15.7	7.0	Th-32.2 MeV	98
$^{32}S(\gamma,n)$						7.0	8.2	16.8	10.0	Th-22.1 MeV	64
$^{35}Cl(\gamma,n)$	12.35	isomeric state			1.0	5.5	9.5			0-30 MeV	125
		ground state			0	6.0	8.5			0-30 MeV	141
					0.5	1.6	2.4				
$^{37}Cl(\gamma,n)$	10.37										
$^{42}Ca(\gamma,xn)$	11.80			1.0	7.0.	21.0	26.0				
$^{45}Sc(\gamma,n)+(\gamma,np)+(\gamma,-2n)$*	11.20				5.7	15.5	18.5			Th-25 MeV	158
				2.5	12.0	28.0	32.0			Th-28.1 MeV	365
$^{45}Sc(\gamma,n)$*											
$^{50}Cr(\gamma,n)$				2.0	7.0	120.0	124.0	16.0	120.0		
								17.0	124.0		

See footnotes at end of table

Table 27. Photonuclear Cross Sections[a] (continued)

Reaction	Threshold MeV	Approximate Cross Section, mbarns 8 MeV	10 MeV	12 MeV	14 MeV	16 MeV	17 MeV	Resonance peaks up to 17 MeV MeV	mbarns	Integrated Cross Section Energy Range	MeV-barns
$^{52}Cr(\gamma,n)$	12.18				15.0	47.0	73.0			Th-26 MeV	640
$^{54}Fe(\gamma,n)$	12.30				5.0	23.0	42.0			0-31 MeV	290
$^{54}Fe(\gamma,n)$					3.5	15.0	27.0				
$^{55}Mn(\gamma,xn)$	10.19			5.0	18.0	54.0	80.0	16.8	85.0	12-25 MeV	627
$^{55}Mn(\gamma,n)$				10.0	22.0	60.0	67.0	15.4	47.0	Th-36.5 MeV	629
								13.7	27.0		
$^{56}Fe(\gamma,n)$	11.25										
$^{58}Ni(\gamma,n)$	12.20				9.5	17.5	21.5			10-25 MeV	185
$^{58}Ni(\gamma,n)$					10.0	18.0	21.0			Th-33.5 MeV	278
$^{63}Cu(\gamma,n)$	10.84			10.0	25.0	66.0	75.0	17.1	75.0	Th-25.1 MeV	498
$^{63}Cu(\gamma,n)$				12.0	28.0	80.0	91.0				
$^{63}Cu(\gamma,n)$				2.5	10.0	50.0	56.0				
$^{64}Zn(\gamma,n)$	11.85			8.0	31.0	65.0	78.0	16.7	73.0	Th-29.5 MeV	703
$^{64}Zn(\gamma,n)+(\gamma,pn)$				5.0	23.0	65.0	68.0			Th-29 MeV	750
										12-22 MeV	2030
										Th-24.1 MeV	397
$^{65}Cu(\gamma,n)$	9.91			30.0	70.0	120.0	137.0			10-28 MeV	437
$^{65}Cu(\gamma,n)$				17.0	40.0	70.0	75.0			Th-27.8 MeV	421
$^{66}Zn(\gamma,xn)$				5.0	17.0	47.0	54.0				
$^{69}Ga(\gamma,n)+(\gamma,pn)$	10.3			19.0	64.0	103.0	115.0	17.0	115.0	Th-26.5 MeV	910
$^{70}Ge(\gamma,n)$	12.1				30.0	47.0	65.0	17.0	160.0	12-20 MeV	590
$^{70}Ge(\gamma,n)$	11.1			15.0	75.0	130.0	160.0			Th-26.5 MeV	687
$^{70}Ge(\gamma,n)$				70.0	130.0	140.0	125.0				
$^{70}Ge(\gamma,n)$			27.0	70.0	130.0	145.0	130.0				
$^{70}Ge(\gamma,n)+(\gamma,pn)$				16.0	55.0	90.0	87.0				

See footnotes at end of table

Table 27. Photonuclear Cross Sections[a] (continued)

Reaction	Threshold MeV	Approximate Cross Section, mbarns						Resonance peaks up to 17 MeV		Integrated Cross Section	
		8 MeV	10 MeV	12 MeV	14 MeV	16 MeV	17 MeV	MeV	mbarns	Energy Range	MeV-barns
$^{71}Ga(\gamma,n)+(\gamma,pn)$	9.27			19.0	64.0	103.0	115.0	17.0	115.0	Th-26.5 MeV	910
$^{133}Cs(\gamma,xn)$	8.99			80.0	162.0	212.0	212.0	15.0	300.0	Th-24.2 MeV	1828
$^{133}Cs(\gamma,n)+(\gamma,pn)$			40.0	80.0	230.0	250.0	175.0			Th-29.5 MeV	1480
$^{181}Ta(\gamma,n)$	7.66		75.0	340.0	350.0	180.0	85.0	14.7	270.0	Th-22 MeV	2970
$^{181}Ta(\gamma,n)$			25.0	90.0	250.0	140.0	65.0	12.5	308.0	Th-24.6 MeV	1300
$^{181}Ta(\gamma,n)$		35.0	100.0	350.0	370.0	440.0	265.0	12.6	440.0	Th-25.2 MeV	2180
$^{181}Ta(\gamma,n)$			80.0	370.0	360.0	410.0	250.0	12.4	370.0		
$^{181}Ta(\gamma,n)$		40.0	80.0	340.0	355.0	180.0	85.0	13.5	365.0		
$^{181}Ta(\gamma,xn)$		20.0	70.0	280.0	290.0	310.0	190.0	15.5	348.0		

[a]Taken from Photonuclear Data Abstract Sheets 1955-1982; NBSIR 83-2742; U.S. Department of Commerce, National Bureau of Standards, 1984-1985.
*Up to 20 MeV, >80% ^{44}Sc (ground state) is formed and <20% ^{44m}Sc is formed.
**Th=threshold

Table 28. Sensitivity of the NaI Well Counter, Net cpm/nCi

Nuclide	100 to 1400 keV	40 to 1400 keV
^{54}Mn	566	621
^{46}Sc	941	994
^{182}Ta	1,221	1,789
^{59}Fe	536	567

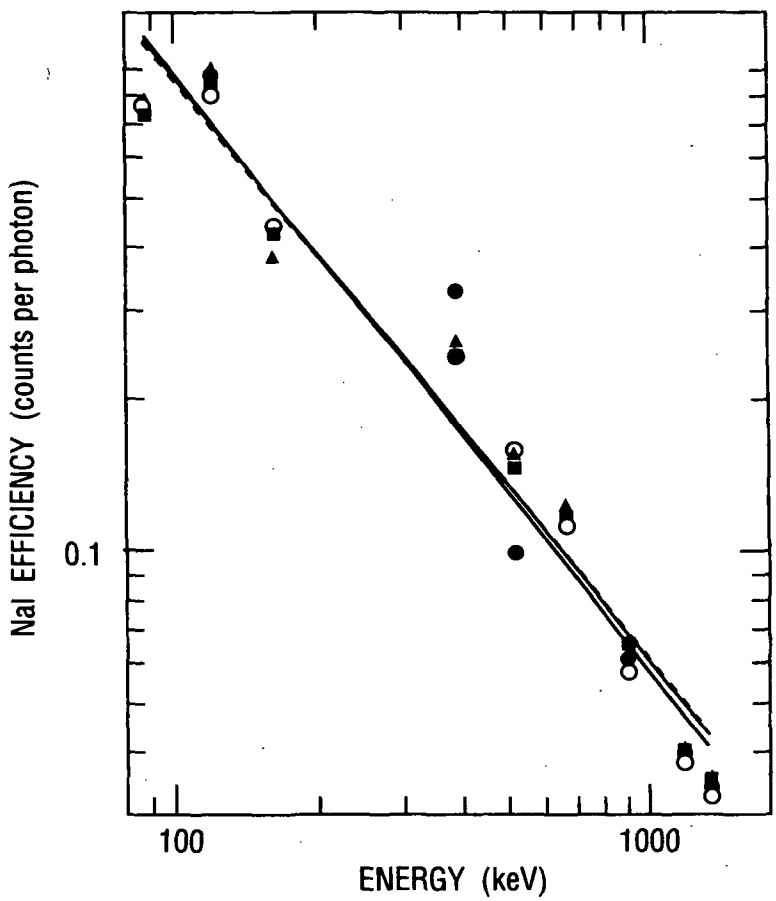

Figure 8. Efficiency curve of the NaI well counter for various standards. Amersham Multigamma Standard 1-1=●; Amersham Multigamma Standard 1-4=▲; Amersham Multigamma Standard 1-3=○; Amersham Multigamma Standard 1-2=■.

The 40 to 1400 keV energy range window was used because of the increased signal-to-noise ratio.

The NaI counting times needed to detect two times exempt concentrations were calculated from the NaI sensitivity, net cpm/nCi for the 40 to 1,400 keV window, and the expected

activity as calculated from equation 14. Gamma-emitting nuclides identified in topaz, ^{46}Sc, ^{54}Mn, ^{182}Ta, and ^{59}Fe, were detected at a 99.9% confidence level in less than one minute using a shielded, well-type NaI detector. If the detector was not shielded, the background count rate (74.4 cpm) for the 40 to 1,400 keV energy window increased, and the required counting time also increased. Although not analyzed in this study, the counting time necessary to detect two times an exempt concentration of ^{134}Cs in 0.1, 0.25, and 0.5 g topaz was calculated to be 9.1, 1.5, and 0.4 minutes, respectively, at the 99.9% confidence interval. These results are based on an assumed NaI sensitivity of 1,400 cpm/nCi for ^{134}Cs.

Similarly, NaI beta sensitivity was determined using NIST-traceable liquid standards. Plastic and glass vials were used. Table 29 summarizes the results (given in net cpm/nCi). Carbon-14 was used to simulate sulfur-35. The net cpm/nCi was about 2.6 times greater in plastic versus glass vials for ^{32}P for a given energy window, but was approximately equal for ^{14}C and ^{36}Cl.

4.5 GM Beta Absorption Analysis

Figures 9 to 24 give the findings from analysis of shielded GM beta absorption of selected neutron-irradiated gems. Irradiated gemstones were centered beneath the GM detector. The maximum variation across the face of the detector for the counting geometry was 4.75 percent of the maximum count. In general, the net count rate decreased with an increase in aluminum filtration. Both log-log and log-linear graphs are given for each topaz to aid in identifying individual isotopes. The half-value-density-thickness of topaz suspected of containing ^{32}P (i.e., #12, 15, 31, and 32) closely followed the expected value of approximately 100 mg/cm^2. Several weeks later, measurements were repeated on several stones to verify the presence of ^{32}P. The GM absorption coefficient remained relatively constant, with a slowly decreasing count rate for stones containing only gamma/beta emitters. This flattened response began at about 450 mg/cm^2, for stones with ^{32}P, while for stones without ^{32}P it occurred at approximately 80 mg/cm^2. Therefore, we could identify the presence of ^{32}P in irradiated topaz by observing the GM response (net cpm) at 0, 80, and 450 mg/cm^2. Curves deviating from the expected values at large mg cm^{-2} thicknesses (4/2/89 GM count on gems 31 and 32) did so because of the statistical variation in low net counts.

Table 29. NaI Sensitivity for Various Gamma-Emitting Liquid Standards

Liquid standard designation	g of liquid standard	nCi/g of standard	Net cpm/(nCi/g) (100 to 1,400 keV window)	Net cpm/nCi (100 to 1,400 keV window)	Net cpm/(nCi/g) (40 to 1,400 keV window)	Net cpm/nCi (40 to 1,400 keV window)	S^2/N^* (100 to 1,400 keV window)	S^2/N^* (40 to 1,400 keV window)
^{46}Sc-A	0.4024	2.15	373	927	395	980	2,181	2,092
^{46}Sc-B	0.4035	17.67	379	939	405	1,004	2,250	2,206
^{46}Sc-C	0.4029	17.37	385	956	402	998	2,324	2,173
^{54}Mn-A	0.4033	3.82	214	531	238	590	718	762
^{54}Mn-B	0.4036	30.17	233	578	252	624	854	853
^{54}Mn-C	0.4032	29.54	238	589	261	648	886	816
^{182}Ta-A	0.3996	12.25	499	1,249	727	1,820	3,901	7,109
^{182}Ta-B	0.4018	12.73	487	1,213	708	1,763	3,722	6,747
^{182}Ta-C	0.3991	12.63	479	1,201	712	1,785	3,598	6,819
^{59}Fe-A	0.4017	11.68	220	548	231	576	760	718
^{59}Fe-B	0.4021	12.71	202	504	215	534	643	621
^{59}Fe-C	0.3995	11.49	222	556	236	590	774	747

*S equals net cpm/(nCi/g). Background (or N) equals 63.8 cpm for the 100 to 1,400 keV window and 74.4 cpm for the 40 to 1,400 keV window.

Table 30. Sensitivities of the NaI Well Counter for Pure Beta Emitters, Net cpm/nCi

	100 to 1,400 keV		40 to 1,400 keV	
	Plastic	Glass	Plastic	Glass
^{32}P	58.1	16.4	77.1	29.8
^{14}C	0.0	0.0	0.2	0.2
^{36}Cl	3.4	3.7	10.3	10.8

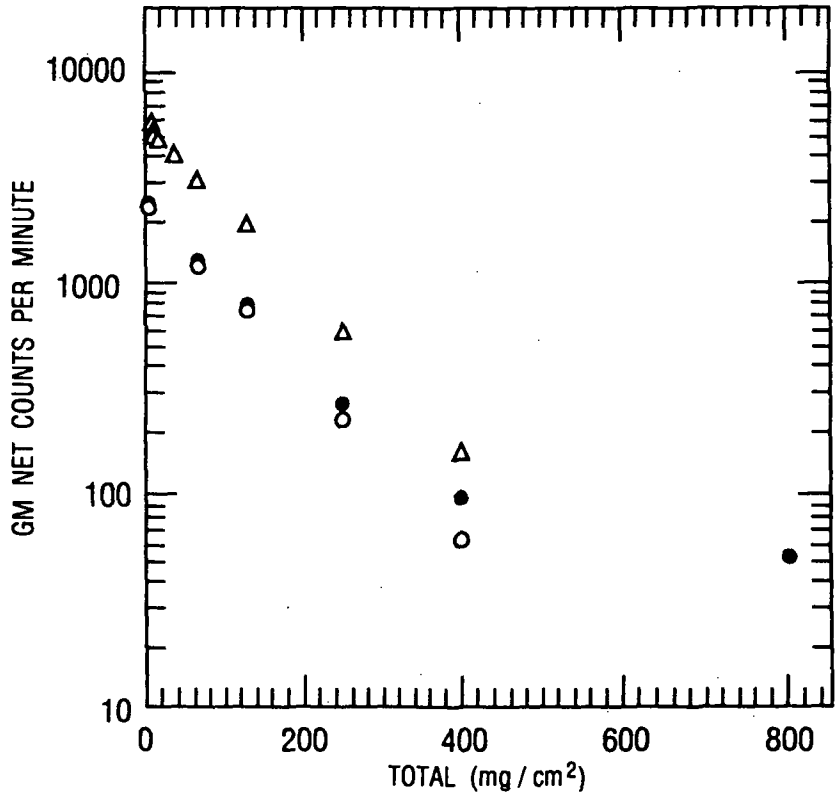

Figure 9. Log-linear GM response for gem #12. Origin: Sri Lanka; HFBR irradiation date: 11/21/88; fast neutron fluence: 1.1 x 10^{18}; mass: 0.5345g; gamma activity present on 4/1/89: ^{59}Fe (0.87 nCi/g of gem), ^{46}Sc (19.35 nCi/g of gem), ^{182}Ta (0.50 nCi/g of gem); five minute counting time; △=3/14/89 GM count, ●=4/2/89 GM count, ○=^{32}P decay corrected GM count on 4/2/89.

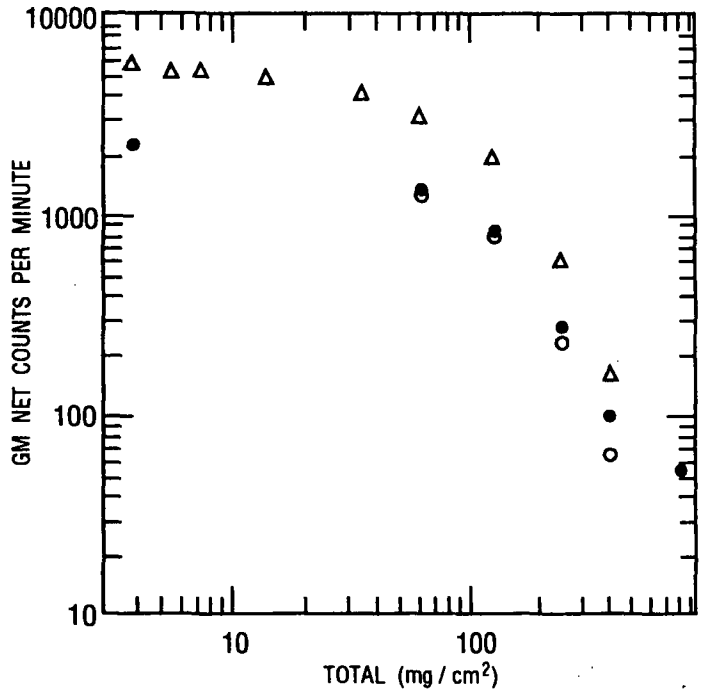

Figure 10. Log-log GM response for gem #12. Origin: Sri Lanka; HFBR irradiation date: 11/21/88; fast neutron fluence: 1.1 x 10^{18}; mass: 0.5345g; gamma activity present on 4/1/89: ^{59}Fe (0.87 nCi/g of gem), ^{46}Sc (19.35 nCi/g of gem), ^{182}Ta (0.50 nCi/g of gem); five minute counting time; △=3/14/89 GM count, ●=4/2/89 GM count, ○=^{32}P decay corrected GM count on 4/2/89.

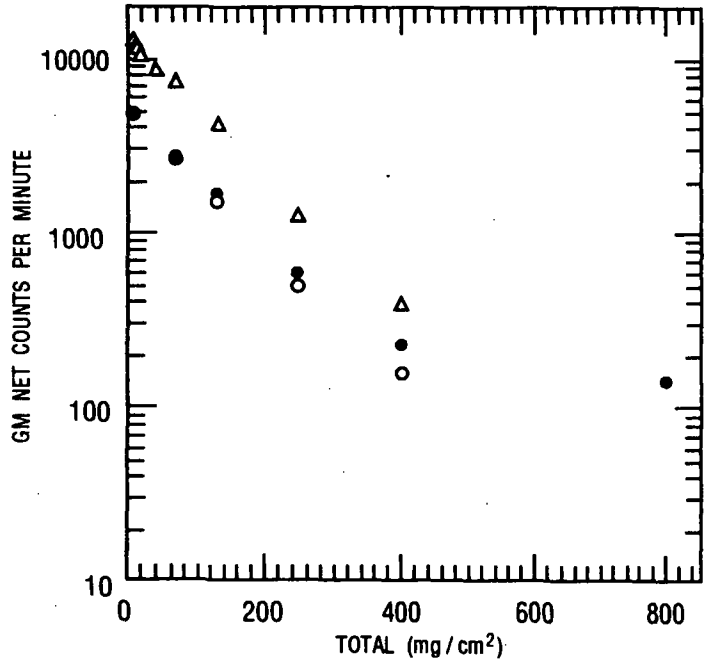

Figure 11. Log-linear GM response for gem #15. Origin: Sri Lanka; HFBR irradiation date: 11/21/88; fast neutron fluence: 1.1 x 10^{18}; mass: 0.5080g; gamma activity present on 4/1/89: ^{59}Fe (1.12 nCi/g of gem), ^{46}Sc (25.47 nCi/g of gem), ^{182}Ta (0.40 nCi/g of gem), ^{51}Cr (1.71 nCi/g of gem); five minute counting time; △=3/15/89 GM count, ●=4/2/89 GM count, ○=^{32}P decay corrected GM count on 4/2/89.

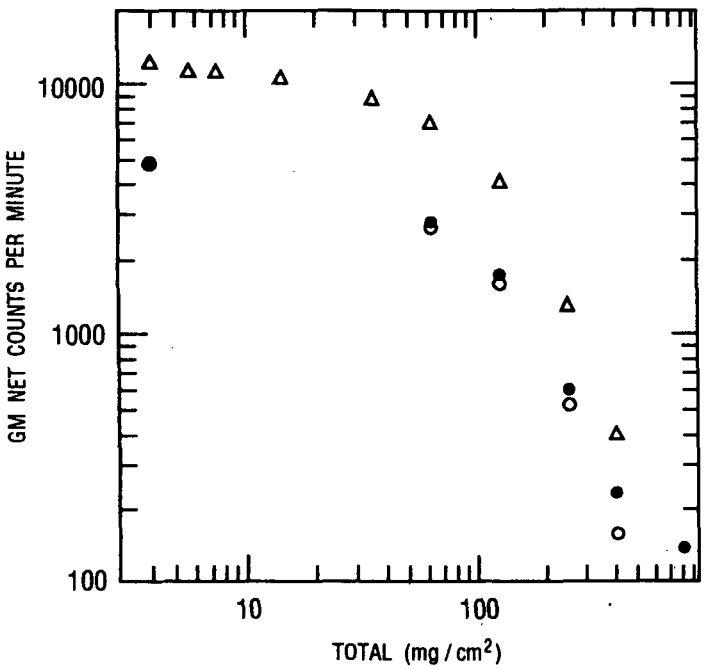

Figure 12. **Log-log GM response for gem #15. Origin: Sri Lanka; HFBR irradiation date: 11/21/88; fast neutron fluence: 1.1 x 10^{18}; mass: 0.5080g; gamma activity present on 4/1/89: ^{59}Fe (1.12 nCi/g of gem), ^{46}Sc (25.47 nCi/g of gem), ^{182}Ta (0.40 nCi/g of gem), ^{51}Cr (1.71 nCi/g of gem); five minute counting time; △=3/15/89 GM count, ●=4/2/89 GM count, ○=^{32}P decay corrected GM count on 4/2/89.**

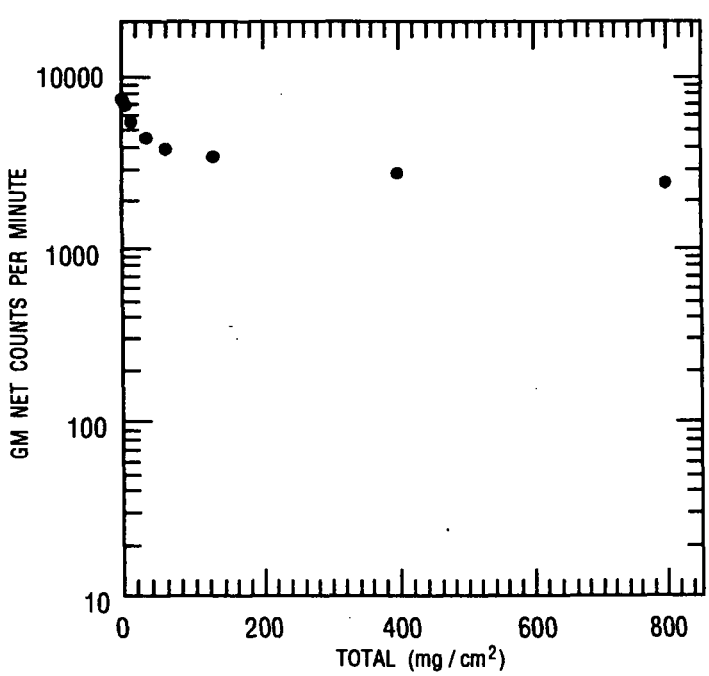

Figure 13. **Log-linear GM response for gem #16. Origin: India; HFBR irradiation date: 11/21/88; fast neutron fluence: 1.1 x 10^{18}; mass: 0.69895g; gamma activity present on 3/11/89: ^{59}Fe (38.5 nCi/g of gem), ^{46}Sc (259.1 nCi/g of gem), ^{182}Ta (19.85 nCi/g of gem); five minute counting time.**

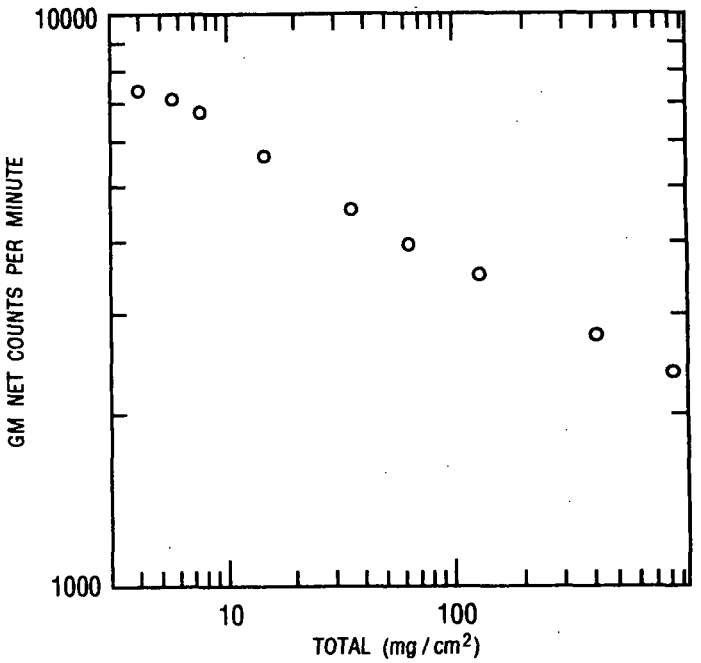

Figure 14. **Log-log GM response for gem #16. Origin: India; HFBR irradiation date: 11/21/88; fast neutron fluence: 1.1 x 10^{18}; mass: 0.69895g; gamma activity present on 3/11/89: ^{59}Fe (38.5 nCi/g of gem), ^{46}Sc (259.1 nCi/g of gem), ^{182}Ta (19.85 nCi/g of gem); five minute counting time.**

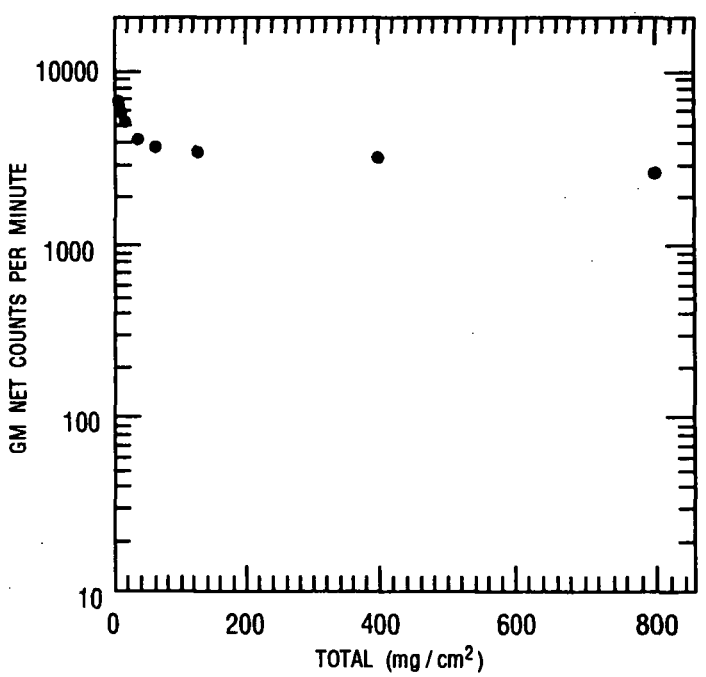

Figure 15. **Log-linear response for gem #17. Origin: India; HFBR irradiation date: 11/21/88; fast neutron fluence: 1.1 x 10^{18}; mass: 0.6311g; gamma activity present on 3/11/89: ^{59}Fe (30.6 nCi/g of gem), ^{46}Sc (420.3 nCi/g of gem), ^{182}Ta (6.10 nCi/g of gem); five minute counting time.**

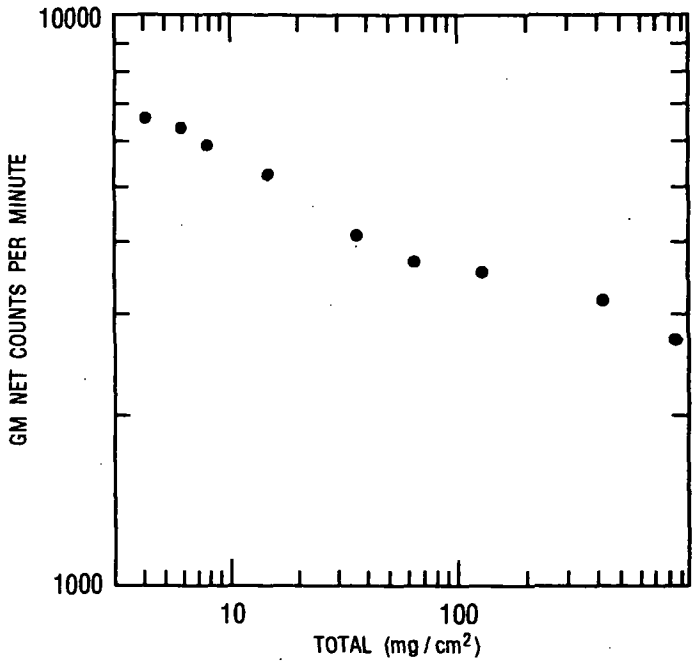

Figure 16. Log-log GM response for gem #17. Origin: India; HFBR irradiation date: 11/21/88; fast neutron fluence: 1.1 x 10^{18}; mass: 0.6311g; gamma activity present on 3/11/89: ^{59}Fe (30.6 nCi/g of gem), ^{46}Sc (420.3 nCi/g of gem), ^{182}Ta (6.10 nCi/g of gem); five minute counting time.

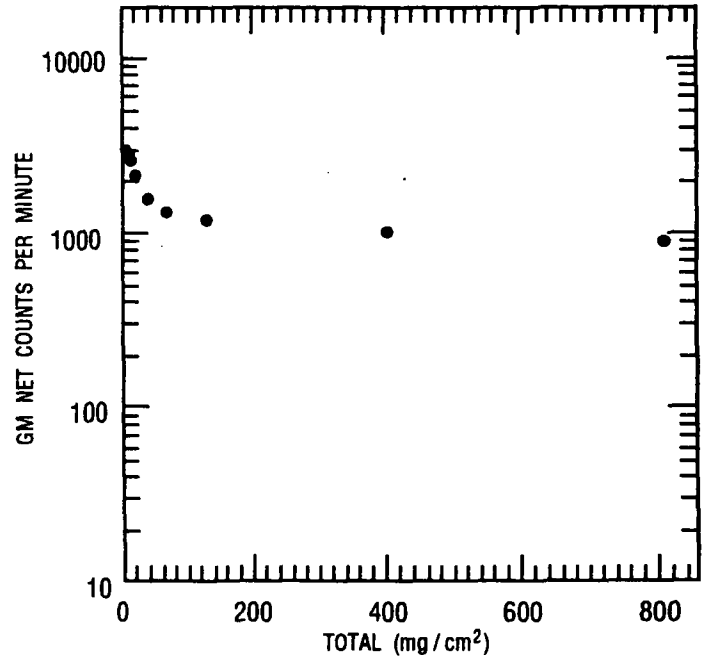

Figure 17. Log-linear GM response for gem #25. Origin: Brazil; HFBR irradiation date: 1/3/89; fast neutron fluence: 1.0 x 10^{18}; mass: 0.1118g; gamma activity present on 3/11/89: ^{59}Fe (2.97 nCi/g of gem), ^{46}Sc (448.3 nCi/g of gem), ^{182}Ta (555.4 nCi/g of gem); five minute counting time.

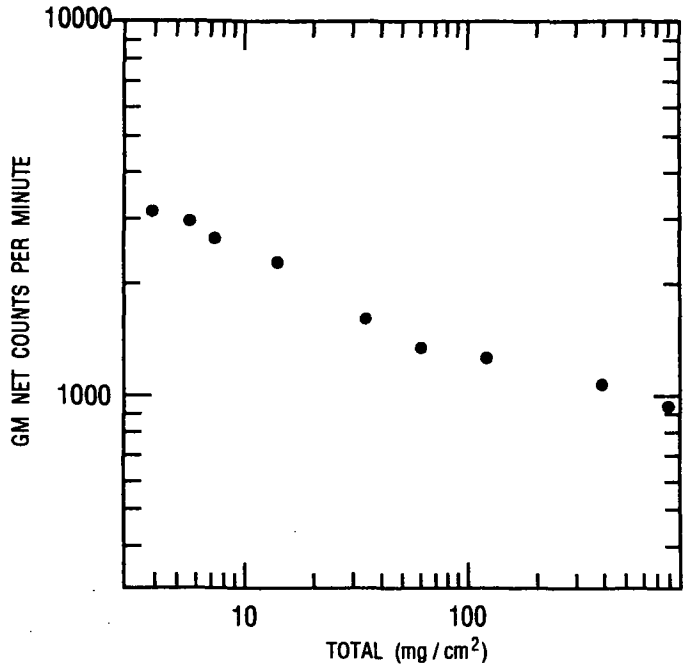

Figure 18. **Log-log GM response for gem #25. Origin: Brazil; HFBR irradiation date: 1/3/89; fast neutron fluence: 1.0 x 10^{18}; mass: 0.1118g; gamma activity present on 3/11/89: ^{59}Fe (2.97 nCi/g of gem), ^{46}Sc (448.3 nCi/g of gem), ^{182}Ta (555.4 nCi/g of gem); five minute counting time.**

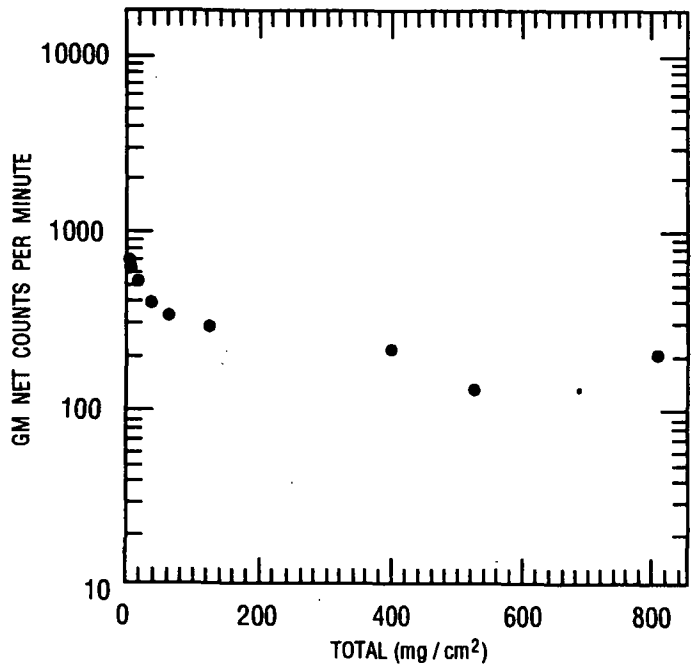

Figure 19. **Log-linear GM response for gem #30. Origin: Brazil; HFBR irradiation date: 1/3/89; fast neutron fluence: 1.0 x 10^{18}; mass: 0.1105g; gamma activity present on 3/11/89: ^{59}Fe (2.61 nCi/g of gem), ^{46}Sc (163.2 nCi/g of gem), ^{182}Ta (7.14 nCi/g of gem); five minute counting time.**

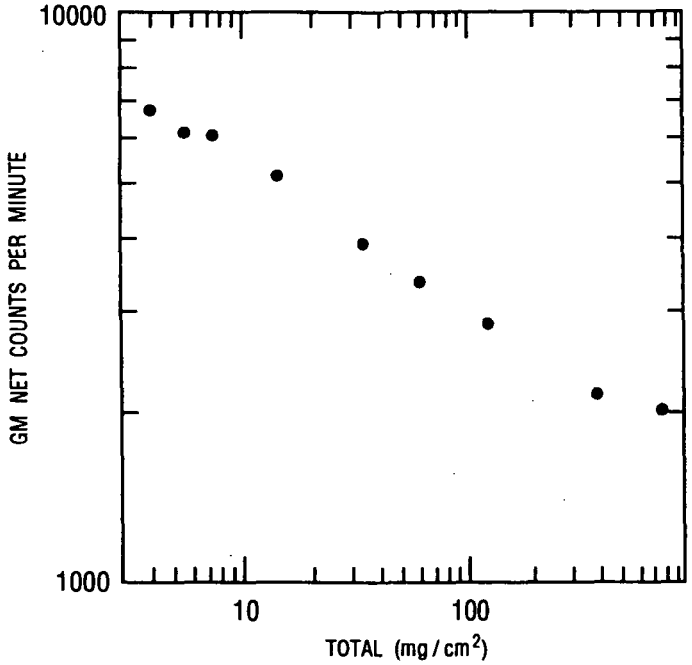

Figure 20. **Log-log GM response for gem #30. Origin: Brazil; HFBR irradiation date: 1/3/89; fast neutron fluence: 1.0 x 10^{18}; mass: 0.1105g; gamma activity present on 3/11/89: ^{59}Fe (2.61 nCi/g of gem), ^{46}Sc (163.2 nCi/g of gem), ^{182}Ta (7.14 nCi/g of gem); five minute counting time.**

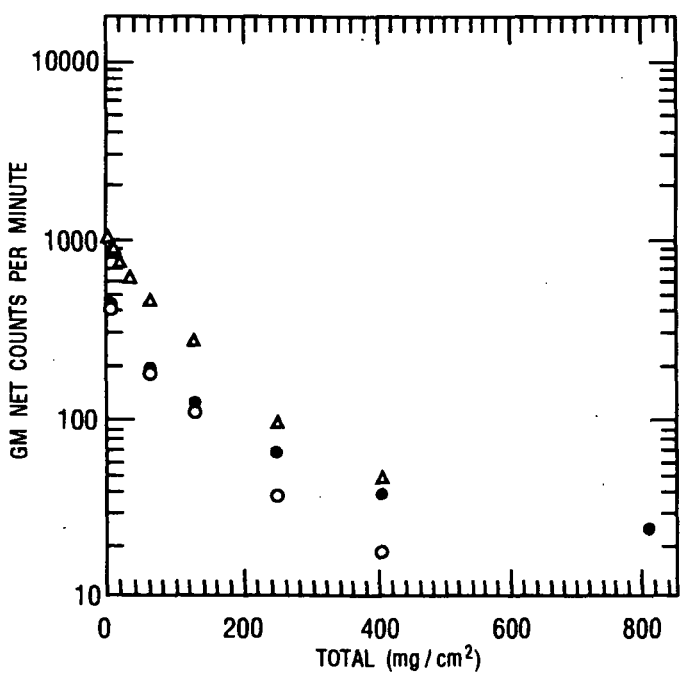

Figure 21. **Log-linear GM response for gem #31. Origin: Sri Lanka; HFBR irradiation date: 1/3/89; fast neutron fluence: 1.0 x 10^{18}; mass: 0.50826g; gamma activity present on 4/1/89: ^{59}Fe (0.064 nCi/g of gem), ^{46}Sc (1.80 nCi/g of gem), ^{182}Ta (4.25 nCi/g of gem); five minute counting time; △=3/14/89 GM count, ●=4/-2/89 GM count, ○=^{32}P decay corrected GM count on 4/2/89.**

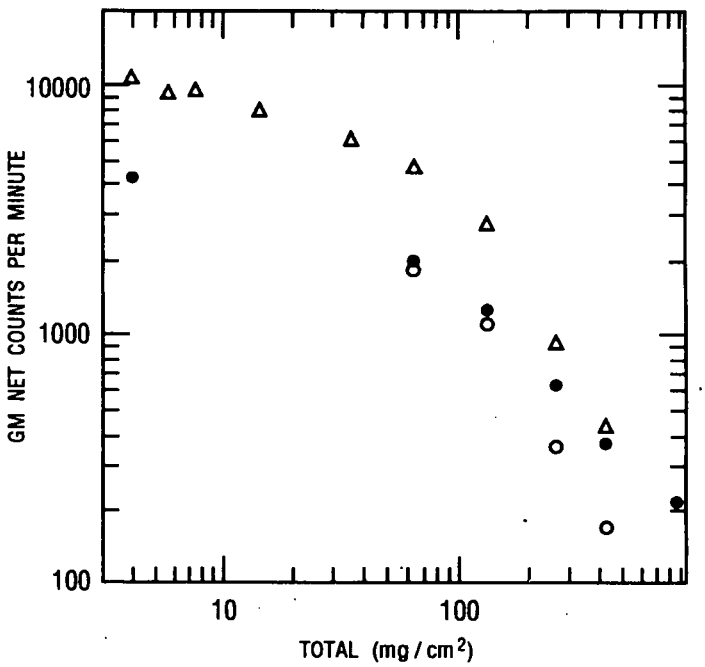

Figure 22. Log-log GM response for gem #31. Origin: Sri Lanka; HFBR irradiation date: 1/3/89; fast neutron fluence: 1.0 x 10^{18}; mass: 0.50826g; gamma activity present on 4/1/89: ^{59}Fe (0.064 nCi/g of gem), ^{46}Sc (1.80 nCi/g of gem), ^{182}Ta (4.25 nCi/g of gem); five minute counting time; △=3/14/89 GM count, ●=4/-2/89 GM count, ○=^{32}P decay corrected GM count on 4/2/89.

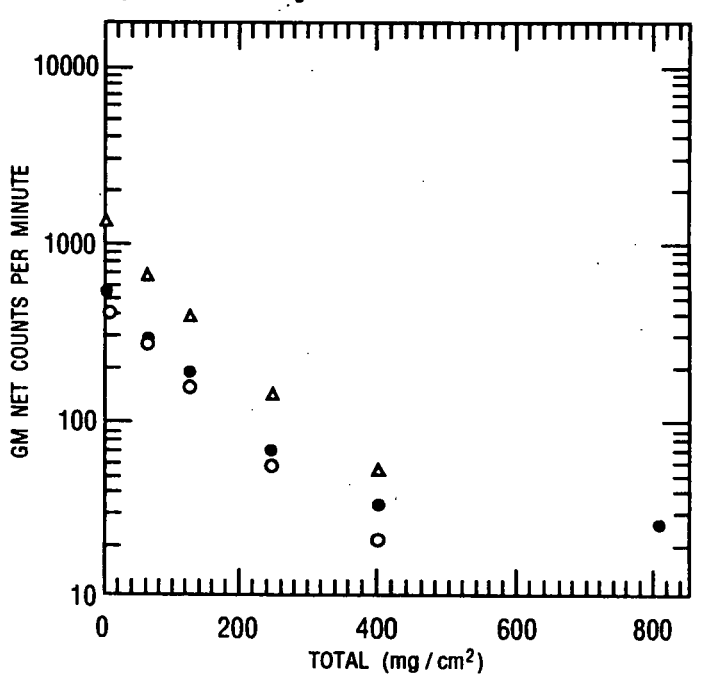

Figure 23. Log-linear GM response for gem #32. Origin: Sri Lanka; HFBR irradiation date: 1/3/89; fast neutron fluence: 1.0 x 10^{18}; mass: 0.51767g; gamma activity present on 4/1/89: ^{59}Fe (0.22 nCi/g of gem), ^{46}Sc (3.22 nCi/g of gem), ^{182}Ta (1.19 nCi/g of gem), ^{51}Cr (0.44 nCi/g of gem); five minute counting time; △=3/14/89 GM count, ●=4/2/89 GM count, ○=^{32}P decay corrected GM count on 4/2/89.

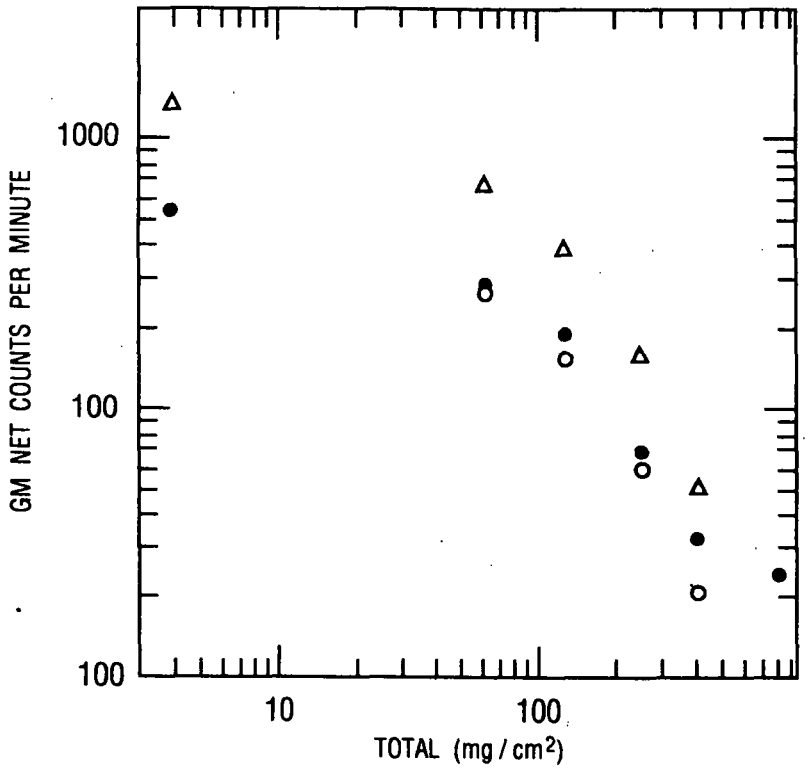

Figure 24. Log-log GM response for gem #32. Origin: Sri Lanka; HFBR irradiation date: 1/3/89; fast neutron fluence: 1.0 x 10^{18}; mass: 0.51767g; gamma activity present on 4/1/89: ^{59}Fe (0.22 nCi/g of gem), ^{46}Sc (3.22 nCi/g of gem), ^{182}Ta (1.19 nCi/g of gem), ^{51}Cr (0.44 nCi/g of gem); five minute counting time; Δ=3/14/89 GM count, ●=4/2/89 GM count, ○=^{32}P decay corrected GM count on 4/2/89.

The near-linear GM absorption characteristics for gems lacking ^{32}P (Figs. 14, 16, 18, and 20) plotted on a log-log scale was unexpected.

Figures 25 to 34 show the GM response to plastic disk samples measuring 13/32" diameter 1/4" deep, of ground topaz (about 0.58 grams of 30 mesh) saturated with standard solutions containing ^{54}Mn, ^{182}Ta, ^{59}Fe, ^{14}C, or ^{36}Cl and then dried. Both log-log and log-linear graphs are included. All the standards were dried at 30 to 40°C for 12 hours before counting. Two different standards, counted for five minutes each, were used for each graph.

The general shape of the curves were similar between gamma emitters, i.e., ^{54}Mn, ^{182}Ta, and ^{59}Fe and between beta emitters, i.e., ^{14}C and ^{36}Cl. The pure beta emitter, ^{36}Cl, could be distinguished from gamma emitters and ^{32}P if ^{36}Cl concentrations predominated. Based on these results, attenuation measurements with a shielded GM counter could not distinguish gamma emitters from each other, nor beta emitters from each other.

GM beta absorption analysis on several RPI LINAC irradiated topaz gems was conducted 17 hours after irradiation. The results, shown in Figures 35 and 36, cannot be used to determine the identity of the beta emitters present.

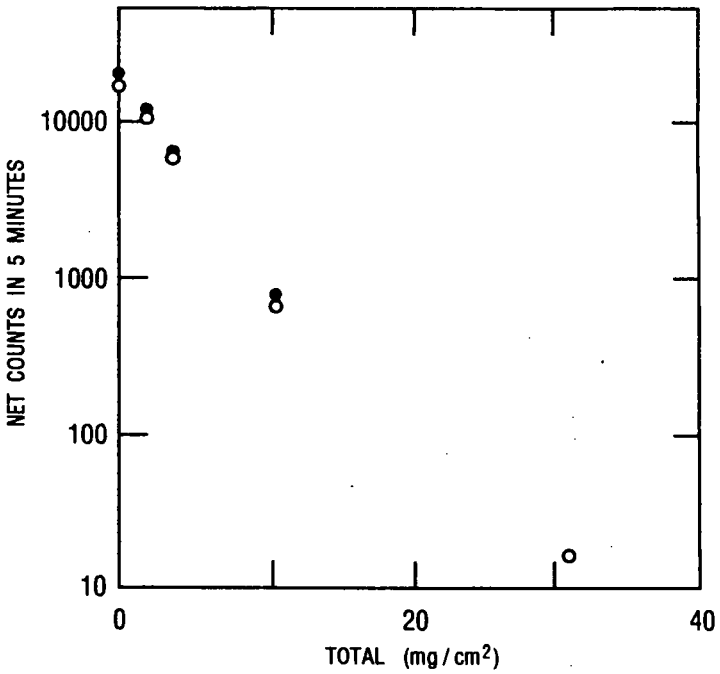

Figure 25. **Log-linear GM response to ^{14}C. nCi/g of ground topaz (30 mesh) as determined on 3/22/89. ●=^{14}C, 387.26 nCi/g; ○=^{14}C, 367.21 nCi/g; five minute counting time.**

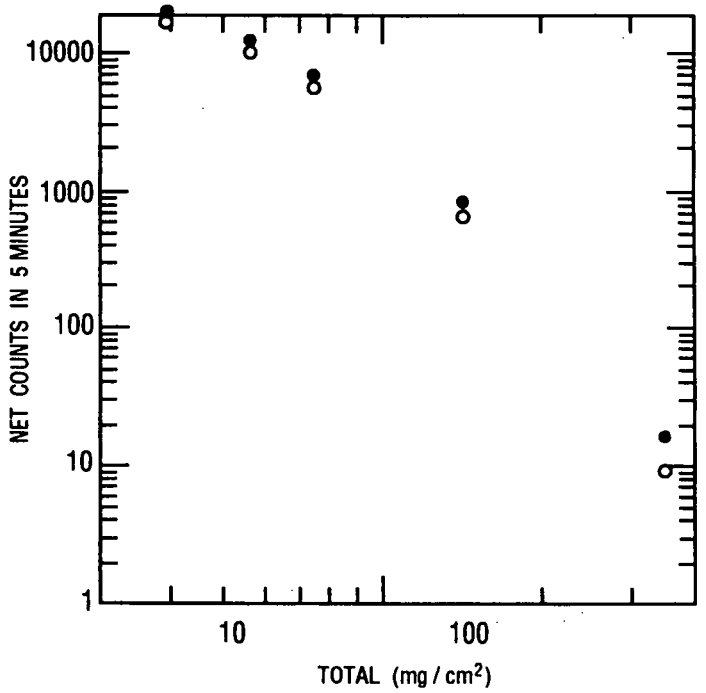

Figure 26. **Log-log GM response to ^{14}C. nCi/g of ground topaz (30 mesh) as determined on 3/22/89. ●=^{14}C, 387.26 nCi/g; ○=^{14}C, 367.21 nCi/g; five minute counting time.**

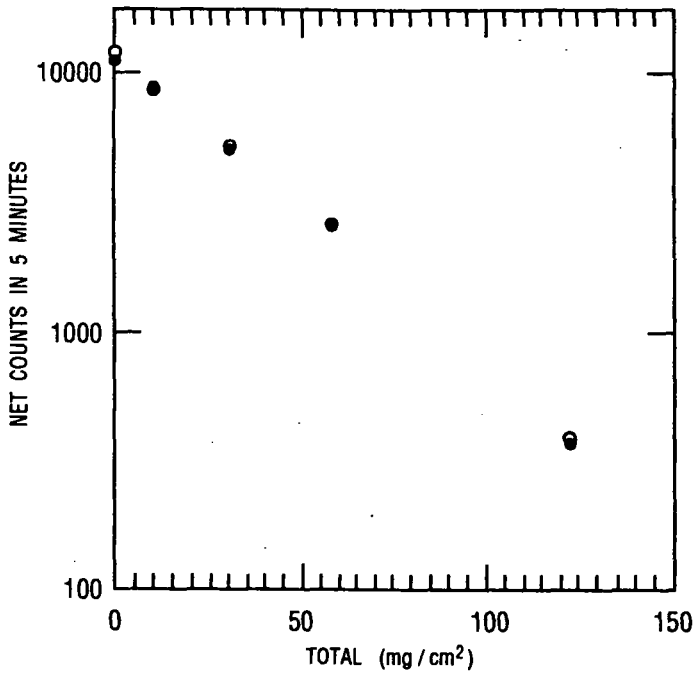

Figure 27. **Log-linear GM response to ^{36}Cl. nCi/g of ground topaz (30 mesh) as determined on 3/22/89. ○=^{36}Cl, 25.91 nCi/g; ●=^{36}Cl, 30.98 nCi/g; five minute counting time.**

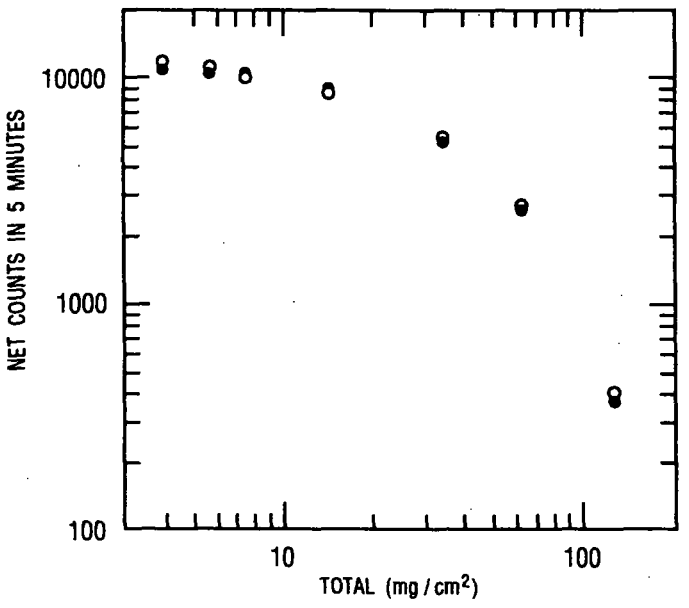

Figure 28. **Log-log GM response to ^{36}Cl. nCi/g of ground topaz (30 mesh) as determined on 3/22/89. ○=^{36}Cl, 25.91 nCi/g; ●=^{36}Cl, 30.98 nCi/g; five minute counting time.**

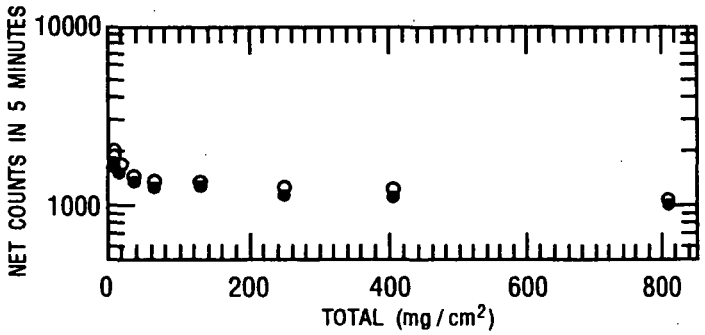

Figure 29. Log-linear GM response to ^{54}Mn. nCi/g of ground topaz (30 mesh) as determined on 3/22/89. ●=^{54}Mn, 79.02 nCi/g; ○=^{54}Mn, 80.34 nCi/g; five minute counting time.

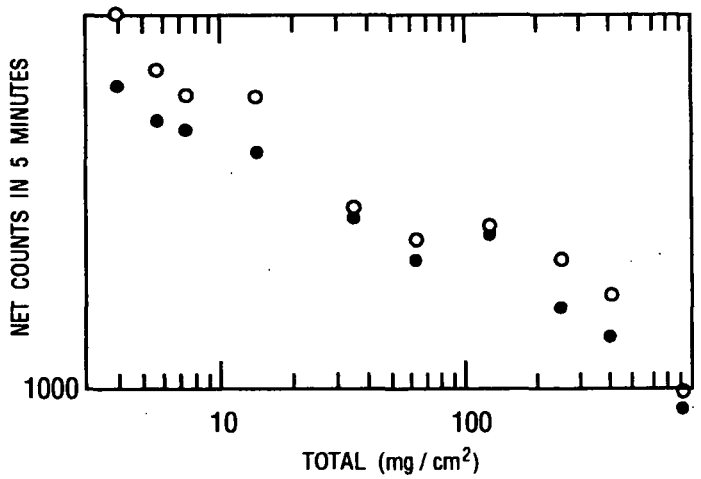

Figure 30. Log-log GM response to ^{54}Mn. nCi/g of ground topaz (30 mesh) as determined on 3/22/89. ●=^{54}Mn, 79.02 nCi/g; ○=^{54}Mn, 80.34 nCi/g; five minute counting time.

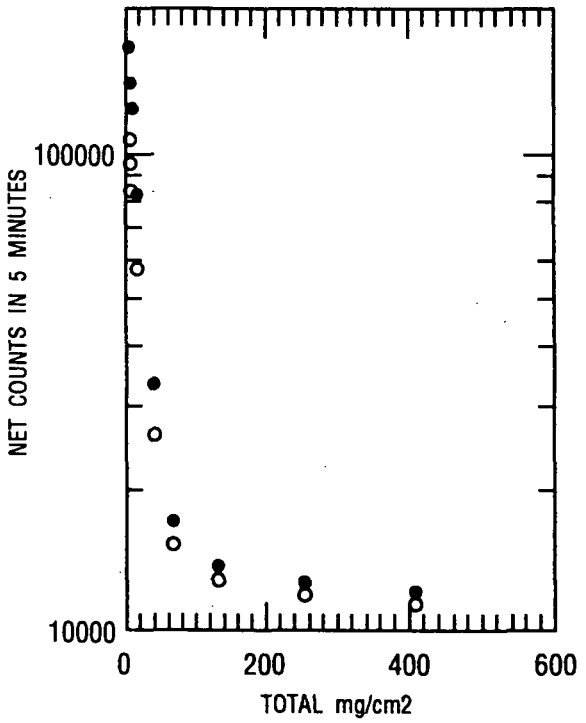

Figure 31. **Log-linear GM response to ^{59}Fe. nCi/g of ground topaz (30 mesh) as determined on 3/22/89. ●=^{59}Fe, 543.91 nCi/g; ○=^{59}Fe, 434.07 nCi/g; five minute counting time.**

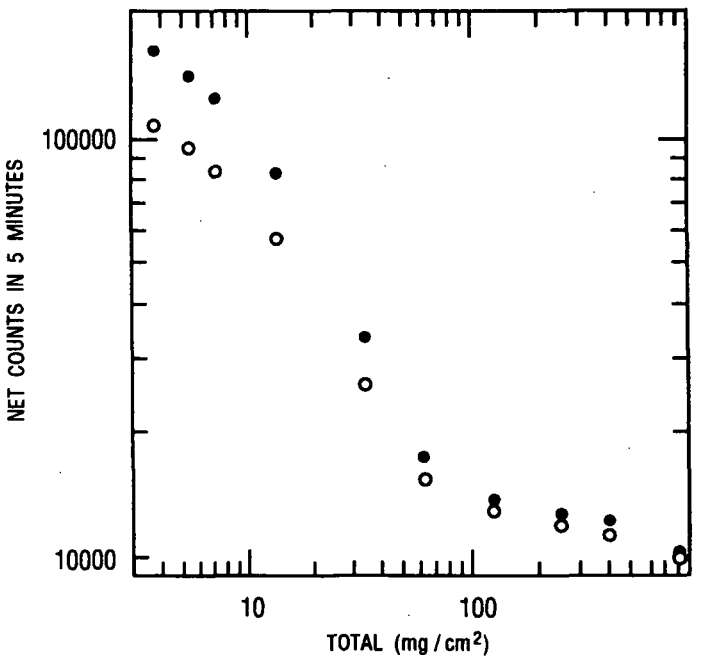

Figure 32. **Log-log GM response to ^{59}Fe. nCi/g of ground topaz (30 mesh) as determined on 3/22/89. ●=^{59}Fe, 543.91 nCi/g; ○=^{59}Fe, 434.07 nCi/g; five minute counting time.**

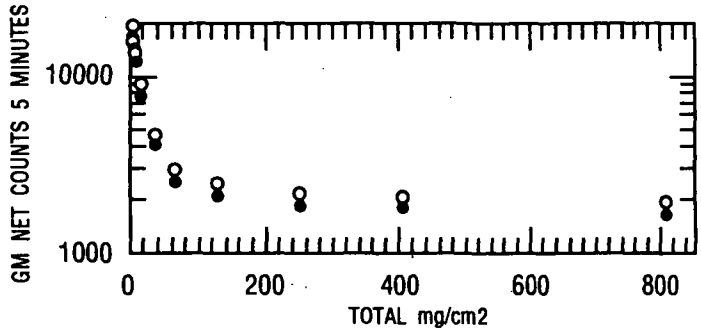

Figure 33. **Log-linear GM response to ^{182}Ta. nCi/g of ground topaz (30 mesh) as determined on 3/22/89. ●=^{182}Ta, 70.89 nCi/g; ○=^{182}Ta, 73.95 nCi/g; five minute counting time.**

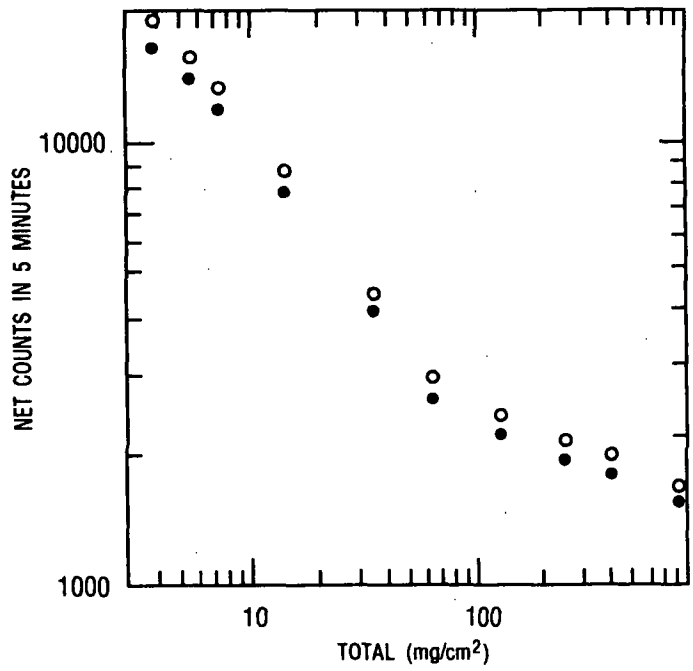

Figure 34. **Log-log GM response to ^{182}Ta. nCi/g of ground topaz (30 mesh) as determined on 3/22/89. ●=^{182}Ta, 70.89 nCi/g; ○=^{182}Ta, 73.95 nCi/g; five minute counting time.**

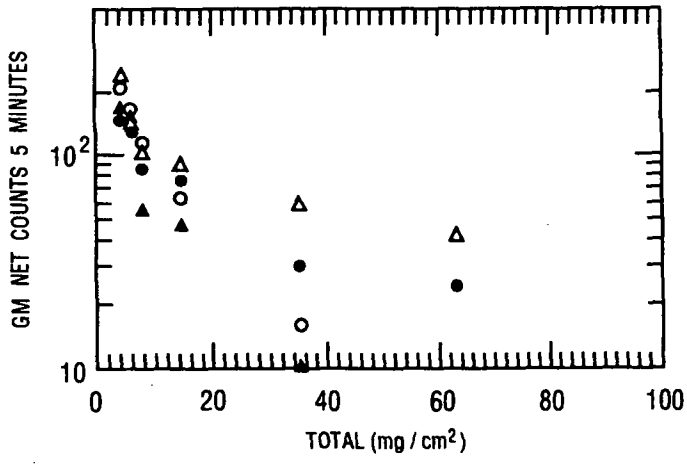

Figure 35. **GM response to electron irradiated topaz (gems #77, 79, 82, 85). RPI LINAC-irradiated topaz. End of irradiation on 15:30 5/18/89, GM counts started on 08:30 5/19/89. ○=Gem 77, △=Gem 79, ●=Gem 82, ▲=Gem 85.**

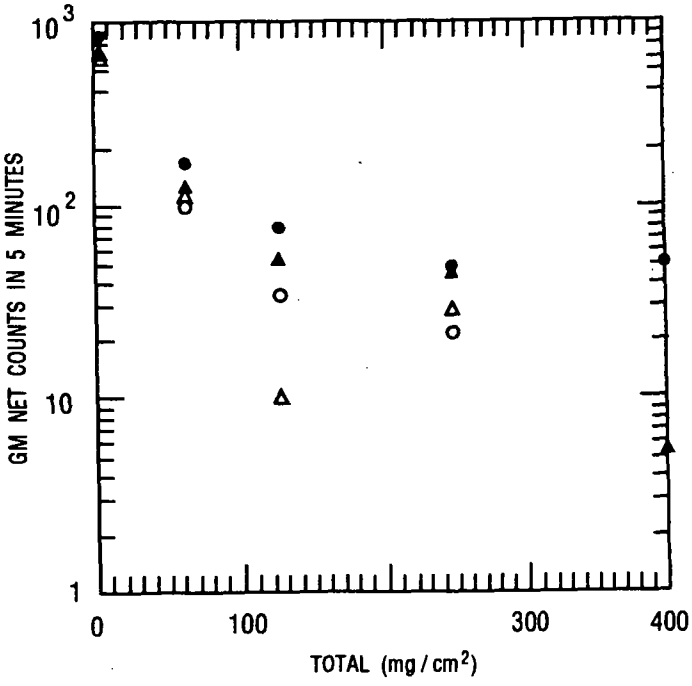

Figure 36. **GM response to electron-irradiated topaz (gems #54, 57, 67, 87). RPI LINAC-irradiated topaz. End of irradiation on 15:30 5/18/89, GM counts started on 08:30 5/19/89. ○=Gem 54, △=Gem 57, ●=Gem 67, ▲=Gem 87.**

The GM sensitivity and net cpm/g for several isotopes contained in the ground topaz samples and identified or suspected is presented in Table 31.

Table 31. GM Detector Response

Nuclide	GM Detector sensitivity, S (net cpm/nCi)	Net cpm/g (S x exempt conc)
^{46}Sc	109	43.7
^{54}Mn	8.3	8.3
^{182}Ta	114	45.8
^{32}P	646	129
$^{14}C(^{35}S)$	17.4	10.4
^{59}Fe	104	62.5
^{36}Cl	157	0.157*

*Not expected nor detected in gems.

The minimum detectable activity for irradiated topaz counted on a GM counter was calculated by the following equation (NCRP, 1978b):

$$MDA = \frac{k_\alpha + k_\beta \sqrt{2bt}}{St} \quad (13)$$

where,

MDA = the minimum detectable activity, nCi
k_α = a constant that reflects the probability of making a Type I error (i.e., stating activity is > MDA, when true activity is < MDA)
k_β = a constant that reflects probability of making a Type II error (i.e, falsely stating activity is < MDA when it is > MDA)
b = the background count rate, e.g., 24 cpm
t = the counting time, e.g., min
S = the sensitivity of the detector, e.g., cpm/nCi

Typical k factors are given in Table 32.

Table 32. k Factors

α or β	k_α or k_β
0.001	3.10
0.005	2.58
0.01	2.33
0.025	1.96
0.05	1.65
0.10	1.28
0.50	0.00

By rearranging equation 11 and solving for the required counting time, t, the following equation was obtained:

$$t = \frac{77.4b}{(SxMDA)^2} \qquad (14)$$

Setting MDA = twice the exempt concentration multiplied by the gem's weight allowed us to calculate the required counting time at a 99.9% confidence level.

The GM detector counting times necessary to detect double the 10CFR30.70 exempt concentrations for various topaz masses are given in Table 33, based on these results. The required counting times were determined from equation 12. The k_α and k_β factors were taken to be 0.001 and the shielded background count rate was assumed to be 24 cpm (this implies there are no other beta emitters in the sample which would contribute to counting rates).

Table 33. Required Counting Time in Minutes to Detect 2x Exempt Concentration Levels With A Shielded GM Detector

Nuclide	Net cpm/g (S x exempt conc.)	Stone mass		
		0.2 g	0.5 g	1.0 g
^{46}Sc	43.7	6.0	1.0	0.2
^{54}Mn	8.3	169.0	27.0	6.7
^{182}Ta	45.8	5.8	0.9	0.2
^{32}P	129.1	0.7	0.1	0.03
^{35}S*	10.4	107.1	17.2	4.3
^{59}Fe	62.5	3.0	0.5	0.1

*^{14}C was used for calibrations because it emits beta particles with nearly the same energy.

The required shielded GM counting times necessary to detect twice the exempt concentration levels of ^{46}Sc, ^{182}Ta, ^{59}Fe, and ^{32}P in irradiated topaz (mass greater than 0.5 g) were ≤ one minute, at 99.9% confidence. An exempt concentration of ^{35}S in a 0.5 g gem would require about 17 minutes counting time. The most restrictive nuclide in the table, ^{54}Mn, would require that a 0.5 g topaz gem be counted for approximately 27 minutes to detect twice an exempt concentration. However, this isotope can be detected more readily by gamma detectors, as described previously.

4.6 Measurements of the GM Survey Meter

All irradiated gems were counted in direct contact with an unshielded Ludlum Model 12 GM, equipped with a Model 44-9 probe. These measurements were compared to the gamma-induced radioactivity for the same gem. Table 34 gives the results. The total gamma activity (nCi) per gram of topaz, corrected for decay, not containing ^{32}P ranged from 1.5 to 635.6 for larger gems (~1 cm^3), and 0.3 to 957.6 for smaller Brazilian stones (~0.33 cm^3). Size distinction was necessary because the GM response was not independent of the stone's mass. The GM response for these observations was 13 to 40 net cpm/(nCi/g) for larger stones, respectively, and 0 to 3 net cpm/(nCi/g), respectively, for the smaller gems. Assuming a background of 50 cpm, an unshielded GM probe would not identify gems exceeding the 10 CFR 30.70 limits. The net cpm/nCi of gamma activity per gram of gem ranged from 18 to 1851 for stones containing ^{32}P. The response of the unshielded GM detector/probe (net cpm/nCi of ^{32}P per gram of topaz) was not known because of the difficulty in quantifying the amount of ^{32}P present. All stones containing ^{32}P were classified as large (~1 cm^3) in this study.

Table 34. Response of Ludlum Model 12 GM Readings with 44-9 Probe Compared to Gamma Emitting Nuclide Concentration[a]

Gem #	Max. cpm table facet exposure (4/11/89)	Decay corrected nCi/g to 4/11/89					Net cpm per nCi/g (assume bkg=50 cpm)
		^{46}Sc	^{59}Fe	$^{182}Ta^{b}$	^{51}Cr	Total	
1	100	1.6	0.5			2.1	24
2	200	10.0	0.7	0.4		11.1	14
3	160	6.5	0.3			6.8	16
4	bkg	0.9	0.5	0.5		1.9	
5	100	2.9	0.3			3.2	16
6	160	7.7	0.5			8.2	13
7	110	0.9	0.4	0.2		1.5	40
8	130	5.1	0.5	0.5		6.1	74
9	180	10.5	0.4			10.9	12
10	bkg	1.5	0.2		<0.1	1.7	
11	550	6.8	0.2	18.7		25.7	19
12*	1700	17.2	0.7	0.5		18.4	90
13	750	5.2	0.1	2.4	0.1	7.8	91
14	3300	291.7	10.3	2.3		304.3	11
15*	3400	22.9	0.9	0.4	1.2	25.4	132
16	5500	253.6	24.9	12.4		290.9	19
17	5500	356.4	19.1	5.6		380.8	14
18	300	6.2	0.4	1.3	0.5	8.4	30
19	220	6.5	0.4	0.5	0.6	8.0	21

See footnotes at end of table

Table 34. Response of Ludlum Model 12 GM Readings with 44-9 Probe Compared to Gamma Emitting Nuclide Concentration[a] (continued)

Gem #	Max. cpm table facet exposure (4/11/89)	Decay corrected nCi/g to 4/11/89					Net cpm per nCi/g (assume bkg=50 cpm)
		^{46}Sc	^{59}Fe	^{182}Ta[b]	^{51}Cr	Total	
20**	500	113.3	3.2	1.7	4.8	123.0	4
21**	650	145.0	1.7	1.7		148.4	4
22**	3100	946.4	8.4	2.8		957.6	3
23**	250			30.3		30.3	7
24**	1500	446.4	3.4			449.8	3
25**	2400	323.1	1.6	400.6		725.3	3
26**	200	47.5	1.5	10.1		59.1	3
27**	1000	79.4	1.9	232.0		313.3	3
28**	120	5.9	2.8	9.7	0.7	19.1	4
29**	180	0.7		27.0		27.7	5
30**	450	120.1	0.4	5.5	1.1	128.1	3
31*	330	1.5	0.1	4.1		5.7	49
32*	450	2.9	0.2	1.3	0.4	4.8	85
33*	240	1.1	0.1	0.7	0.3	2.2	87
34*	200	1.4	0.1	4.2		5.6	26
35*	600	1.9		28.5	0.4	30.8	18
36	8500	1.7		633.9		635.6	13
37**	bkg	1.4	0.6			2.0	
38**	100	5.7	0.6		1.1	7.4	7

See footnotes at end of table

Table 34. Response of Ludlum Model 12 GM Readings with 44-9 Probe Compared to Gamma Emitting Nuclide Concentration[a] (continued)

Gem #	Max. cpm table facet exposure (4/11/89)	Decay corrected nCi/g to 4/11/89					Net cpm per nCi/g (assume bkg=50 cpm)
		^{46}Sc	^{59}Fe	^{182}Ta[b]	^{51}Cr	Total	
39**	220	71.0	0.6			71.6	2
40**	180	40.3	0.9	1.9		43.1	3
41**	bkg	5.6	0.7			6.3	
42**	bkg	7.3				7.3	
43**	100	1.0	0.2			1.2	43
44**	bkg	0.2	0.1			0.3	
45**	bkg	0.7	0.1			0.8	
46**	bkg	0.3	0.1			0.4	
47*	7500	13.4	10.8	41.7	0.5	66.4	112
48*	62000	25.2	4.5	3.4		33.4	1851
49	1400	120.8	2.6	1.7		125.1	11
50*	12300	17.2	5.6	0.8		23.6	518
51	1100	138.6	2.7	2.3		143.6	7
Bkg	50-75						

*Contains ^{32}P, although gem #35 has decayed to background levels of radiation.
**Small Brazilian stones
[a]Stones placed on the center of probe face. The probe has mylar windows with a thickness of 1.4 to 2.0 mg cm^{-2}. Model 12 GM with 44-9 probe was calibrated 4/4/89.
[b]1221 keV pack.

4.7 Results from the Gas-Flow Proportional Counter

Gas-flow proportional counting with beta absorption analysis on selected topaz (some containing ^{32}P) was conducted, using Tracerlab E-3A aluminum absorbers (S/N 406). An Eberline hemispherical, windowless gas-flow counter supplied with P-10 gas was used. The high voltage was established at 2,425 volts with a ^{36}Cl NIST-traceable source. We gave a minimum 30-sec slow purge (2 bubbles per sec) before each count. A Canberra counter timer (Model 1776), Canberra high voltage power supply (Model 3002), and a Canberra pulse discriminator (set at 6 μsec) were used.

Repeated one-minute counts on individual stones showed an increase with each successive measurement. This unusual effect was greatest when aluminum filters were added. We speculated that the increased count was due to one or more of the following events:

- air leakage from under the aluminum filter;
- electronic perturbations caused by the plastic/aluminum interface;
- water in the P-10 gas line;
- secondary electrons produced in aluminum.

Rubbing a topaz with a cloth can induce a positive charge (Webster, 1983) and, thereby, affect bare wire gas-flow proportional counters by increasing the total number of counts. This charge may last from minutes to hours. Therefore, the results of beta absorption studies using a windowless gas-flow counter should be viewed cautiously. Figure 37 gives the results of gas-flow analyses on selected stones. A mean and high/low range are given for any particular density thickness. There was a large range of net counts at any total mg/cm^2.

4.8 Results from a Plastic Scintillator

We used a plastic scintillator (0.01" Bicron B1) to determine beta activity in topaz gems. Infinitely thin beta standards, ^{36}Cl, ^{14}C, and ^{32}P, covering a wide range of beta energies and radioactive source diameters (1/4" to 1/2") were used to determine the efficiency of the plastic scintillator.

Compared to GM efficiency at the same source-to-detector-distance (1.5 cm), the efficiency of the plastic scintillator was greater for all three isotopes at two different source diameters (see Table 35). The plastic scintillator and GM sensitivity, measured in net cpm/nCi, did not vary with the diameter of the source because the source-to-detector distance was much smaller than the diameter of the detector's face. Table 36 lists the beta sensitivities (net cpm/nCi) for both GM and 0.01" plastic scintillator detectors.

The plastic scintillator response for ^{14}C (and, therefore, ^{35}S) is 207 percent greater than for GM detectors, presumably because of the attenuation of betas in the GM's mica covering. As expected, this effect diminishes with an increase in beta energy (only 14 percent greater efficiency for ^{32}P).

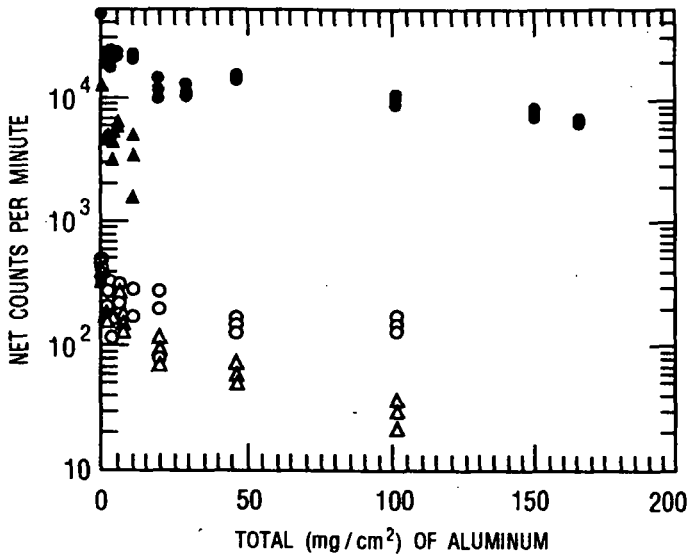

Figure 37. **Beta absorption analysis of irradiated topaz with a windowless gas-flow proportional counter.**
○ = Gem 3, △ = Gem 10, ● = Gem 12, ▲ = Gem 14.

Table 35. Measurements of Infinitely Thin Beta Source

	6/16/89 activity, μCi	6/16/89 0.01" plastic scint. cpm[a]	6/16/89 GM, cpm[b]
^{36}Cl*	0.0159	14,500 ± 121	10,300 ± 102
^{36}Cl-I	0.0522	47,200 ± 217	33,500 ± 183
^{36}Cl-II	0.0548	49,100 ± 222	35,000 ± 187
^{36}Cl-III	0.0552	50,000 ± 224	35,500 ± 188
^{14}C*	0.1752	79,500 ± 282	27,850 ± 167
^{14}C-I	0.5920	305,000 ± 552	86,400 ± 294
^{14}C-II	0.6642	357,000 ± 598	102,350 ± 452
^{14}C-III	0.6494	361,000 ± 601	104,000 ± 323
^{32}P*	0.0094	9,200 ± 96	7,900 ± 89
^{32}P-I	0.0361	35,200 ± 188	29,500 ± 172
^{32}P-II	0.0346	32,500 ± 180	27,900 ± 167
^{32}P-III	0.0335	33,600 ± 183	26,400 ± 163

*1/4" diameter source; all others were 1/2" diameter.
[a]SRM set at 737 V. 1 minute counting time. Bkg=29 cpm.
^{32}P standards counted at approximately 10:45 a.m.
[b]SRM set at 905 V. 1 minute counting time. Bkg=23 cpm.
^{32}P standards counted at approximately 11:00 a.m.

Table 36. Comparison of Sensitivities of a GM and 0.01" Plastic Scintillator Detector, net cpm/nCi

Nuclide	GM Sensitivity	0.01" Plastic Scintillator Sensitivity
^{32}P	853.4 (n=8)	974.0 (n=4)
^{14}C	167.5 (n=8)	515.6 (n=4)
^{36}Cl	695.3 (n=8)	904.5 (n=4)

4.9 Results of Liquid Scintillation Measurements

Liquid scintillation measurements were made on irradiated topaz to determine if beta emitters could be identified and quantified. One ml aliquots of liquid ^{32}P, ^{14}C, and ^{3}H standards were added to 5 ml of scintillation cocktail (Beckman HP) in a plastic scintillation vial. Integrated counts were obtained from channel 0 to 999, channel 50 to 999, etc., for both liquid standards and for the irradiated topaz. Standard graphs determined by this method are shown in Figure 38.

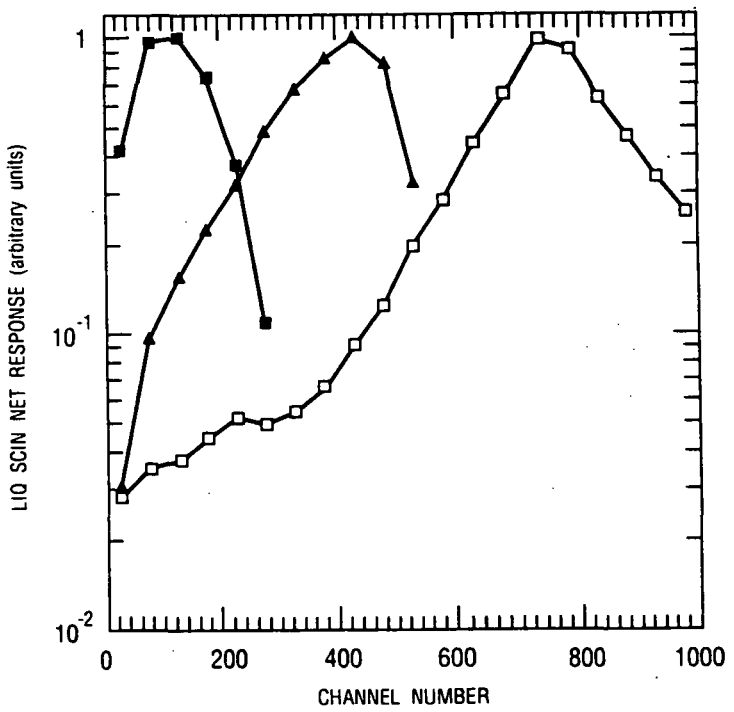

Figure 38. Response of a liquid scintillation counter to ^{3}H, ^{14}C, and ^{32}P. ■=^{3}H, ▲=^{14}C, □=^{32}P.

Irradiated gems were placed in 5 ml of scintillation cocktail (Beckman HP) and counted for five minutes. Examples of integrated counts obtained for gems #12, 15, 25, 30, 31, and 32 are given in Figures 39 to 44, respectively. The curves from stones containing varying amounts of ^{32}P (#12, 15, 31, and 32) were not diagnostic for ^{32}P. This result suggested that the detector's response was predominately due to ^{32}P, and not to low levels of gamma emitters that may be present and that also emit beta emissions, i.e., ^{182}Ta, ^{46}Sc, and ^{59}Fe. The presence of ^{32}P in these stones was verified 68 days later (or 4.75 ^{32}P half-lives) by repeating the liquid-scintillation measurements. The results indicate that a liquid scintillation detector may not be sufficient for topaz beta spectroscopy, but may be an alternative to a GM detector for determining total (open channel) beta activity.

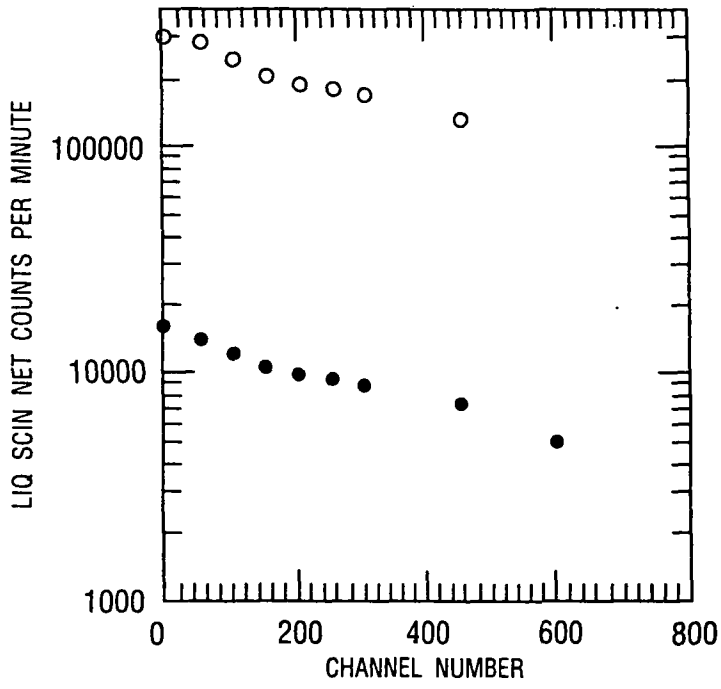

Figure 39. Liquid scintillation counter response to gem #12. Origin: Sri Lanka; HFBR Irradiation Date: 11/21/88; Fast Neutron Fluence: 1.1 x 10^{18}; Mass: 0.5345 g; o=Liquid scintillation measurement made on 1/23/89; •=Liquid scintillation made on 4/1/89; five minute counting time.

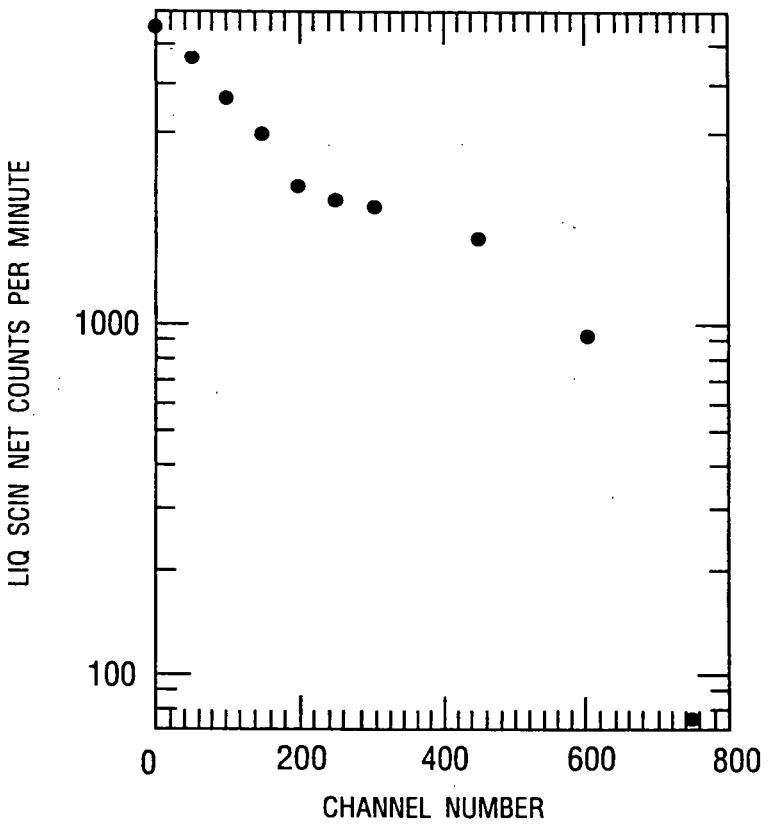

Figure 44. **Liquid scintillation counter response to gem #32. Origin: Sri Lanka; HFBR Irradiation Date: 1/3/89; Fast Neutron Fluence: 1.0 x 10^{18}; Mass: 0.51767g; Liquid scintillation measurements made on 4/1/89; five minute counting time.**

Table 37 compares liquid scintillation (open channel) and gas flow proportional (no absorbers) detectors. The results are not directly comparable, because of the six-day difference between the counts from the liquid scintillation and the gas flow detector. The ten topaz gems studied (none containing ^{32}P) all exhibited a larger liquid-scintillation count. The sensitivity of liquid scintillation (net cpm/(nCi/g) of topaz) ranged from approximately 40 to 3,400, while that of the gas flow counter ranged from 5 to 70 net cpm/(nCi/g). Therefore, neither of these counters would be useful for determining the gamma activity per gram of topaz.

Table 37. Comparisons of Measurements from Liquid Scintillation and Gas-Flow Proportional Counter

Gem #	Net cpm liq. scint[a] 2/10/89	Net cpm windowless gas flow[b] 2/16/89	Decay corrected nCi/g				Total nCi/g (gamma) of gem
			^{46}Sc	^{59}Fe	^{182}Ta[c]	^{51}Cr	
37	1,317±18	232±17	2.2	1.5			3.7
38	2,190±22	389±21	9.0	1.4		4.2	14.6
39	4,913±32	831±30	111.9	1.4			113.3
40	3,896±29	730±28	63.5	2.1	2.7		68.3
41	1,981±21	389±21	8.9	1.6			10.5
42	1,088±17	62±11	11.5				11.5
43	231±10	28±9	1.5	0.4			1.9
44	1,318±18	36±10	0.3	0.3			0.6
45	396±11	35±10	1.1	0.3			1.4
46	2,240±22	40±10	0.4	0.2			0.6

[a]5 minute count. Bkg = 139.8 cpm.
[b]1 minute count. Bkg = 27.5 cpm.
[c]1221 keV peak.

4.10 Determination of Alpha Emitters

The alpha content of unirradiated topaz from India, Brazil, Sri Lanka, Nigeria, and Africa was determined during 13- to 40-hour counting times, using a brass-shielded 2" ZnS/PM (photomultiplier) tube combination. No alpha activity above background was detected. The ZnS detector efficiency was approximately 39% for a NIST ^{241}Am reference source.

4.11 Elemental Determination by X-Ray Fluorescence

Studies of X-ray fluorescence were made on non-irradiated topaz from India, Sri Lanka, and Brazil. Generally, cross-sections for x-ray production (x-ray fluorescence) by charged particles are several orders of magnitude higher than those for nuclear reactions. The beam was spread out over an area of 1 cm^2 or more on the sample for trace analysis using x-ray fluorescence. Resolution was ±160 eV, and the detector was altered to reduce detection of low-energy x-ray emissions.

Iron, nickel, copper, germanium, zinc, and gallium were found in all samples. The K_α x-ray emission line was always the most intense. The iron K_β intensity was approximately 20 percent of the K_α intensity, as expected.

The elements found in topaz (in decreasing order of intensity) were the following: Ge (9.8eV), Ga (9.2eV), Fe (6.39eV), Ni (7.46eV), Cu (8.15eV), and Zn (8.6eV) for Sri Lankian and Indian stones. For Brazilian stones, the ranking was: Ga (9.2eV), Ge (9.8eV), Fe (6.39eV), Ni (7.46eV), Cu (8.15eV), and Zn (8.6eV). The amount of germanium was highest in the Sri Lankian topaz. The amount of iron was highest for the Brazilian topaz, a finding supported by neutron activation studies of topaz containing ^{59}Fe at a given neutron fluence. The amount of gallium was highest in the Brazilian topaz. This result should be confirmed by neutron activation analysis of stones shortly after irradiation.

Germanium (determined by x-ray fluorescence) would be neutron activated via (n,γ) reactions (Table 38).

Table 38. Activation Products of Germanium[a]

Parent Isotope	Percent abundance of parent	Ther. neutron cross-section barns	Activation product	T½ of product, hr
^{70}Ge	20.6	3.2	^{71}Ge	268.8
^{74}Ge	36.7	0.3	^{75}Ge	1.4
^{76}Ge	7.7	0.1	^{77}Ge	11.3

[a]From Bureau of Radiological Health, 1970.

Based on a review of the half-lives and emission spectra, the detection of only ^{77}Ge would be expected. ^{77}Ge was found in BNL irradiated topaz #38 (Brazil), and #47-51 (Nigeria), and was positively identified only because of the relatively long period (several months) needed to allow the activity to decay to acceptable levels. Also, an initial short count was conducted on each sample to ensure that all gems containing short-lived activity could be

analyzed within a relatively short period (<1 day). This short counting-time raised the lower level of detection, making analysis of nuclides with photopeaks of small relative intensity very difficult.

4.12 Determination of Pure Beta Emitters

The potential reactions that create pure beta emitters during neutron irradiation are listed in Table 39. Our selection of the pure beta emitters was based on their potential for skin exposure. The mass of parent (precursor) nuclide needed to produce an exempt concentration of pure beta-emitting end-product above the exemption level was calculated (see Table 40) using equation 8. The mass of parent nuclide depended on the fluence rate and irradiation time.

Table 39. Cross-Sections For Reactions That Produce Beta-Emitting Nuclides

Parent nuclide (fractional abundance[a])	Reaction	End product	14 MeV neutron cross section, b	Thermal neutron cross section, b
^{32}S (0.95)	n,p	^{32}P	0.2517[e]	
^{33}S (0.0076)	n,p	^{33}P	0.2450[d]	
^{34}S (0.0422)	n,γ	^{35}S		0.27[a]
^{35}Cl (0.7553)	n,p	^{35}S	0.100[c]	
^{35}Cl (0.7553)	n,α	^{32}P	0.130[f]	
^{35}Cl (0.7553)	n,γ	^{36}Cl		41.8[c]
^{31}P (1.0)	n,γ	^{32}P		0.199[b]

[a]Bureau of Radiological Health, 1970.
[b]BNL-NCS-31451, 1982.
[c]McLane et al., 1988.
[d]^{33}S (n,p) values derived from $_{16}S$ values in BNL-NCS-31451, 1982.
[e]Threshold at 949 keV Ref: BNL-NCS-31451, 1982.
[f]Threshold at 3 MeV Ref: McLane et al., 1988.

The thermal neutron cross-section was used for all (n,γ) reactions and the 14 MeV neutron cross-section for all (n,p) and (n,α) reactions. In addition, two different post-irradiation times were chosen, i.e., t = 0 days, and t = 30 days.

In Table 40, Case 1 is defined as a fast neutron fluence rate of 7.5 x 10^{11} fast neutrons/(cm^2 sec) and an irradiation time of 405.55 hr. The thermal fluence rate was not considered because cadmium shielding was used during this irradiation. Case 2 is defined as a fast neutron fluence rate of 3 x 10^{14} fast neutrons/(cm^2 sec), a thermal neutron fluence rate of 2 x 10^{14} thermal neutrons $cm^{-2}sec^{-1}$, and an irradiation time of 0.93 hrs.

Because of the relatively large amount of ^{35}Cl needed to produce ^{36}Cl and the evidence from x-ray flourescence and PIXE analysis, that such concentration did not exist, the production

of detectable amounts of ^{36}Cl via thermal neutron activation is unlikely. On the other hand, ^{32}P, ^{33}P, and ^{35}S are likely to be produced via fast neutron reactions at or above exempt concentration levels.

Table 40. Mass of Parent Nuclide in Grams Needed to Produce a Concentration of End Product at or Above the Exempt Level In a 1 Gram Topaz

Reaction	Case 1 t=0 days	Case 2 t=0 days	Case 1 t=30 days	Case 2 t=30 days
$^{32}S(n,p)^{32}P$	$3.9x10^{-9}$	$2.9x10^{-9}$	$1.7x10^{-8}$	$1.2x10^{-8}$
$^{33}S(n,p)^{33}P$	$7.4x10^{-7}$	$6.5x10^{-7}$	$7.7x10^{-6}$	$1.5x10^{-6}$
$^{34}S(n,\gamma)^{35}S$		$1.7x10^{-6}$	$3.9x10^{-8}$	$2.2x10^{-6}$
$^{35}Cl(n,p)^{35}S$	$1.9x10^{-7}$	$1.9x10^{-7}$	$2.3x10^{-7}$	$2.4x10^{-7}$
$^{35}Cl(n,\alpha)^{32}P$	$1.1x10^{-8}$	$7.9x10^{-9}$	$4.5x10^{-8}$	$3.4x10^{-8}$
$^{35}Cl(n,\gamma)^{36}Cl$*		$6.9x10^{-3}$		$6.9x10^{-3}$
$^{31}P(n,\gamma)^{32}P$		$5.1x10^{-9}$		$2.2x10^{-8}$

*Exempt concentration for this study assumed to be 1/5 that for ^{38}Cl based on relative β emissions.

To calculate the total amount of end product requires the summation of all products produced by thermal- and fast-neutron reactions. The most restrictive reactions (the smallest mass of parent nuclide necessary to produce 10 CFR 30.70 exempt concentrations) appear to be those of ^{32}S (n,p) ^{32}P, ^{33}S (n,p) ^{33}P, and ^{35}Cl (n,p) ^{35}S in the production of ^{32}P, ^{33}P, and ^{35}S, respectively. The existence of these parent nuclides could neither be confirmed nor denied by x-ray fluorescence or PIXE analysis because of the small amount of parent nuclide required.

End products produced via (n,γ) reactions are directly related to thermal neutron fluence, and reducing the fluence would reduce the amount of these radioactive end products.

In an attempt to determine parent nuclide composition, an irradiated Nigerian topaz was heated to 950°C with Na_2CO_3 acting as a flux. Although unirradiated topaz fused with Na_2CO_3 at this temperature, the irradiated topaz only partially fused indicating possibly surface hardening caused by irradiation. Higher temperatures (up to 1,200°C) and a different chemical flux, i.e., NaF, will be used in a future attempt to fuse irradiated topaz. At such temperatures, topaz decomposes to the mineral mullite, $Al_6Si_2O_{13}$, with the loss of silicon tetrafluoride and water. The synthesis of topaz is difficult because of the temperature of decomposition.

PIXE analysis was conducted on non-irradiated Brazilian, Sri Lankian, and Indian topaz to determine the concentrations of components with a low atomic number. Pellets made up of approximately 20 percent (by volume) of topaz and 80 percent of graphite were subjected to 3,000 psi pressure. Graphite was necessary to reduce the internal buildup charge caused by proton interaction in the topaz. Fluorine, aluminum, silicon, and calcium were found in

all samples. Sulphur, chlorine, and phosphorus, the precursors for pure beta emitters, ^{35}S and ^{32}P, were conspicuously absent. NBS Standard SRM 89 containing 0.23 percent, 0.03 percent, and 0.05 percent (nominal weight) of P_2O_5, SO_3, and Cl, respectively, was used to determine if P, S, or Cl (the precursors of beta emitters) could be detected. None of these elements were detected. The PIXE minimum detectable level (MDL) is a non-uniform function of atomic number, due to the variation of proton cross-section with proton energy. Also, different matrix compositions alter the proton stopping- power, although this effect is minimal for trace elements with concentrations less than 10 ppm. A change in proton stopping-power changes the mass per unit area penetrated by the beam. Previous PIXE research using a 2.55 MeV proton beam and a Ge(Li) detector (although the detector contained absorbers) gave the following MDLs (values approximate): P - 1000 ppm; S - 425 ppm, and Cl - 250 ppm. The lowest MDLs (at less than 10 ppm) included Ni, Zn, Ga, and Ge (Carlsson and Akselsson, 1981).

4.13 Results of Autoradiography

Autoradiography was performed on irradiated gemstones to determine if film could be used as a screening technique for exempt concentrations of induced radioactivity. Assuming that the beta emissions from beta/gamma emitters identified in topaz cause most of the blackening on the film and that the MeV/disintegration from these beta emissions are approximately equal, then all net darkening values can be normalized. The variables considered were the topaz-film interface and the presence of other beta- emitting nuclides not detected by gamma ray spectroscopy (i.e., ^{32}P and ^{35}S). For our comparisons of net darkening, we assumed that there was a uniform concentration of beta-emitting isotopes within irradiated topaz.

Carbon paper interfacing was chosen because of its opaqueness and its low density thickness (see Table 41). An opaque material eliminated any self-scintillations within the gemstone.

Table 41. Density Thickness of Film Interfacing Material

Material	mg/cm^2
Double-sided mylar	6.79
"Reynolds Wrap" mylar	5.81
Carbon paper	3.25

The normalized net darkening (absorption in density units) per hr divided by the total nCi of gamma emitter per gram of stone (abbreviated NDC) gave values of approximately 0.0004 to 0.0007 on bare film, and 0.0002 to 0.0004 on carbon-paper interface, irrespective of high concentrations of ^{182}Ta (gem #23), ^{46}Sc (gem #3), or ^{59}Fe.

The net darkening per hour was low, even for an individual topaz containing a large total activity (nCi per gram of topaz). For example, stone #14 contained over 500 nCi/g (total) of ^{46}Sc, ^{59}Fe, and ^{182}Ta, but only yielded 0.0001 to 0.0002 NDC.

For stones known to contain ^{32}P, i.e., #12, 15, and 31-34, the NDC ranged from 0.0019 (gem 34) to 0.0047 (gem 33) on bare film. Carbon-paper interfacing reduced the reading

by about 35 to 40 percent. The presence of ^{32}P did not affect this ratio as much as low-energy beta-emitters because the energy of the 1.71 MeV beta was sufficient to penetrate the carbon paper.

Overall, the presence of ^{32}P increased the net darkening on bare film and carbon-paper interfacing by a factor of 2.7 to 11.8. Allowing 42 days for decay reduced the net darkening by gem #12 from 0.01699 NDC to 0.0023, and by gem #15 from 0.0114 to 0.0017. This decrease in darkening closely followed the radioactive decay of ^{32}P ($T_{½}$ = 14.3d).

A rim-darkening effect was noted on bare film for gems #42-46. The NDC ranged from 0.0015 to 0.0467 on the rim to 0.0012 to 0.0382 in the center (film contact point) of the topaz. A low-energy beta-emitter such as ^{35}S may be responsible for this occurrence. Carbon paper (3.25 mg/cm^2) would attenuate a large fraction of ^{35}S particles (max beta range = 32 mg/cm^2). Table 42 lists the counting times needed to measure exempt concentrations in gemstones, 0.4 nCi/g and 1.0 nCi/g, on bare film and with a carbon-paper interface.

Table 42. Autoradiography Exposure Time Necessary to Detect Exempt Concentration Levels in Topaz, hr.

Bare Film		Carbon Paper Interfacing	
0.4 nC/g	1.0 nC/g	0.4 nC/g	1.0 nC/g
833	333	1666	666

Assumes bare film level of 0.0006 NDC and 0.0003 on the carbon paper interface.
Assumes a minimum visible darkening of 0.20 (bkg = 0.17).

Therefore, autoradiography has limited importance for screening exempt concentrations of γ/β emitters typically found in neutron-irradiated topaz (i.e., ^{46}Sc, ^{56}Fe and ^{182}Ta).

Assuming an NDC of 0.015, a counting time of 66.7 hr would be required to detect ^{32}P occurring in a neutron-irradiated gemstone (1.1 x 10^{18} fast neutrons/cm^2) 72 days after irradiation. The film's response to topaz containing ^{32}P is unknown because of the difficulty in making synthetic topaz containing a known amount of ^{32}P. The 66.7 hrs is thought to be a conservative estimate, and shorter exposure times may be used if analysis is conducted a few weeks after irradiation.

Carbon paper or other light-proof material will attenuate any internally generated luminescence. The density thickness of carbon paper (or other light-proof material) should be small to minimize beta attenuation.

4.14 TLD Results

To determine the extent of direct exposure from irradiated topaz, LiF TLD chips (0.125" x 0.125" x 0.035") were taped onto irradiated gemstones and left for approximately 18 days. The results in Table 43 indicate that the beta-gamma dose from irradiated gems not containing ^{32}P (as determined by shielded GM beta absorption analysis) ranged from 23 to 39 mrad/(nCi g) of topaz, even though the relative amounts of ^{46}Sc, ^{59}Fe, ^{182}Ta, and ^{51}Cr

varied by an order of magnitude from gem to gem. The TLD response to an irradiated gem containing both gamma-emitting nuclides and ^{32}P ranged from 94 to 1089 mrad/(nCi/g) of gem. The wide variation was due to ^{32}P decay that occurred before TLD measurement. The increased values due to ^{32}P stressed the importance of identifying the high-energy beta emitters present. Once identified, gems containing short-lived nuclides should be held for radioactive decay before being released to the public.

Using the decay-corrected activity listed in Table 43 and the beta surface dose-rate from individual nuclides listed in Table 44, the calculated beta exposure was compared to the TLD exposure from BNL-irradiated topaz without ^{32}P. The results are listed in Table 45.

Both beta and gamma emissions cause exposure in TLD chips. However, beta emissions predominate and are the only type of emission considered in the calculations in Table 45. The TLD response compared to calculated exposure ranged from 43% (in gem #36) to 62% (in gem #3).

As discussed previously, the gamma-emitting nuclides identified in BNL-irradiated topaz, ^{46}Sc, ^{59}Fe, and ^{182}Ta also emit beta radiations. The TLD response to beta particles is nonlinear and is approximately 20% higher for high-energy beta sources (^{90}Sr-Y), and 5% lower for low-energy beta sources (^{204}Tl) (Ben-Shachar et al., 1989).

Table 43. *Measurements of TLD Gemstone Exposure*[a]

Gem #	Net cpm GM[b] (open window)	nCoul[c] (bkg sub)	Dose, mrad (2.51 nCoul =200 mrad)	Decay corrected nCi/g				Total nCi/g of gem	mrad per nCi/g
				^{46}Sc	^{59}Fe	^{182}Ta[d]	^{51}Cr		
3	123±13	3.49±2.06	279	9.2	0.5			9.7	29
4	35±9	1.17±1.38	94	1.3	0.9	0.7		2.9	33
10	35±9	0.88±1.27	70	2.2	0.4		0.1	2.7	27
11	667±27	16.73±4.18	1336	9.6	0.3	23.9		33.8	39
12*	5791±76	354.53±18.85	28306	24.1	1.3	0.6		26.0	1089
14	4394±67	126.83±11.29	10126	409.4	19.5	2.9		431.8	23
15*	12443±112	452.23±21.28	36106	32.1	1.7	0.5	3.4	37.7	958
19	267±18	11.83±3.54	944	9.1	0.8	0.6	1.6	12.1	78
31*	1026±33	44.23±6.71	3532	2.1	0.1	5.2		7.4	472
32*	1330±37	54.53±7.43	4354	4.0	0.4	1.7	1.0	7.1	620
33*	581±25	25.53±5.12	2039	1.6	0.2	0.9	0.8	3.5	595
34*	485±23	19.83±4.53	1584	2.0	0.1	5.4		7.5	211
35*	1273±36	47.23±6.93	3771	2.6		36.4	1.0	40.0	94
36	11843±109	390.03±19.77	31140	2.4		811.5		813.9	38

*Contains ^{32}P as determined by GM beta absorption study.

[a]Gems taped onto topaz on 2/24/89, 13:30. Removed 3/13/89, 8:30. 0.125" x 0.125" .x 0.035" LiF chips supplied by Harshaw. Chips initially annealed, exposed to 200 mR (1 mR ≈ 1 mrad) then reannealed. Chips with exposures greater than 1 standard deviation from the mean were not used in this study.

[b]Shielded GM bkg 95% CI = 23.7±8.4 cpm (n=12). One sigma error level is listed.

[c]TLD bkg 95% confidence interval = 0.366±0.046 nCoul (n=3). One sigma error level is listed.

[d]1221 keV peak.

Table 44. Radioactive Nuclide Data for Radioactive Gemstones[a]

Nuclide	Half-life	Gamma keV[b]	Beta keV[c]	r[d]	Gamma dose rate[e] (μrad/day)	Beta dose rate[f] (mrad/day)	Exempt concentration[g] (nCi/g)
Sodium-22	2.60a	2187	194	12.0	0.0025	0.0025	0.001
Phosphorus-32	14.2d	-	695	-	-	8.5	0.2
Phosphorus-33	25d	-	248	-	-	0.019	0.001
Sulphur-35	87d	-	49	-	-	0.74	0.6
Scandium-46	84d	2009	112	10.9	1.8	1.1	0.4
Chromium-51	28d	33	4	0.2	1.3	1.9	20.0
Manganese-54	312d	836	4	4.7	1.9	0.1	1.0
Cobalt-58	71d	977	34	5.5	2.3	0.9	1.0
Iron-59	44.5d	1188	117	6.4	1.6	1.8	0.6
Cobalt-60	5.27a	2504	97	13.2	2.7	1.2	0.5
Zinc-65	244d	585	7	2.7	1.1	0.2	1.0
Strontium-85	65d	518	9	3.0	1.2	0.2	1.0
Niobium-95	35d	764	44	4.2	1.7	1.1	1.0
Zirconium-95	64d	738	116	4.1	1.0	1.7	0.6
Tin-113	115d	23	6	1.7	0.6	0.1	0.9
Antimony-124	60d	1352	334	9.3	0.3	1.9	0.2
Antimony-125	2.73a	443	99	2.7	1.1	2.5	1.0
Barium-133	10.54a	404	54	2.4	0.001	0.0014	0.001[h]
Cesium-134	2.06a	1555	163	8.7	0.3	0.4	0.09
Cerium-141	32.5d	77	170	0.4	0.1	3.9	0.9
Europium-152	13.33a	1162	136	5.3	1.4	2.0	0.6
Tantalum-182	115d	1301	212	6.3	1.1	2.1	0.4

[a]Adapted from Ashbough, 1988. ^{32}P, ^{33}P, and ^{35}S added as potential contaminants.
[b]Average gamma and x-ray energy per disintegration.
[c]Average beta and electron energy per disintegration.
[d]Specific gamma ray constant (μrad/hr at 1 cm per nCi).
[e]Photon dose rate (μrad/day) at 7.62 cm per gram of topaz containing an exempt concentration of isotope listed. Gem worn 24 hours a day.
[f]Surface dose rate (mrad/day) due to β's and electrons for a gem that is thick in comparison to the average β energy emitted and contains an exempt concentration of the isotope listed. Gem worn 24 hours a day.
[g]Current exempt concentrations for reactor-irradiated faceted topaz as in 10 CFR 30.70.
[h]No value given in 10 CFR 30.70.

Table 45. Calculated Beta Dose Compared to Measured TLD Dose, mrad

Gem #	Calculated	TLD
3	453	279
4	166	94
10	123	70
11	2,640	1,336
14	20,467	10,126
36	72,953	31,140

In part, this difference in response explains some of the discrepancy between the calculated and measured TLD exposures. Other significant potential sources of difference include attenuation in the TLD chips and nonuniform distribution of nuclides within the topaz.

4.15 Estimates of Somatic Risk

4.15.1 Gamma Risk Estimate

Cancer risk estimates were made using the latest risk factors and organ-weighting factors suggested in ICRP Publication 60 (ICRP, 1991). For this purpose, it was assumed that total cancer risk could be approximated as three times that due to breast tissue (one part due to breast, one to thyroid, and one to the rest of the body). Therefore, the effective dose was estimated as three times the effective breast dose.

Since the isotopes decay during the year, the dose per year was obtained from the integral of dose rate, $\dot{D}$.

$$D = \dot{D} \int_0^t e^{-\lambda t} dt \tag{15}$$

$$= \dot{D} \ (1 - e^{-\lambda t})/\lambda \tag{16}$$

where

λ is the decay constant for the isotope of interest, day^{-1}, and

t is the decay time (365 days in this example).

First year doses to individuals wearing 30 carats (6 grams) of topaz containing an exempt concentration of the specific isotopes of concern are shown in Table 46 for the case of wearing the stones 8 hours per day, 365 days of the year at an effective distance of three inches.

Breast and thyroid tissues were assumed to be effectively three inches from stones containing exempt quantities of the most important isotopes. Initial gamma dose rates at three inches were as given in the sixth column of Table 44 and multiplied by 10^6 to convert μrad to rad (or rem, since 1 rad = 1 rem for gamma radiation). Based on ICRP 60, risk is estimated as 4 X 10^{-4} per Sv (4 x 10^{-6}/rem) for gamma exposures to the whole body, and breast and thyroid have weighting factors of 0.05 compared to the whole body. For exposures of 8 hours per day, the cancer risk per year per gram (5 carat) of stone is then:

$$R_\gamma = g \times 1/3 \times 3 \times 0.05 \times (4 \times 10^{-6})\ \dot{D}\ (1 - e^{-\lambda t})/\lambda \qquad (17)$$

where

g	=	grams of topaz
1/3	=	a factor to account for the assumed wearing for 8 of 24 hours each day.
3	=	the factor to account for breast, thyroid, and rest of body risks
0.05	=	the weighting factor
$\dot{D}$	=	initial dose rate at 3", rad/day

A summary of results for first year individual and collective effective doses due to gamma irradiation is given in Table 46. An affected U.S. population of 2.25 million owning a 5-carat pendant (one year of U.S. purchases, based on data in Section 1), worn 8 hr/day, was assumed for collective dose estimates. Also, a 30- carat topaz was selected to estimate the maximum effective dose an individual wearing a pendant containing a single gem would receive from gamma radiation.

Table 46. First Year Individual and Collective Effective Dose Due to Gamma Radiation Emitted from an Irradiated Topaz Gem Containing an Exempt Concentration of the Indicated Isotope

Individual Effective Dose, μrem		Collective Effective Dose, person-rem
Nuclide	30 carat	5 carat
^{182}Ta	49	18
^{59}Fe	31	12
^{124}Sb	21	8
^{46}Sc	62	23
^{54}Mn	146	55
^{51}Cr	20	8
^{134}Cs	30	11

Integrated doses may need to be calculated for longer than one year if a nuclide has a half-life longer than a few months. Among the gamma/beta emitters listed in Table 46, ^{134}Cs is of special interest because of its long half-life and small 10 CFR 30.70 exempt concentration, 0.09 nCi/g. If the stone contained an exempt concentration of both ^{182}Ta

and ^{134}Cs, the relative contribution to dose due to ^{134}Cs would increase in three years from five percent to 1,500 percent when compared to ^{182}Ta because of differing half-lives.

The one-year integrated risk estimates for individuals wearing 30 carat topaz gems are listed in Table 47 for several gamma emitting nuclides.

Table 47. First Year Risk Estimate Due to Gamma radiation Emitted from a 30 Carat Irradiated Topaz Gem

Nuclide	Individual gamma risk estimate
^{182}Ta	1.9×10^{-8}
^{59}Fe	1.2×10^{-8}
^{124}Sb	8.4×10^{-9}
^{46}Sc	2.5×10^{-8}
^{54}Mn	5.8×10^{-8}
^{51}Cr	8.0×10^{-9}
^{134}Cs	1.2×10^{-8}

As can be seen, all individual risk estimates were a factor of about 2 to 10 less than a risk level of 10^{-7} per year, the NCRP negligible individual risk level (NIRL) (NCRP, 1987). The calculated risk estimates were well within NIRL levels even if the topaz-bearing pendant were worn 24 hours per day (instead of 8), except for ^{54}Mn. A ^{54}Mn risk value of 1.8×10^{-7} resulted when a 30 carat topaz pendant was worn 24 hours per day. These estimates indicate that further efforts to reduce gamma radiation levels are probably unwarranted.

It would require concentration levels of 3.4 (for ^{54}Mn) to 25 (for ^{51}Cr) greater than the present exempt concentration levels listed in 10 CFR 30.70 for a one gram (5 carat) topaz to exceed the NCRP NIRL level of 10^{-7} for a gem worn 24 hr/day for 365 days/yr. Identification of topaz containing this high activity could be clearly established by gamma spectroscopy (germanium or NaI (Tl)) and GM detector measurements.

4.15.2 Beta Risk Estimate

The dose rate due to beta particle emission was calculated by using the following equation (Loevinger et al., 1956):

$$\dot{D}_\beta = 2.13\ (E_\beta)(\tau)$$

where

$\dot{D}_\beta$ = beta dose rate in rads/hr due to beta particles in an infinite, plane slab of infinite thickness
$E\beta$ = average beta energy (in MeV) per beta disintegration
τ = concentration of beta emitter in topaz, $\mu Ci/g$

The surface dose rate was estimated as $D_\beta/2$ to account for 2π emission geometry. This equation assumed a uniform concentration of beta emitters within topaz.

Using this equation, the surface dose rate due to beta emission from major nuclides found or expected in this study was estimated. The results are given in the 7th column of Table 44.

Examination of gamma dose rates at 7.62 cm (3"), given in the 6th column of Table 44, and surface beta dose rates from Table 44 indicated larger beta surface dose rates than gamma dose rates for isotopes that emit both gamma and beta emissions. For the beta-gamma emitting isotopes found in this study, the beta surface dose rates were 58 (^{54}Mn) to 2,375 (^{124}Sb) times greater than the gamma dose rate at 7.62 cm, and 39,000 times greater for ^{141}Ce, which was not found in BNL gems.

The beta dose estimates reflect doses expected from thick gems (relative to the range of average betas emitted). Thinner topaz may give somewhat greater integral gems doses (dose x volume of the tissue exposed) due to less self-absorption of beta radiation. For example, the estimated dose averaged over one cm^2 at 7.0 mg/cm^2 depth in tissue from an infinitely thin 1/4" or 1/2" diameter source, having average beta energy of 0.49 MeV, is 2.8 mrad/hr per nCi, or about 90 times greater than expected at the surface of a thick gem with the same activity. These higher doses per nCi would present concerns mainly for the higher energy beta emitters, especially ^{32}P, since, for medium and low energy emitters, self-absorption is significant even in fairly thin gems (e.g., 1/16" to 1/8" thick). However, if release criterion are expressed as a dose rate at the topaz surface, the problem of variations in self-absorption with topaz thickness is avoided.

Beta risk estimates were made assuming a risk of fatal radiation-induced skin cancer of 10^{-10}/(rad cm^2) of exposed skin (see page 18 section 2). For maximum individual risk estimates, it was assumed that six one-gram stones of the irradiated topaz are worn 8 hours per day and that each gram effectively irradiates a one cm^2 area of skin at the dose rates listed in Table 44. No shielding from topaz mountings or effective distance away from the skin was taken into consideration. These factors were chosen to assure conservatism in risk estimates.

The one-year integrated beta dose $D_{I\beta}$ was estimated in a fashion similar to that employed for the integrated yearly gamma dose using the following equation:

$$D_{I\beta} = \frac{\dot{D}_\beta}{\lambda}(1 - e^{-\lambda t}),\ \text{mrem-cm}^2 \qquad (19)$$

Individual and estimates of collective yearly integrated dose from beta radiation are given in Table 48. Assumptions used in the calculation of collective dose were the same as those in the estimates of gamma emission risk.

Table 48. First Year Individual and Collective Dose Due to Beta Radiation Emitted from Irradiated Topaz*

Nuclide	First year individual dose, mrad-cm^2	First year collective dose, person-rad-cm^2
	30 carat	5 carat
^{22}Na	4.8	3,600
^{32}P	213	160,000
^{33}P	2.0	1,575
^{35}S	261	198,000
^{59}Fe	345	258,750
^{124}Sb	486	364,500
^{46}Sc	381	285,750
^{182}Ta	930	697,500
^{134}Cs	345	258,750

*Based on assumed 8 hr/day, 365 day/yr wearing of a 6 gram (30 carat) stone with an exempt concentration of the nuclides listed for estimating maximum individual dose, or an average of 1 gram (5 carat) stones worn by 2.25 million persons for collective dose estimates.

4.16 Beta Particle Detection with GM Counters

The dose rate due to beta particle exposure was approximated by the following equation (Blatz, 1959):

$$\dot{D}_\beta = (5.76 \times 10^{-5})(\phi)(S/\rho) \quad (20)$$

where

$\dot{D}_\beta$ = absorbed dose rate due to beta radiation, rads/hr
ϕ = fluence rate of beta particles, number of betas/cm^2-sec
S/ρ = mass stopping power, MeV-cm^2/g

The skin cancer risk, R_β, was calculated by using the following equation:

$$9R_\beta = nfD_\beta R_s \text{ year}^{-1} \quad (21)$$

where

- n = number of one gram topaz stones worn
- f = fraction of day stones are worn
- D_β = the one year integrated from a one gram stone containing an exempt concentration of the isotope, mrad-cm^2/day.
- R_s = total somatic risk estimate for induction of skin cancer, 10^{-13}/(mrem-cm^2).

The estimates of one-year integrated individual risk from beta emissions for several nuclides are listed in Table 49. These risk levels were less than 10^{-3} of the NCRP NIRL level of 10^{-7} (NCRP, 1987).

Table 49. First Year Risk Estimates Due to Beta Radiation Emitted from Irradiated Topaz*

Nuclide	Individual beta risk estimate
^{22}Na	5x10^{-13}
^{32}P	2x10^{-11}
^{33}P	2x10^{-13}
^{35}S	3x10^{-11}
^{59}Fe	3x10^{-11}
^{124}Sb	5x10^{-11}
^{46}Sc	4x10^{-11}
^{182}Ta	9x10^{-11}
^{134}Cs	3x10^{-11}

*Based on wearing six one-gram stones (total 30 carats) initially containing an exempt concentration of the isotope and worn 8 hr/day for 365 days.

By rearranging Eq. 21, the number of betas/cm^2-second was estimated as shown in Table 50.

Table 50. Betas/cm^2-sec Emitted from Irradiated Topaz Containing Exempt Concentrations of Nuclides

Nuclide	Avg. β keV/dis (from Table 44)	S/ρ in MeV-cm^2/g (based on ave. β keV/dis) for SiO_2 in ICRU, 1984)	β/cm^2-sec
^{22}Na	194	2.3	0.0016
^{32}P	695	1.6	1.6
^{33}P	248	2.1	0.0065
^{35}S	49	5.4	0.1
^{59}Fe	117	3.1	0.4
^{124}Sb	384	1.8	0.8
^{46}Sc	112	3.1	0.3
^{182}Ta	212	2.2	0.7
^{134}Cs	163	2.6	0.1

The mass stopping power for topaz was approximated by SiO_2 (ionization potential = 139.2 eV and ρ = 2.32 g/cm^3). The calculated value of β/cm^2-sec closely approximated the general rule of 100 β/cm^2-sec = 10 mrad/hr to the skin (Shapiro, 1981). If the number of betas/cm^2-sec is known, then the number of betas/sec for various size table facets (largest facet) can be determined as shown in Table 51.

Table 51. Betas/sec from Topaz Containing a 10 CFR 30.70 Exempt Concentration for Various Facet Areas

Nuclide	β/cm^2-sec	Betas/sec from area		
		Facet Area		
		0.0625 cm^2	0.25 cm^2	1.0 cm^2
^{22}Na	0.0016	0.0001	0.0004	0.0016
^{32}P	1.6	0.10	0.40	1.6
^{33}P	0.0065	0.0004	0.02	0.0065
^{35}S	0.1	0.01	0.03	0.10
^{59}Fe	0.4	0.03	0.11	0.4
^{124}Sb	0.8	0.05	0.19	0.8
^{46}Sc	0.3	0.02	0.07	0.3
^{182}Ta	0.7	0.04	0.18	0.7
^{134}Cs	0.1	0.01	0.03	0.1

Knowing the number of betas/sec leads to the total number of betas emitted for 60 and 300 sec GM counting times (see Table 52).

Table 52. Total Betas Emitted from Facet Areas During a 60 and 300 Second GM Analysis of Irradiated Topaz Containing Nuclides at 10 CFR 30.70 Exempt Concentration Levels

Nuclides	Betas emitted					
	Facet Area					
	0.0625 cm^2		0.25 cm^2		1.0 cm^2	
	60 sec	300 sec	60 sec	300 sec	60 sec	300 sec
^{22}Na	0.096	0.48	0.38	1.9	1.5	7.6
^{32}P	6.0	30.0	24.0	120.0	94.8	474.0
^{33}P	0.39	2.0	1.6	7.8	6.2	31.2
^{35}S	0.4	1.9	1.5	7.5	6.0	30.0
^{59}Fe	1.6	7.8	6.3	31.5	25.2	126.0
^{124}Sb	2.9	14.4	11.4	57.0	46.2	231.0
^{46}Sc	1.0	5.1	4.1	20.3	16.2	81.0
^{182}Ta	2.6	13.2	10.6	53.1	42.6	213.0
^{134}Cs	0.4	1.8	1.7	8.3	6.6	33.0

Assuming a shielded GM detector efficiency of 70 percent and a background radiation level of 24 cpm, the concentration of nuclide necessary to yield net counting rates of twice background was calculated. Results are given in Table 53. It should be noted that, for some low energy beta emitters such as ^{35}S, the concentration necessary for GM detection will be larger than the stated value is because the GM counter's efficiency for low energy beta emitters is less than 70%. Overall GM efficiency can be increased by using multiple GM detectors simultaneously.

Table 53. Concentration of Nuclide in Topaz Needed to Yield Net Beta Counting Rates Equal to Twice Background Using a GM Detector*

Nuclide	Facet Area		
	0.0625 cm^2	0.25 cm^2	1.0 cm^2
^{22}Na	11,000 x exempt	2,750 x exempt	688 x exempt
^{32}P	11 x exempt	3 x exempt	< exempt
^{33}P	2,750 x exempt	688 x exempt	172 x exempt
^{35}S	185 x exempt	46 x exempt	11 x exempt
^{59}Fe	44 x exempt	11 x exempt	3 x exempt
^{124}Sb	24 x exempt	6 x exempt	exempt
^{46}Sc	67 x exempt	17 x exempt	4 x exempt
^{182}Ta	25 x exempt	6 x exempt	2 x exempt
^{134}Cs	190 x exempt	48 x exempt	10 x exempt

*Background = 24 cpm

These results indicate that except for ^{124}Sb, a shielded GM detector could not be used to determine near exempt concentrations at twice background levels in topaz having a table facet area less than 1 cm^2. However, based on skin cancer risk estimates, even the most restrictive beta emitter, ^{182}Ta, could be detected at the smallest facet size at radiation levels greater than twice background with a shielded GM detector without exceeding the 10^{-7} risk level.

5. DISCUSSION

Counting equipment must be carefully calibrated if minimum detectable levels in topaz are to be determined. Minimum detectable levels are important if exempt concentrations, as listed in 10 CFR 30.70, are to be determined in irradiated topaz. In this study, irradiated gems were counted singly on all radiation equipment. Sampling large batches of irradiated topaz to determine average concentration levels (nCi/g of gem) does not ensure that individual gems will not occasionally exceed an exempt concentration level because the majority of activity, for any particular nuclide, could be concentrated in one or a few stones.

Tables 54-57 summarize the detection sensitivties for the equipment used in this study; only the major nuclides that we found are included.

A NaI(Tl) detector, similar to the one used in this study, should be used to examine individual stones and to quantify gamma-emitting nuclides with counting times less than five minutes for individual stones. The NaI sensitivity (net cpm/nCi) should initially be determined for all nuclides identified, using germanium gamma spectroscopy and counting times long enough to detect exempt concentrations of any gamma-emitting isotopes that may be present. Batches of 40 to 50 gems are often counted simultaneously to identify these isotopes. If single-channel NaI analysis only is available, the nuclide having the smallest NaI sensitivity (net cpm per exempt concentration) should be used as a cutoff value for a topaz containing a mixture of several gamma-emitting nuclides. The product of NaI sensitivity (net cpm/nCi), exempt concentration (nCi/g), and the mass of the stone (g) yields net cpm. An irradiated topaz should not be released to the public if it exceeds the cpm obtained from this product. Alternatively, multichannel analysis could be used to quantify all gamma-or positron-emitting nuclides that may be present. The NaI sensitivity for beta-emitting nuclides ^{32}P, ^{14}C, and ^{36}Cl is due to bremsstrahlung detection. Of the beta-emitting nuclides, only ^{32}P could be detected on a NaI detector at a 95 percent confidence interval using a 100 to 1400 keV window setting.

The GM sensitivity for the gamma/beta emitting nuclides ^{46}Sc, ^{182}Ta, and ^{59}Fe is nearly independent of the nuclide. The GM sensitivity to ^{32}P is approximately six times as great as it is to typical gamma/beta emitters. The sensitivity for ^{54}Mn and ^{14}C (or ^{35}S) is very low, and excludes their detection by a shielded GM detector (except at very large concentrations).

The degree of self-absorption could be estimated when infinitely thin beta sources were compared to saturated ground-topaz standards (Table 56). The GM net cpm/nCi of the ground-topaz standards was approximately 76, 23, and 10 percent of the infinitely thin standards GM net cpm/nCi for ^{32}P, ^{35}Cl, and ^{14}C, respectively.

The plastic scintillator is an alternative to a shielded GM detector in the analysis of beta particles. As Table 57 shows, a 0.01" plastic scintillator is appreciably better for detecting ^{14}C (or ^{35}S), assuming the same source-to-detector distance.

Table 54. Sensitivies of NaI Detectors for BNL Topaz

Nuclide	NaI[a] 100 to 1,400 keV window		NaI[a] 40 to 1,400 keV window		# of samples
	Net cpm/(nCi g)	Net cpm/nCi	Net cpm/(nCi g)	Net cpm/nCi	
^{46}Sc	379 ± 12	941 ± 28	401 ± 10	994 ± 24	3
^{54}Mn	228 ± 24	566 ± 61	250 ± 23	621 ± 56	3
^{182}Ta	488 ± 19	1,221 ± 49	716 ± 19	1,789 ± 56	3
^{59}Fe	215 ± 20	536 ± 55	227 ± 21	567 ± 57	3
^{32}P		16 ± 5		30 ± 6	1
^{14}C		Not detectable		0.2 ± 5.4	1
^{36}Cl		4 ± 5		11 ± 6	1

[a]Liquid standards in glass vials (approx. 0.5 cm^3 volume in a round bottom vial of 12 mm inside diameter); D.S. Davidson 1024 analyzer Model 1056B: Ortec Model 485 amp: Ortec Model 113 preamp: Bertan Model 313A HV power supply (set at 1250 V); Ludlum 44-12 NaI detector. Five minute counting time. Two sigma standard deviation except for ^{32}P, ^{14}C, and ^{36}Cl where two sigma standard error of the single sample point was used.

Table 55. Sensitivities of GM Detection Equipment for BNL Topaz[a]

Nuclide	Net cpm/(nCi g)	Net cpm/nCi	Counting Time (min.)	
^{46}Sc	54	108	5	
	50	104		
	24*	115*		
		$x = 109 \pm 11$		
^{54}Mn	4.5	7.9	5	
	5.0	8.4		
	1.6*	8.5		
		$x = 8.3 \pm 0.6$		
^{182}Ta	63	112	1	
	72	133		
	68	121		
		$x_1 = 122 \pm 21$		
				$x_T = 114 \pm 38$
	52	87	5	
	47	96		
	38*	136*		
		$x_5 = 107 \pm 51$		
^{59}Fe	58	110	1	
	58	148		
	75	99		
		$x_1 = 119 \pm 50$		
				$x_T = 104 \pm 50$
	60	111	5	
	50	78		
	16*	80*		
		$x_5 = 90 \pm 36$		

*9/32" diameter standard.

[a]13/32" diameter x 0.2" ground topaz standards; Eberline SRM 200 equipped with HP210 probe; HV=905V; 3.94 mg/cm^2 (total) density thickness; GM probe surrounded with 2" thick lead shielding. Two sigma standard deviation used.

Table 56. Sensitivities of GM Detection Equipment for Standards

Nuclide	Net cpm/(nCi/g)$^{-1}$	GM[a] Net cpm/nCi	Counting time (min)	GM measurements on infinitely thin beta sources[b] Net cpm/nCi	# of samples	Counting time (min)
^{32}P	335	633	1	853±90	8	1
	359	558				
	345	713				
	370	678				
	306	714				
	114*	579*				
		x = 646±131				
^{14}C	10.5	19.4	5	168±28	8	1
	9.3	16.5				
	3.4*	16.4*				
		x = 17.4±3.3				
^{36}Cl	85	132	5	695±110	8	1
	75	147				
	42*	193*				
		x = 157±62				

*9/32" diameter standard.

[a]13/32" diameter x 0.2" ground topaz standards; Eberline SRM 200 equipped with HP210 probe; HV=905V; 3.94 mg/cm^2 (total) density thickness; GM probe surrounded with 2" thick lead shielding. Two sigma standard deviation used.

[b]1/4" and 1/2" diameter standards; HV=905V; 3.94 mg/cm^2 (total) density thickness; GM probe surrounded with 2" lead thickness. Two sigma standard deviation used.

Table 57. Sensitivities of Plastic Scintillator and Autoradiography for Standards and BNL Topaz

Nuclide	0.01" Plastic scintillator measurements on infinitely thin beta sources[a]			Autoradiography[b]	
	cpm/nCi	# of samples	Counting time (min)	Bare film (net darkening by gem/hr per nCi x10^{-5})	Carbon paper interface (net darkening by gem/hr per nCi x10^{-5})
^{46}Sc					
^{54}Mn				0.4 to 0.7	0.2 to 0.4
^{182}Ta					
^{59}Fe					
^{32}P	974±51	4	1	1.9 to 4.7[c]	1.1 to 2.8[c]
^{14}C	516±87	4	1		
^{36}Cl	904±13	4	1		

[a]1/4" and 1/2" diameter standards; Eberline SRM 200 equipped with Bicron B1 probe; HV=737V; Source-to-detector distance equal to GM measurement distance; plastic scintillator surrounded with 2" lead. Two sigma standard deviation used.

[b]Kodak OMAT AR film; room temperature exposure. No enhancement techniques used; BKG *fogging* = 0.17 net darkening. Assume 0.20 necessary for visual identification.

[c]Amount of darkening due to ^{32}P will depend on homogenicity of activity within gem (and therefore the self-absorption), the decay time since the end of irradiation and presumably, neutron flux.

There is a possibility that scintillation can occur within the irradiated topaz, indicating that low-energy beta interactions are occurring. Such low-energy beta emissions would not be detected by GM or gas-flow proportional counters because of self-absorption. The plastic scintillator could detect their presence because of this scintillation. The sensitivity of the plastic scintillator for beta emissions associated with elements emitting both beta and gamma radiations, i.e., ^{46}Sc, ^{182}Ta, and ^{59}Fe, was not determined. However, because we assumed that plastic scintillators would only be used for isotopes that emit only beta particles then the plastic scintillator and/or bare PM tube may be important for low-energy beta screening. The efficiency of the plastic scintillator in detecting gamma radiation was less than 0.1 percent for ^{241}Am, and 1 to 2 percent for ^{54}Mn (non-beta emitters).

The use of autoradiography to evaluate activated topaz appears attractive because many stones could be treated simultaneously, and the film would provide a permanent record for compliance and legal purposes. Also, the only requirements for autoradiography (using Kodak OMAT AR film) are a light-tight box and a method of film-processing (either automatic or manual). Autoradiography is extremely cost-effective and can be used by individuals that are not trained to use complicated radiation-detection equipment. However, long exposure times are needed.

The response of the film to ^{46}Sc, ^{54}Mn, ^{182}Ta, and ^{59}Fe was nearly independent of nuclide for both the bare film and the carbon paper interface. The film's response was diminished by a factor of approximately two by placing carbon paper between the stones and film. A rim-darkening effect was noted on bare film for several irradiated topaz; we speculated that internal reflections caused the stone to luminesce at the rim. Interfacing a piece of carbon paper between the stone and film reduced darkening to below detectable levels during a 24-hour exposure. A low-energy beta emitter such as ^{35}S may be responsible for this occurrence. An exposure time of 833 hours would be required to detect a concentration of 0.4 nCi/g of ^{46}Sc, ^{54}Mn, ^{182}Ta, or ^{59}Fe for bare film. A concentration of 1 nCi/g would reduce this time to 333 hr. Counting times for film with carbon paper interfacing would be approximately twice as long.

Many pure beta emitters can be produced by neutron-or electron-beam irradiation. Most possibilities can be rejected for one or more of the following reasons: (1) the half-life is too short, (2) radionuclides of the same element which have gamma-ray emissions would be produced and detected by gamma-ray spectroscopy, (3) the amount of the element needed to produce 10 CFR 30.70 levels is on the order of milligrams, and (4) 10 CFR 30.70 levels could not be produced from irradiation of the pure element. Of those isotopes remaining, ^{32}P, and ^{35}S pose the greatest concern for skin exposure. Destructive chemical analysis using high temperatures and a chemical fluence, such as NaF, is necessary to estimate the amount of precursor elements in topaz that would be activated to create these nuclides.

Most beta particles that occur in topaz are essentially self-absorbed, even in the smallest topaz stone; the range of betas from all isotopes found or expected in BNL-HFBR irradiated stones have a range of approximately 2.2 mm. Therefore, surface emissions will account for the largest percentage of total beta emissions. The topaz was considered as an infinite medium for beta emissions because of this limited range.

The ICRP (1991) recommends an annual skin dose limit to workers of 500 mSv (50 rem) to control nonstochastic effects. The annual dose equivalent to the skin, or lens of the eye, of nonoccupationally exposed individuals should not exceed 50 mSv (5 rem) for a single product (for either a safety or non-safety product). Where the skin is nonuniformly irradiated, the average dose over 1 cm^2 in the region of the highest dose should be estimat-

ed and related to the above limit. In the 1991 revision of 10 CFR 20, NRC recommends a limit of 50 rem/yr averaged over 1 cm^2 of the skin for workers. The skin dose to topaz braders is reduced by remote handling tools, such as tweezers. Furthermore, smaller and smaller quantities are dispersed to additional distributors. Thus, the maximum dose is reduced even further to any individual.

The effective dose equivalent to the most highly exposed individual non-user (e.g., family member of the individual that owns an irradiated topaz) will be much lower than that to the user; therefore, no assessment of individual non-user dose is necessary.

The concept of reasonable negligible risks is considered frequently in societal and individual activities. Levels of risk often are selected, based on the size of the risk compared with other natural or human uses. NCRP Report No. 91 (NCRP, 1987) recommended a Negligible Individual Risk Level (NIRL) below which efforts to reduce radiation exposure to an individual were unwarranted. NCRP recommended that scenarios be disregarded with probabilities of less than one in ten million. The uncertainties of radiation risk when compared with natural background would be on the order of 10's of mrem, and levels below this would be considered below regulatory concern.

The Nuclear Energy Agency (OECD) recommended an individual dose equivalent limit of 5 μS_v (0.5 mrem) per year or a skin exposure of 5 mSv in a year for users of consumer products that were not safety-related (NEA, 1985). This level corresponds to a few percent of the annual dose limit for members of the public recommended by the ICRP. The 5 μSv/yr allows an individual to be exposed to radiation doses from several practices. (A higher dose to users is considered acceptable from a product contributing to safety.) The above recommendation assumes that the source of radiation, i.e, wearing topaz rings, is inherently safe under normal and accidental conditions.

Alternate criteria presented here are based on limiting beta and photon doses and dose rates. Maximum individual photon-dose estimates were made assuming in that a person wears a 6 g topaz 8 hr/day at an assumed effective distance of three inches from breast tissues. A beta limit is based on evaluating the surface dose rate. Both levels are intended to reduce the risk of fatal cancers to $<10^{-7}$, the NCRP NIRL level, and the yearly effective dose equivalent to less than 0.25 millirem for all isotopes identified in this study. Integrated first year gamma risk estimates for the above topaz pendant were 0.58 (^{54}Mn) to 0.08 (^{51}Cr) of the NCRP NIRL level.

From this research, procedures were developed to aid domestic reactor groups and importers of treated gems, wishing to be licensed by the NRC, to distribute irradiated topaz to persons exempt from licensing.

6. CONCLUSION

All nuclides identified in this study can be detected using these procedures except ^{35}S, ^{51}Cr, and ^{124}Sb. GM and NaI sensitivity has yet to be determined for the latter two isotopes. ^{35}S is unlikely to be generated by neutron activation; destructive analysis of irradiated topaz may be needed to identify and quantify this nuclide.

Procedures needed to ensure that irradiated topaz has safe levels of residual radioactivity include the following:

(i) A quality-assurance program, incorporating information on energy and efficiency calibration, is expected to be developed and maintained by groups or individuals wishing to be licensed. Also, the quality-assurance program must include techniques to assure the stability of the detector and low levels of background radiation.

(ii) After irradiation, the topaz should not be analyzed for about two to three weeks to allow radioactive decay of neutron-produced ^{77}As, ^{183}Ta, ^{72}Ga, ^{24}Na, and all isotopes produced by electron-beam irradiation.

(iii) Gems that are ready for analysis should be placed in an ultrasonic bath in mild acid solution for 30 minutes or more to remove surface contamination.

(iv) Analysis by germanium spectroscopy is necessary to identify all gamma- or positron-emitting nuclides. Batches of topaz counted on a germanum detector with 20% relative efficiency will require 1 to 3 hours, depending on the detector's geometry and efficiency. The detector element should be surrounded by a minimum of 4" steel and lined with cadmium to reduce background levels of radiation. Analysis can be conducted at the irradiation site, or at another certified laboratory.

(v) Topaz should be segregated into lots based on mass, to permit quantitative analysis in units of activity per gram, or for estimates of dose or risk per gram.

(vi) A 2" lead shielded GM detector with window thickness of 1.4 to 2.0 mg/cm^2 will be required to analyze individual topaz for beta particle emission. The table facet of the stone should be placed as close as possible to the detector's face. A one-minute count on a 0.5 g or larger topaz with a table-facet area of at least 0.25 cm^2 will detect an exempt concentration level at 2x background (bkg = 24 cpm). All stones with a count rate greater than two times background should be stored for further radioactive decay.

If necessary, ^{32}P can be identified by the shape of a GM beta absorption curve at 0, 80, and 450 mg/cm^2.

The activated isotopes in topaz smaller than 0.5 g can be detected at twice background levels if longer counting times are used.

(vii) All topaz passing GM analysis in step (vii) should be analyzed on a well-type NaI detector (2" thick x 1 1/2" diameter). Exempt concentrations of ^{54}Mn and ^{134}Cs can be identified at twice background levels (bkg = 74 cpm) during a 2-minute count for topaz with a mass greater than 0.5 grams. Smaller stones require longer counting times.

REFERENCES

American National Standard Institute (ANSI), ANSI N42.14-1978, "Calibration and Usage of Germanium Detectors for Measurement of Gamma-Ray Emission of Radionuclides," New York.

Ashbaugh, C.E., "Gemstone Irradiation and Radioactivity," Gems & Gemology, 24:196-213, 1988.

Atomic Energy Commission, "Products Intended for Use by General Public (Consumer Products)," 30 Federal Register 3462, March 16, 1965.

Attix, F.H., Roesch, W.C. and Tochilin, E. (eds.), Radiation Dosimetry, Vol 1., Fundamentals, 2nd ed., Academic Press, New York, p. 128-135, 1968.

Benada, J., Randa, Z., Kuncif, J. and Vobecky, M., Nondestructive Neutron Activation Analysis of Mineral Materials II, Ceskoslovenska Akademie Ved. Rez. Ustav Jaderneho Vyzkumu, 1972.

Ben-Shachar, B., Levine, S.H. and Hoffman, J.M., "Beta Skin Dose Determination Using TLDs, Monte-Carlo Calculations, and Extrapolation Chamber," Health Physics, 57:917-925, 1989.

Blatz, H. (ed.), Radiation Hygiene Handbook, 1st ed., McGraw-Hill Book Company, Inc., New York, p.14-5, 1959.

Brookhaven National Laboratory, "Guidebook for the ENDF/B-V Nuclear Data Files," BNL-NCS-31451/EPRI NP-2510/RP975-1/ENDF-328, 1982.

Bureau of Radiological Health (BRH) and the Training Institute Environmental Control Administration, Radiological Health Handbook, Revised Edition, U.S. Government Printing Office, Washington, D.C., 1970.

Carlsson, L. and Akselsson, K.R., "Rapid Determination of Major and Trace Elements in Geological Material with Proton-Induced X-Ray and Gamma-Ray Emission," Nuclear Inst. Methods, 1811: 531-537, 1981.

Code of Federal Regulations, Vol. 56, No. 98, Title 10, Part 20, Section 20.101; 1991.

Code of Federal Regulations, Title 10, Part 30, August 31, 1984.

Crookes, W., "On Acquired Radio-Activity," Phil. Trans. Royal Society, London, Series A, 214:433-445, 1914.

Crowningshield, R., "Irradiated Topaz and Radioactivity," Gems & Gemology, 17:215-217, 1981.

Dickinson, A.C. and Moore, W.J., "Paramagnetic Resonance of Metal Ions and Defect Centers in Topaz," J. Phy. Chem., 71:231-240, 1967.

Foord, E., Jackson, L.L., Taggart, J.E., Crock, J.G. and King, T.V.V., "Environment of Crystallization of Topaz as Determined from Crystal Chemistry and Infrared Spectra," U.S. Geological Society Abstracts, 20:A224, 1988.

Fournier, R., "Process for Irradiating Topaz and the Product Resulting Therefrom," U.S. Patent 4,749,869 filed May 14, 1986, issued June 7, 1988.

Fritsch, E. and Rossman, G.R., "An Update on Color in Gems, Part 1: Introduction and Colors Caused by Dispersed Metal Ions," Gems & Gemology, 23:126-139, 1987.

Hahn, E.J., "Autoradiography: A Review of Basic Principles," American Laboratory, 15:64-71, 1983.

Harbottle, G., "Activation Analysis in Archeology," Radiochemistry, Vol. 3, A Review of the Literature Published During 1974 and 1975, Edited by G.W.A. Newton, Burlington House, London, p. 33-72, 1976.

Harshaw/Filtrol, "Thermoluminescence Dosimetry (TLD) Materials," Performance Specification Pamphlet TL203-2, 1988.

Heide, F., "Bemerkungen zur Verteilung von Spurenelementen im Topas," Chem. Erde. 25:230-236, 1966.

International Commission on Radiation Units and Measurements (ICRU), "Measurement of Low-Level Radioactivity," ICRU Report 22, Washington, D.C., 1972.

International Commission on Radiation Units and Measurements (ICRU), "Stopping Powers for Electrons and Positrons," ICRU Report 37, Washington, D.C., 1984.

International Commission on Radiological Protection (ICRP), "Report of the Task Group on Reference Man," ICRP Publication 23, Pergamon Press, Oxford, U.K., pp. 86-102, 1975.

International Commission on Radiological Protection (ICRP), "Recommendations of the International Commission on Radiological Protection," ICRP Publication 26, Pergamon Press, Oxford, U.K., 1977.

International Commission on Radiological Protection (ICRP), "Limits for Intakes of Radionuclides by Workers, Part 1," ICRP Publication 30, Pergamon Press, Oxford, U.K., 1979.

International Commission on Radiological Protection (ICRP), "Radionuclide Transformations: Energy and Intensity of Emissions," ICRP Publication 38, Pergamon Press, Oxford, U.K., 1983.

International Commission of Radiological Protection (ICRP), "1990 Recommendations of the International Commission on Radiological Protection," ICRP Publication 60, Pergamon Press, Oxford, U.K., 1991.

Jeweler's Gemstone Reference, "A Guide to Gemstone Enhancement, Care and Handling," Modern Jeweler, September 1985.

Johns, H.E. and Cunningham, J.R., The Physics of Radiology, 3rd Edition, Charles C. Thomas, Springfield, Illinois, p. 272-282, 1978.

Koch, R.C., Activation Analysis Handbook, Academic Press, New York, 1960.

Levy, P.W. (ed.), Radiation Effects in Optical Materials, SPIE, 541:1-24, 1985.

Loevinger, R., Japha, E.M., and Brownell, G.L., "Discrete Radioisotope Sources," Radiation Dosimetry, Hine, G.J and Brownell, G.L. (eds.), Academic Press, New York, p. 723, 1956.

McLane, V., Dunford, C.L., and Rose, P.F., Neutron Cross Sections, Volume 2, Academic Press, New York, 1988.

Nassau, K., The Physics and Chemistry of Color, John Wiley & Sons, Inc., New York, p. 187, 1983.

Nassau, K., Gemstone Enhancement, Butterworths, London, p. 165, 1984.

Nassau, K., "Altering the Color of Topaz," Gems & Gemology, 21:26-34, 1985.

Nassau, K. and Prescott, B.E., "Blue and Brown Topaz Produced by Gamma Irradiation," American Mineralogist, 60:705-709, 1975.

National Academy of Sciences/National Research Council, The Effects on Populations of Exposure to Low Levels of Ionizing Radiation, BEIR III, Committee on the Biological Effects of Ionizing Radiation, National Academy Press, Washington, D.C., 1980.

National Academy of Sciences/National Research Council, Health Effects of Exposure to Low Levels of Ionizing Radiation, BEIR V, Committee on the Biological Effects of Ionizing Radiation, National Academy Press, Washington, D.C., 1990.

National Bureau of Standards, "Photonuclear Data - Abstract Sheets 1955-1982," NBSIR 83-2742, U.S. Government Printing Office, Washington, D.C., 1984.

National Council on Radiation Protection and Measurements (NCRP), "Instrumentation and Monitoring Methods for Radiation Protection," NCRP Report No. 57, Washington, D.C., 1978a.

National Council on Radiation Protection and Measurements (NCRP), "A Handbook of Radioactivity Measurement Procedures," NCRP Report No. 58, Washington, D.C., 1978b.

National Council on Radiation Protection and Measurements (NCRP), "Recommendations on Limits for Exposure to Ionizing Radiation," NCRP Report No. 91, Washington, D.C., 1987.

National Jeweler Newsmagazine, Gralla Publications, 32:8,25,76,77,78, 1988.

Nero, A.V., A Guidebook to Nuclear Reactors, University of California Press, Ltd., p. 4-16, 1979.

Nuclear Data Inc., ND66 Multichannel Analyzer/Remote Terminal Operator's Instruction Manual 07-0088, Schaumburg, Illinois, p. 14-7, 1981.

Nuclear Energy Agency, Organisation for Economic Co-Operation and Development, A Guide for Controlling Consumer Products Containing Radioactive Substance, NEA, Paris, 1985.

Nuclear Regulatory Commission, "Suspension of Exemption Permitting Use of Glass Enamel and Glass Enamel Frit Containing Small Amounts of Uranium," 48 Federal Register 33697, July 25, 1983.

Nuclear Regulatory Commission, "Glass Enamel and Glass Enamel Frit Containing Small Amounts of Uranium," 49 Federal Register 35611, September 11, 1984.

Nuclear Regulatory Commission, Memorandum to Victor Stello, Jr. from Hugh Thompson, Jr., dated September 28, 1987, SECY-87-559, 1987b.

ORTEC, Experiments in Nuclear Science, 2nd edition, ORTEC Publication AN 34, New York, p. 9, 1976.

Overman, R.T. and Clark, H.M., "The Laboratory Characterization of Radiation," Radioisotope Techniques, McGraw-Hill Book Company, Inc., New York, p. 210-223, 1960.

Petrov, I. and Berdesinski, W., "Untersuchung Kunstlich Farbveranderter Blauer Topas (vorlaufige mitteilung)," Z. Dt. Gemmol. Ges., 24:16-19, 1975.

Pough, F.H. and Rogers, T.H., "Experiments in X-Ray Irradiations of Gem Stones," American Mineralogist, 32:31-43, 1947.

Raju, K.S., "Topaz - On Neutron Irradiation," Int. J. App. Rad. Isotopes, 32:929-930, 1981.

Schmetzer, K., "Colour and Irradiation-Induced Defects in Topaz Treated with High-Energy Electrons," J. Gem., 20:362-368, 1987.

Shapiro, J., Radiation Protection: A Guide for Scientists and Physicians, 2nd edition, Harvard University Press, Cambridge, Massachusetts, p.112, 142, 1981.

Shore, R.E., "Overview of Radiation-Induced Skin Cancer in Humans," Int. J. Radiat. Biol., 37:809-827, 1990.

Swanstrom, R. and Slank, P.R., "X-ray Intensified Screens Greatly Enhance the Detection by Autoradiography of the Radioactive Isotopes ^{32}P and ^{125}I," Analytical Biochemistry, 86:184-192, 1978.

Tessmer, C.F., "Penetration and Absorption of Ionizing Radiations," Conference on Biology of Cutaneous Cancer, Nat'l Cancer Inst. Monograph No. 10, p. 393-431, 1963.

Traub, R.J., Reece, W.D., Scherpelz, R.I., and Sigalla, L.A., "Dose Calculation for Contamination of the Skin Using the Computer Code VARSKIN," NUREG/CR-4418, PNL-5610, 1987.

U.S. Department of Commerce, "Maximum Permissible Body Burdens and Maximum Permissible Concentrations of Radionuclides in Air and in Water for Occupational Exposure," National Bureau of Standards Handbook 69, Superintendent of Documents, Washington D.C., 1959.

Webster, R., Gems: Their Sources, Descriptions and Identification, 4th edition, Butterworths, London, p. 691-692, 1983.

Yeh, S.J. and Harbottle, G., "Intercomparison of the Asaro-Perlman and Brookhaven Archaeological Ceramic Analytical Standards," J. Radioanalytical & Nuc. Chem., 97:279-291, 1986.

APPENDIX A

Gem Terminology

carat	unit of gem mass. 1 carat = 0.2 g.
cloisonne	a kind of enamelware in which the surface decoration is formed by different colors of enamel separated by thin strips of metal set on edge.
color center	defects that cause light absorption (that may or may not be in the visible range). May involve a vacancy (hole or electron color center) or a defect plus an adjacent impurity. X, Y, and Z color centers result from absorption bands being observed in the X, Y, and Z axis, respectively, when a polarized electric field is applied. Peak absorption of light for F centers occurs between the wavelengths of 400 and 700 μm.
fluvial	formed by the action of flowing water: girdle setting edge.
greisen	a granite rock composed chiefly of quartz and mica.
hydrothermal	hot magmatic rock that is rich in water.
pavilion	lower half of the stone.
pegmatite	a coarse-grained igneous rock, largely granite, sometimes rich in rare elements.
pendeloque cut	pear-shaped modification of the brilliant cut rhyolite, a glassy volcanic rock, similar to granite in composition and usually exhibiting flow lines.
step cut (or trap cut)	table facet surrounded by a series of step-like rectangular facets which increase in steepness towards the girdle. In the lower part of the stone, the rectangular facets decrease in steepness as they progress towards the basal facet.
table facet	the largest flat surface on the gem.
USGS	United States Geologic Survey.
VHN	Vickers hardness number. A measure of a materials hardness determined by applying a known load to a sphere of standard diameter pressing on plane of material and measuring indentation.

APPENDIX B

Radiation Terminology

ANSI	American National Standards Institute
attenuation	process by which a beam of radiation is reduced in intensity when passing through material.
autoradiography	photographic method of recording the spatial distribution of radioactivity within an object.
beta particle	charged particle emitted from the nucleus of an atom with a mass and charge equal to that of an electron (9.109×10^{-28}g). Beta particles have an energy range from zero to a maximum. The most probable energy is about 1/3 of the maximum.
bremsstrahlung	radiation produced by deacceleration of charged particles passing through matter.
CFR	Code of Federal Regulations.
cpm	counts per minute.
epithermal neutrons	neutrons having an intermediate energy range of 0.5 eV to 100 keV.
erythema	increased redness of the skin due to swelling of the capillaries with blood.
eV	electron volt, a unit of energy equal to the energy gained by an electron in passing through a potential difference of one volt. Multiples of electron volt include kiloelectron volt (keV) = 10^3 eV, and megaelectron volt (MeV) = 10^6 eV.
exempt concentration	concentration of radioactive material listed in 10 CFR 30.70 Schedule A which does not require a specific or general license for the receipt, possession, or use of any by-product contained within the product.
fast neutron	neutrons having an energy greater than 100 keV. All neutrons are initially fast.

fission, nuclear	splitting of a nucleus into at least two nuclei and resulting in the release of a large amount of energy.
fluence	number of particles passing through a unit cross-sectional area, e.g., neutrons/cm^2.
fluence rate	number of particles passing through a unit cross-sectional area per unit of time, e.g., neutrons/(cm^2 sec).
gamma ray	electromagnetic radiation emitted from an energetically unstable nucleus-gas flow proportional counter charged-particle detector in which the charge collected is proportional to the counter charge produced by the initial ionizing event.
Ge(Li) detector	lithium drifted germanium detector used in gamma spectroscopy.
GM	Geiger Muller counter. Operated in the region in which the charge collected per ionizing event is essentially independent of the number of primary ions produced in the initial ionizing event.
HFBR	BNL High Flux Beam Reactor.
IAEA	International Atomic Energy Agency.
ICRP	International Commission on Radiation Protection.
intrinsic germanium detector	essentially pure germanium detector used for gamma spectroscopy.
isotopes	nuclides having the same number of protons in the nucleus but differing in the number of neutrons, i.e., nuclides with similar atomic number but different mass numbers.
K_α	characteristic x-rays emitted as a result of an electron in the L shell filling a vacancy in the K shell.
K_β	characteristic x-rays emitted as a result of an electron in the M shell filling a vacancy in the K shell.
LINAC	linear accelerator.
MDL	minimum detectable level.
(n,α)	atomic reaction in which a neutron interacts with a nucleus, emitting an alpha particle.
(n,γ)	atomic reaction in which a neutron interacts with a nucleus, emitting a gamma ray.

(n,p)	atomic reaction in which a neutron interacts with a nucleus, emitting a proton.
(n,2n)	atomic reaction in which a neutron interacts with nucleus, emitting two neutrons.
NaI(Tl)	sodium iodide detector doped with thallium. Used for gamma spectroscopy analysis.
nCi/g	nanocurie (or 10^{-9} Curie) per gram of material.
neutron	subatomic particle having a mass of 1.674×10^{-24}g. The neutron is electrically neutral.
NIRL	the negligible individual fatal risk level of 10^{-7} per year.
NIST	National Institute of Standards and Technology. Replaced National Bureau of Standards (NBS).
nonstochastic	severity of effect increases with dose above some threshold, e.g., skin erythema.
NRC	Nuclear Regulatory Commission.
nuclide	any atomic nucleus specified by its atomic number (Z), atomic mass (A), and energy state.
photonuclear reaction	reaction in which a high energy gamma ray or x-ray (typical minimum energy of 6 to 13 MeV) interacts with an atom and, most typically, a neutron is emitted. Also called photodisintegration.
photopeak	photoelectric absorption peak in gamma spectroscopy corresponding to a particular photo energy emitted by a radionuclide.
PIXE	proton induced x-ray fluorescence.
positron	particle equal in mass to the electron but possessing a positive charge.
proton	subatomic particle with a mass of 1.672×10^{-24} g and having a positive electrical charge.
RPI	Renssalaer Polytechnic Institute

scintillation detector	theory of operation based on detection of fluorescent radiation (usually visible light) emitted when an electron returns from an excited state to a valance state. Light, or scintillations, are detected by a photomultiplier tube. The size of the pulse is proportional to the energy deposited in the crystal.
signal-to-noise	net detector response divided by the detector background response.
stochastic	probability of effect is proportional to dose, e.g., in carcinogenesis.
sum of ratios	ratio between the concentration of radionuclides present in activated topaz and the exempt concentration listed in 10CFR 30.70 Schedule A. The sum of these ratios for all isotopes identified in irradiated topaz must not exceed one, i.e., unity.
T 1/2	radioactive half-life.
thermal neutron	neutron having a most probable energy of 0.025 eV.
TLD	thermoluminescent dosimeter.
transition element	element in which an outer electron shell is only partially filled.
x-ray fluorescence	emission of characteristic x-rays after matter is irradiated with high energy electrons.

APPENDIX C

Summary of Counting Equipment (Non-Gamma Spectroscopy) Used In This Study

Description	Manufacturer/ Model	Serial Number	Date of last calibration	Comments
Gamma scintillator	Ludlum/125	15475		
GM	Victoreen/700	63691	1/6/88	
GM	Eberline/HP 210L	706382	2/13/89	897 volt plateau
Radiation monitor	Eberline/SRM-200	276	2/23/89	Used for GM and plastic scintillator probes
Liquid scintillation counter	Searle Analytic/ Analytic 92 Model 6892			
Windowless gas flow proportional counter	Eberline			2425 volt plateau
Counter/timer	Canberra/1776			Used in conjunction with windowless gas flow counter
High voltage power supply	Canberra/3002			Used in conjunction with windowless gas flow counter
Sample holder	Ludlum/180-2			Used with Eberline HP 210L GM probe
Survey meter	Ludlum/Model 3	44200	10/4/88	Used with 44-9 probe
GM pancake probe	Ludlum/Model 44-9	PRO30039	10/4/88	
Survey meter	Ludlum/Model 12	65231	4/4/89	Used with 44-9 probe
GM pancake probe	Ludlum/Model 44-9	PRO55651	4/4/89	
NaI(Tl) well-type scintillation detector	Ludlum/44-12	PRO55652		
Plastic scintillator	Bicron/B1			Equipped with interchangeable 0.0001", 0.001", 0.01", and 0.1" plastic scintillators

APPENDIX D

Summary of Non-Counting Equipment Used in This Study

Description	Manufacturer/ Model	Serial Number	Date of last calibration	Comments
Pan balance[a]	Metter/AC100	824079	3/88	Automatic zeroing capability (not used since 1/89)
Pan balance[a]	Mettler/AE100	C38657	3/88	Automatic zeroing capability
Pan balance[a]	Mettler	224220	4/88	Manual zeroing
Refractometer	Gem Instruments/ Duplex II			
Utility lamp	Gem Industries	409		
TLD reader	Harshaw/2000			
Calibrated sieves	W.S. Tyler			
Optical densitometer	Macbeth/TD502LB	1164A		Calibrated with Macbeth opal glass density strip (PN 29002670)
Longwave UV lamp	UVP, Inc./ UVL-56 Blak-Ray			750 $\mu W/cm^2$ @ 6"
Shortwave UV lamp	UVP, Inc./ UVL-54 Mineralight			580 $\mu W/cm^2$ @ 6"
UV viewing cabinet	UVP, Inc./ CC-10 Chromato-Vue			

[a]All balances are calibrated yearly as part of Brookhaven's quality assurance program and have an accuracy of ±0.0001 g.

APPENDIX E

Germanium Detectors Used in This Study

Manufacturer	Serial Number	BNL Designation	Detector Volume (cm^3)	Resolution (FWHM at 1.33 MeV)	Rel. eff. at 1.33 MeV[c] %	Pulser	High Voltage Supply	Preamp	Spectroscopy, Amp
PGT[a]	1727	6A	95.0	1.74	19.0	-	PGT 5 KV Model 315	PGT RG11A/C	PGT Model 340
Ortec[b]	8001-2021T	2	100.1	2.00	20.5	-	Ortec 5 KV Model 459	Ortec Model 120-4F	Ortec 472A
PGT[a]	1591	12	62.0	1.62	13.5	Ortec Research	PGT 5 KV Model 315A	PGT RG11B/C	Tennelac TC 244 with pileup rejector

[a]Princeton Gamma Tech, Princeton, N.J. 08540
[b]EG&G Ortec, Oak Ridge, TN 37831
[c]Relative efficiency of germanium detector as compared to a 3' x 3" NaI(Tl) detector.

APPENDIX F

Frequencies of Testing the Germanium Detector's Performance

	PGT 12	Ortec 2	PGT 6A
Background	1,800-3,600 sec Whenever a series of samples is run.	60,000 sec Weekly	60,000 sec Weekly
		7,200-9,000 sec Whenever a series of samples is run	7,200-9,000 sec Whenever a series of samples is run.
keV/channel	Whenever a series of samples is run.	Weekly	Weekly
Efficiency calibration* using NBS traceable standard	Whenever a series of samples is run.	Weekly	Weekly
Resolution	Monthly	Weekly	Weekly

*At least 10,000 net counts must be accumulated for each calibration peak or the percent error of the peak area (as determined by the Nuclear Data peak search routine) must be less than 2%.

APPENDIX G

Comparison of Neutron-Irradiated Ohio Red Standards[a] (Net Count Rate (cpm) per mg)

Nuclide	Energy keV	Ohio Red Standard Identification							
		107D.S14[b] (top)	107.S16[b] (bottom)	107D.S30[c] (top)	107D.S29[c] (middle)	107D.S28[c] (bottom)	107.S06[d] (top)	107.S10[d] (middle)	107.S15[d] (bottom)
^{141}Ce	145	56.5±.3	58.9±.4	176.6±3.2	176.1±3.0	169.2±3.1	16.1±.2	16.9±.2	15.2±.1
^{59}Fe	1099	69.7±.1	69.9±.1	201.9±1.4	205.7±1.2	205.5±1.2	21.9±.1	21.8±.1	21.4±.1
^{51}Cr	320	19.5±.2	18.7±.2	22.7±1.6	33.3±1.6	21.6±1.6	3.7±.2	2.8±.1	3.9±.1
^{134}Cs	604	9.0±.1	8.6±.2	55.9±1.2	55.4±4.3	55.3±1.2	18.8±.1	21.3±.1	20.4±.1
^{46}Sc	889	244.9±.2	241.6±.2	743.8±2.2	743.4±2.2	762.5±24.4	52.5±.2	52.0±.2	51.9±.1
^{60}Co	1173	10.4±.1	9.3±.1	36.1±.6	37.6±.6	36.1±.6	3.7±.1	3.8±.1	3.9±.1
	1332	9.1±.1	8.6±.1	30.6±.4	31.7±.4	30.1±.4	4.0±.1	4.1±.1	4.2±.1

[a]Ohio Red standards placed at top, middle, or bottom of topaz irradiation packet during neutron bombardment. All standards decay corrected to time = 0 following irradiation.

[b]Thermal neutron fluence = 3×10^{18} neutrons/cm^2; HFBR port V10.

[c]Thermal neutron fluence = 9.21×10^{18} neutrons/cm^2; HFBR port V14.

[d]Thermal neutron fluence = 6.6×10^{17} neutrons/cm^2; HFBR port V15.

NRC FORM 335 (2-89) NRCM 1102, 3201, 3202

U.S. NUCLEAR REGULATORY COMMISSION

BIBLIOGRAPHIC DATA SHEET

(See instructions on the reverse)

1. REPORT NUMBER (Assigned by NRC, Add Vol., Supp., Rev., and Addendum Numbers, if any.)

NUREG/CR- 5883
BNL-NUREG-52330

2. TITLE AND SUBTITLE

Health Risk Assessment of Irradiated Topaz

3. DATE REPORT PUBLISHED

MONTH	YEAR
January	1993

4. FIN OR GRANT NUMBER

A-3982

5. AUTHOR(S)

K. Nelson, J.W. Baum

6. TYPE OF REPORT

Technical

7. PERIOD COVERED *(Inclusive Dates)*

8. PERFORMING ORGANIZATION – NAME AND ADDRESS *(If NRC, provide Division, Office or Region, U.S. Nuclear Regulatory Commission, and mailing address; if contractor, provide name and mailing address.)*

Brookhaven National Laboratory
Upton, New York 11973

9. SPONSORING ORGANIZATION – NAME AND ADDRESS *(If NRC, type "Same as above"; if contractor, provide NRC Division, Office or Region, U.S. Nuclear Regulatory Commission, and mailing address.)*

Division of Regulatory Applications
Office of Nuclear Regulatory Research
U.S. Nuclear Regulatory Commission
Washington, D.C. 20555

10. SUPPLEMENTARY NOTES

11. ABSTRACT *(200 words or less)*

Irradiated topaz gemstones are currently processed for color improvement by subjecting clear stones to neutron or high-energy electron irradiations, which leads to activation of trace elements in the stones. Assessment of the risk to consumers required the identification and quantification of the resultant radionuclides and the attendant exposure. Representative stones from Brazil, India, Nigeria, and Sri Lanka were irradiated and analyzed for gamma ray and beta particle emissions, using sodium iodide and germanium spectrometers; and Geiger-Muller, plastic and liquid scintillation, autoradiography, and thermoluminescent-dosimetry measurement techniques. Based on these studies and other information derived from published literature, dose and related risk estimates were made for typical user conditions. New criteria and methods for routine assays for acceptable release, based on gross beta and gross photon emissions from the stones, were also developed.

12. KEY WORDS/DESCRIPTORS *(List words or phrases that will assist researchers in locating the report.)*

Irradiation, Neutrons, Electrons, Radiation Hazards, Health Hazards, Health Hazards- Risk Assessment, Consumer Protection, Radiation Detectors, Dose Rates, Gamma Radiation, Beta Particles, Radiation Detection, Radioisotopes- Doses, Consumer Products.

13. AVAILABILITY STATEMENT

Unlimited

14. SECURITY CLASSIFICATION

(This Page) Unclassified

(This Report) Unclassified

15. NUMBER OF PAGES

16. PRICE

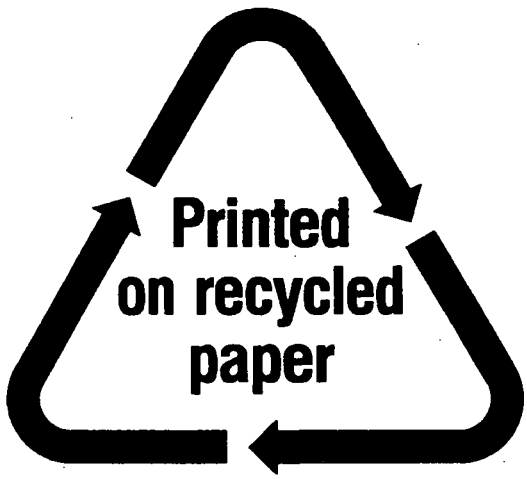

Federal Recycling Program

UNITED STATES
NUCLEAR REGULATORY COMMISSION
WASHINGTON, D.C. 20555-0001